RECHARGE ESTIMATION AND SUSTAINABILITY ASSESSMENT OF GROUNDWATER RESOURCES IN THE NORTH CHINA PLAIN

by

GUOLIANG CAO

Dr. CHUNMIAO ZHENG, COMMITTEE CHAIR
Dr. RONA J. DONAHOE
Dr. GEOFF R. TICK
Dr. TIM MASTERLARK
Dr. BRIDGET R. SCANLON

A DISSERTATION

Submitted in partial fulfillment of the requirements
for the degree of Doctor of Philosophy
in the Department of Geological Sciences
in the Graduate School of
The University of Alabama

TUSCALOOSA, ALABAMA

2011

ABSTRACT

Sustainable use of groundwater resources requires a comprehensive understanding of the groundwater flow system, including recharge mechanisms and system dynamics to quantify future availability and variability of groundwater resources in response to climatic conditions (recharge) and human activities (pumping). This dissertation explores sustainability issues in the North China Plain (NCP), a region plagued by one of the worst groundwater overuse and depletion problems globally. The dissertation is organized as three closely related but self-contained papers.

The first paper describes the development of a regional, three-dimensional groundwater flow model, and its application in investigating the overall flow dynamics of the groundwater system across the NCP under both predevelopment and post-development conditions. The output from the groundwater model provides estimates of groundwater depletion rates over the post-development period, which average about 4 km^3/yr. Mean annual groundwater recharge of the overall plain, as estimated through calibration of the groundwater model is ~120 mm, which is in reasonable agreement with previously reported values based on the regional water balance method. Groundwater storage depletion, as estimated from groundwater level fluctuation data and from the numerical simulation is highly correlated with variations in precipitation. The numerical model makes it possible to integrate the available hydrologic data, providing a comprehensive approach to evaluate sustainability of groundwater resources in the NCP. The results show a severe imbalance between groundwater recharge and groundwater extraction (the

primary discharge). Finally, some strategies that have been conducted towards more sustainable groundwater management in the NCP are discussed.

In the work discussed in the second paper, as a way of mitigating the uncertainty inherent in specifying groundwater recharge as a calibration parameter (as commonly done in regional groundwater modeling), a simplified vertical one-dimensional unsaturated zone flow model was coupled with the regional three-dimensional saturated zone flow model. This allows more realistic simulation of the recharge process at the interface between the unsaturated and saturated zones. Soil hydraulic parameters were estimated using pedotransfer functions. Simulation over 12 years (1993–2008) was performed across the NCP. Simulated mean annual recharge ranges from ≤360 mm in the piedmont area to ≤260 mm in the middle and coastal plain areas, with a mean of ~150 mm across the NCP; this figure represents 18% of the average annual precipitation plus irrigation. Variability in soil texture and hydraulic properties is primarily responsible for the large range in simulated recharge rates. Increasing thickness of the unsaturated zone with groundwater depletion was shown to have little effect on long term mean groundwater recharge.

The third paper discusses the application of direct simulation of groundwater mean age using a solute transport model to help calibrate the flow model parameters, including recharge rates. The simulated age distribution and the recalibrated flow model were then used to characterize the flow regime both under natural conditions and under conditions as altered by groundwater pumping. The model results indicate that simulated groundwater age in the NCP is affected both by the paleo-hydrologic conditions and by extensive groundwater pumping. Flow path analysis, water budget calculations, and the simulated groundwater age distribution all

indicate that the lateral flow to the deep aquifer zone in the NCP is limited, and that the primary water input to the deep aquifer zone is downward leakage from the shallow aquifer zone; the extensive pumping of deep groundwater in recent decades has increased this downward flow. These results confirm that regional pumping has altered the flow regime in the deep aquifer zone, and that widely distributed vertical leakage has become a dominant process shaping the flow pattern both in the shallow and deep aquifers of the NCP.

DEDICATION

This dissertation is dedicated to my wife, Dongmei, for her love and support.

LIST OF ABBREVIATIONS AND SYMBOLS

<	Less than
=	Equal
$\Delta\theta$	Change of soil water storage
Δ_p	Slope of the saturated vapor pressure curve
A	Groundwater mean age
α_L	Longitudinal dispersivity
α_V	Vertical dispersivity separately, and the
α_T	Transverse dispersivity
BCs	Boundary conditions
CIGEM	China Institute of Geo-Environmental Monitoring
ET	Evapotranspiration
ET_p	potential evapotranspiration
ET_a	actual evapotranspiration
ET_w	Wet environment evapotranspiration
ε	Brooks-Corey exponent
f_T	Vapor transfer coefficient
HWCC	Hai River Water Resources Commission
IDW	Inverse distance weighting
I_r	Irrigation

Ks	Saturated hydraulic conductivity
$K(\theta)$	is unsaturated hydraulic conductivity
ME	The mean error
NCP	North China Plain
PTFs	Pedo-transfer functions
P	Precipitation
Q_{TP}	Net available energy adjusted to the equilibrium temperature
R_p	Potential recharge to the vadose zone
RH	Relative humidity
RMSE	Root mean square error
SNWD	South-to-North Water Diversion
SRTM	Shuttle radar topography mapping
σ	Stefan-Boltzman constant
θ	Volumetric water content
θ_r	Residual water content
θ_s	Saturated water content
T	Air temperature
T_p	Equilibrium and air temperature
T_{dew}	Dew point temperature
TDS	Dissolved solids
t	Time

WUE	Water use efficiency
z	Elevation in the vertical direction

ACKNOWLEDGMENTS

I would like to thank my research advisor, Dr. Chunmiao Zheng, for his guidance and encouragement during my Ph.D. program. In the past four years, Dr. Zheng has had a significant role in both my scientific and personal development. As a role model to me in the field of hydrogeology, especially groundwater modeling, it is he who taught me that modeling is not just matching observations and simulations, but a way of exploring and understanding the true hydrogeological behavior of a groundwater system.

I also would like to thank Dr. Rona J. Donahoe, Dr. Geoff R. Tick, and Dr. Tim Masterlark for serving as my dissertation committee members and for their valuable comments on my dissertation. Their classes greatly enriched my knowledge base for further study and research.

For her invaluable contribution to my dissertation, I want to give my special thanks to Dr. Bridget Scanlon of University of Texas-Austin. Her constructive suggestions and helpful editing helped me improve my writing and challenged me to become a better hydrogeologist.

For data collection and logistical support, I would like to thank Dr. Jie Liu at Peking University and other colleagues at China Institute of Geo-Environmental Monitoring and China Institute of Water Resources and Hydropower Research. Special thanks are given to China Geological Survey for most of the basic hydrogeologic data for the modeling work.

Finally, I am indebted to my wife Dongmei and my son Yuechuan. They made my life complete and colorful!

CONTENTS

LIST OF TABLES

LIST OF FIGURES

CHAPTER 1

INTRODUCTION

Groundwater sustainability is commonly defined as groundwater development in a manner that can be maintained throughout entire hydrologic system for an indefinite time without causing unacceptable environmental, economic, or social consequences (Alley et al., 1999). It is clear that both groundwater quantity and quality must be considered based on this definition of sustainability. However, sustainability in terms of quantity alone may be studied and evaluated separately, or in advance of, sustainability in terms of water quality, and in fact this is often done in practice. The sustainability of a groundwater pumping activity in terms of quantity alone—i.e., the hydraulic sustainability—is ultimately possible only if a hydraulic balance or equilibrium can be established in the groundwater system under the pumping regime. As pointed out by Theis (1940), a groundwater utilization system is sustainable only when pumping, as an additional discharge term imposed on a natural system which was originally in a state of equilibrium, is balanced by the sum of increases in recharge and decreases in natural discharge. In practical terms, increases in recharge or decreases in natural discharge can rarely be identified, confirmed, or quantified without a detailed analysis of the original flow regime, the regime as it exists under pumping, and the process of transition between them. Again in practical terms, such an analysis and assessment of impact of different groundwater development scenarios can only be done through simulation (Zhou, 2009).

Accurate water balance and information on groundwater dynamics are important bases for assessment of sustainability of groundwater resources at a basin scale (Alley et al., 1999 and

2004). To properly manage groundwater resources, managers need reliable information on inputs (recharge) and outputs (pumpage and natural discharge) within the groundwater basin. As a critical component of the water balance, the groundwater recharge rate and its spatial and temporal variability are essential in any analysis of groundwater systems (Sophocleous, 2005). As one of the most overexploited aquifers in the world (Kendy et al., 2003; Liu et al., 2008), the North China Plain (NCP) aquifer has been subject to very heavy withdrawals since the 1970s (Liu et al., 2001). Since the 1960s many hydrogeological studies have been conducted in the NCP. Most of these studies were designed to evaluate the groundwater system, and to develop an understanding of its evolution in response to pumpage. Against the overall background of serious water shortages and deterioration of ecological systems, groundwater sustainability has become the central concept guiding the development and management of the NCP aquifer system in the 21^{th} century (Zhang, 2003; Zhang et al., 2004; Zhang et al., 2009; Wu et al., 2010).

The North China Plain (NCP) refers to an area in northeastern China, having generally low elevation (altitude of <100 m above mean sea level), and bordered on the north by the Yanshan Mountains, on the east by the Bohai Sea, on the south by the Yellow River and on the west by the Taihang Mountains (Figure 1.1) (Wu et al., 1992). The total area of the NCP as defined is ~140,000 km^2. The NCP covers the entire plains of Hebei Province, Beijing Municipality, Tianjin Municipality, and the northern parts of the plains of Shandong and Henan Provinces. The population of the NCP, based on 2000 state census data, is ~105 million (National Bureau of Statistics of China, 2003) with a population density of ~800 persons per km^2 (Figure 1.2). The NCP is the dominant national center for wheat and maize production and is an extremely important economic, political, and cultural region of China, producing ~15% of

China's total gross domestic product (GDP) and ~ 10% of total grain production based on 2009 statistical data (China Statistical Yearbook, 2010).

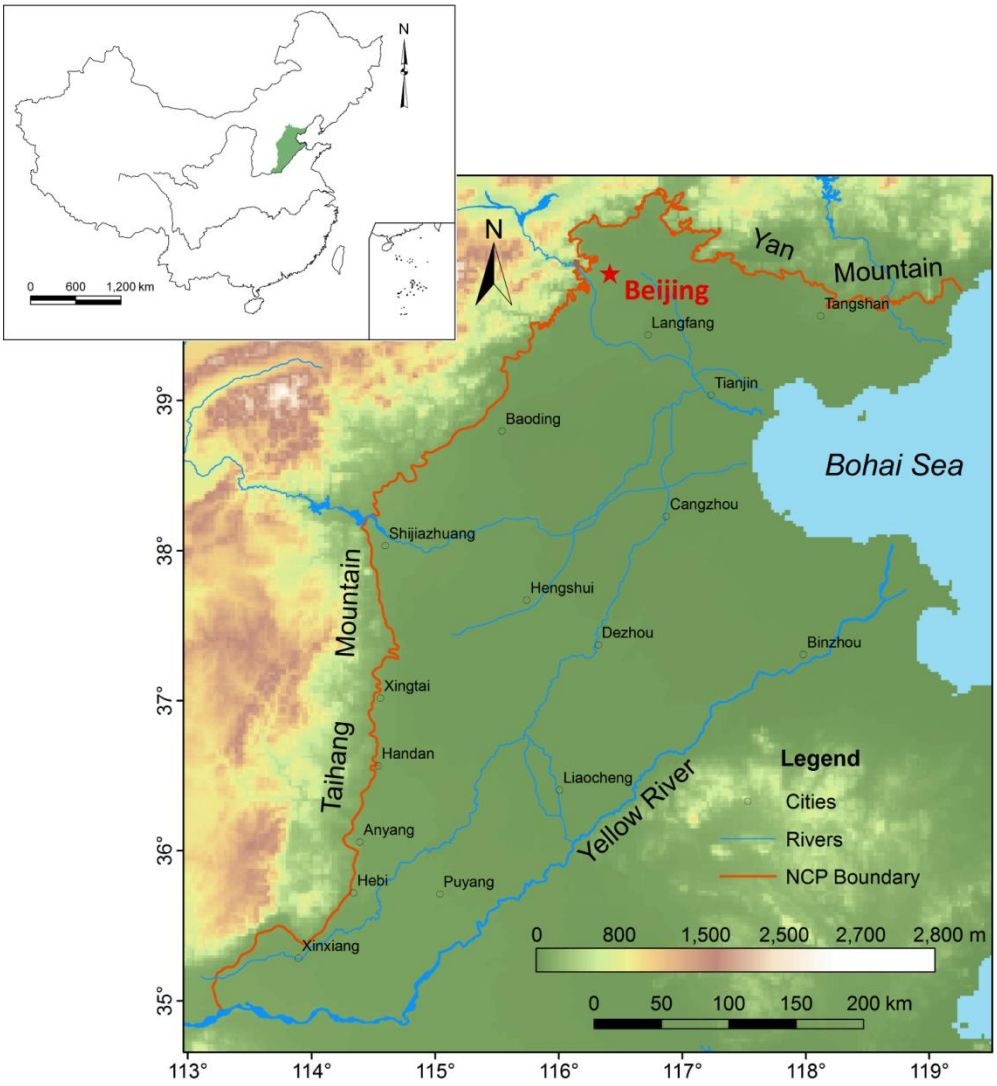

Figure 1.1. Location and topography of the North China Plain.

The factors affecting recharge in the NCP can be divided into two major categories: natural climate fluctuations and effect of human activity. Although mean annual precipitation is 500~600 mm, temporal and spatial distribution is uneven, with 50 to 80% of the total concentrated during the summer monsoon months (July–September), and a generally decreasing

trend from southeast to northwest (Chen, 1999). Superimposed on the seasonal variation, there has been a long-term decrease in mean annual precipitation from ~600 mm in the 1950s to ~ 500 mm in the 2000s (Figure 1.3). Effects of human activity on recharge include changes in the interaction between surface water and groundwater and changes in the groundwater cycling pattern, which in turn may alter both areas and process of recharge. Besides the three main river systems—the Yellow River, the Hai River, and the Luan River, there are nearly 60 small rivers, such as the Tuhai and the Majia Rivers in the NCP. Under natural conditions with little pumping and water table depths ranging from 0–5 m in the central and coastal plain to 1–10 m in the piedmont plain (Zhu and Liu, 1995), these rivers acted primarily as discharge channels of groundwater system. In the early stages of groundwater development, as water levels fell, most of the draining reaches would have been converted to a losing condition, recharging the groundwater system. However, with long-term reduction in precipitation and interception of streamflow by upstream reservoirs, most of the river reaches in the NCP are now dry or carry flow only seasonally. As a result of this, leakage from rivers to groundwater has declined; for example, leakage from the Yellow River decreased by ~50% in 2000 relative to that in 1980 (Fei et al., 2009). Groundwater recharge from sources other than streams leakage, including precipitation and irrigation return flow, and discharge by pumping have become the primary terms in the basin groundwater balance equation.

Previous studies indicated that recharge from infiltration of precipitation accounts for approximately 70–80% of total natural groundwater recharge in the NCP (Chen, 1999; Chen and Ma, 2002). A common approach used in recharge estimation in the NCP is to assume that a certain fraction of precipitation and of the applied irrigation water percolates to the water table, regardless of the quantity applied (Kendy et al., 2003). The percentage of precipitation as

recharge, or “precipitation infiltration coefficient”, was determined for different water table depth and soil property areas, using precipitation and recharge typically calculated using water level fluctuations in the 1980s (Chen, 1999). A data set of irrigation return flow, as percentage of applied irrigation water, was determined in the 1980s, and was updated according to changes in water table depth and irrigation methods. Estimates of annual groundwater recharge from precipitation and irrigation return flow based on this method range from 70 to 180 mm/yr (Zhu and Zheng, 1983; Liu and Wei, 1989; Chen, 1999; Water Resources Department of the Hebei Province, 2003; Ren, 2007). Because the value of the recharge coefficient depends on soil properties, unsaturated zone thickness, and precipitation amount, the recharge coefficient varies spatially and temporally (Li, 2009). These recharge estimates represented long time average values for different periods and did not provide information on recharge variations with time. Moreover, recharge estimation neglecting unsaturated zone flow processes is considered inappropriate in arid regions with thick unsaturated zone (Hunt et al., 2008). As a result of the decades of heavy groundwater exploitation in the NCP, the thickness of the unsaturated zone has increased from 2–15 m in the 1970s to 8–30 m, at present, and up to 30–56 m in some local areas (Zhang et al., 2004). Ignoring unsaturated zone processes and using the recharge coefficients obtained for overly sediments during times of shallow water table could be problematic for estimation of groundwater recharge under current conditions (Zhang et al., 2007). Finally, water level rises used in this method cannot distinguish areal recharge and lateral inflow, which is a significant source of groundwater recharge in the NCP (Kendy et al., 2003).

Many researchers have used environmental tracer methods (Li et al., 2007; Wang et al., 2008; Liu et al., 2009; von Rohden et al., 2010) to estimate local groundwater recharge. Averaging of numerous such local values would then be necessary to obtain a regional recharge

estimates. Some researchers have attempted to estimate recharge by unsaturated zone water budget calculation based on Richards' equation (e.g. Lu et al., 2011). This time consuming method leads to an estimate of recharge at local point characterized by the parameters used in the calculation. However, a large amount of data, including thickness and hydraulic properties of the unsaturated zone, rainfall patterns, irrigation types and regimes, land use, evapotranspiration, etc. would be needed for the number of local calculations to obtain regional recharge estimates. Considering the available data in the NCP, regionalization of point recharge estimates does not seem practical.

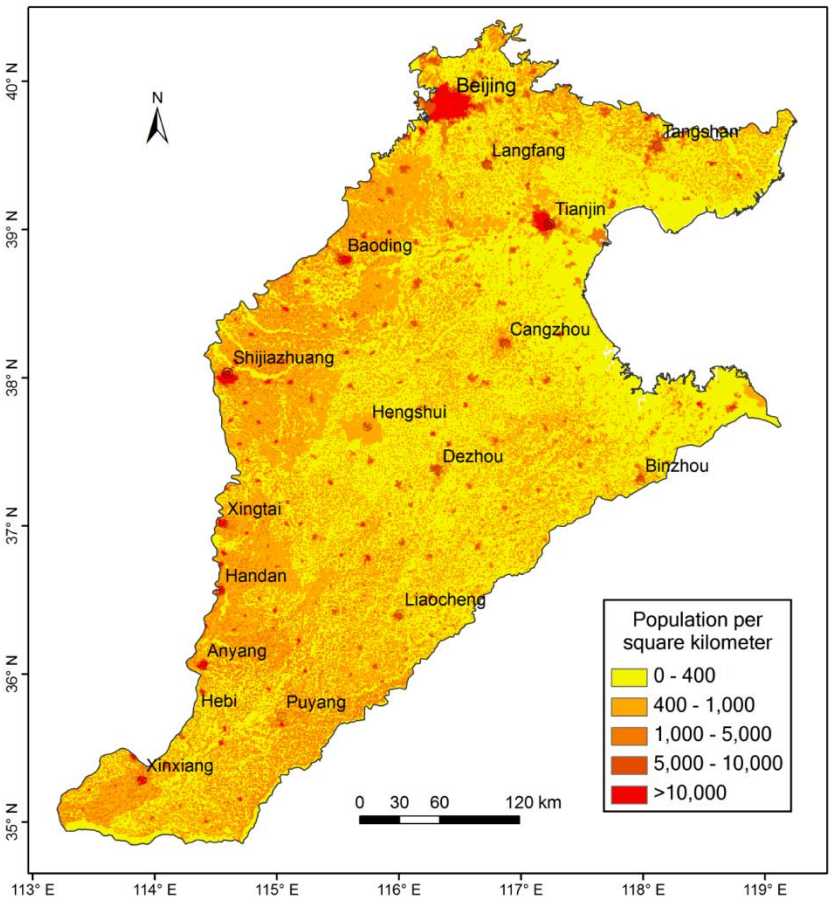

Figure 1.2. Population density in the NCP based on population on 2003.

This dissertation includes three closely related papers using flow model and transport model to estimate the recharge distribution and assess groundwater sustainability in the NCP. The first paper uses a regional multi-layer, three dimensional flow model to simulate both the predevelopment flow regime, and groundwater dynamics during the development of groundwater utilization (1960–2008). The groundwater recharge rate and its spatial and temporal variability were calibrated as the critical model inputs. The results of the regional flow model provide an overall picture of the predevelopment condition of the aquifer system, of the response of that system to intense development, and of the resulting variations of each term of groundwater balance.

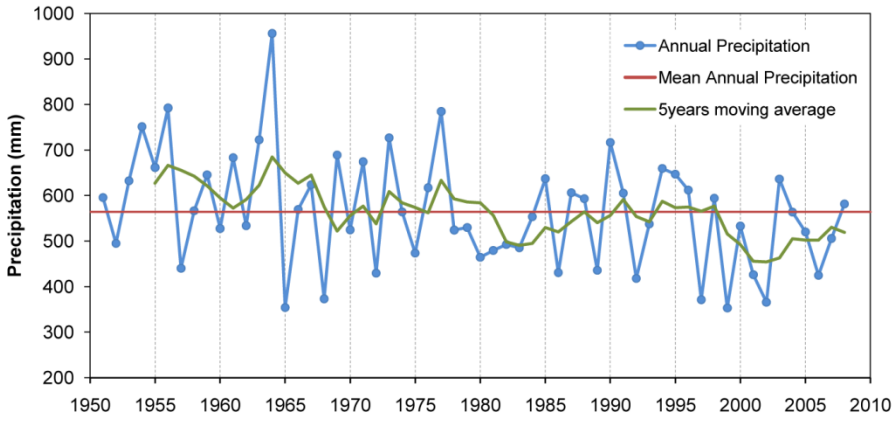

Figure 1.3. Precipitation in the NCP from 1951 to 2008 based on measured precipitation data at 23 meteorological stations across the NCP.

The flow model in the first paper focuses on the saturated zone of the NCP aquifer. The recharge estimated through model calibration depends on the accuracy of the hydraulic parameters and flow data used in the model. However, the available groundwater withdrawals are estimated based on the average water consumption norms (Liu et al., 2004), and accurate groundwater withdrawal information is generally not available. Moreover, because groundwater

no longer discharges to rivers, no flow data available can help to achieve a unique solution for the inverse modeling of recharge. Although this problem has been overcome to some extent by using the same hydraulic parameters verified by previous models, a better method is needed for the reliable recharge estimates.

The second paper introduces an integrated model of the soil water balance and unsaturated flow to estimate groundwater recharge and travel time of water from the land surface to the water table. Actual evapotranspiration, as a critical term in the soil water budget equation, was estimated by a method employing the complementary relationship hypothesis of evapotranspiration. A one dimensional homogeneous unsaturated flow model is used to simulate the delay of recharge through the unsaturated zone, and the required soil hydraulic parameters are estimated using pedotransfer functions. The complexity of the soil-plant system was ignored by using this model construction, and only basic meteorological data and soil data were required as model inputs.

The deep groundwater zone is the primary source of water supply for the central and coastal plains. Recharge to this zone, and renewability of its groundwater, must therefore be considered in any evaluation of sustainable groundwater development (Zhang, 2003; Zhang et al., 2004; Chen et al., 2009). The third paper attempts to calibrate the steady sate flow model in the first stage using isotopic groundwater age, using a mean age transport model. The impacts of assumed paleo-hydraulic conditions and recent decades of intense groundwater pumping are also evaluated. Flow regime alternation is assessed through groundwater dynamics and flow paths analyses. Simulated groundwater age distribution and water budget calculation in the deep aquifer zone are then used to evaluate the sustainability of its groundwater development.

References

Alley, W.M., T.E. Reilly, and O.L. Franke. 1999. Sustainability of ground-water resources. *U.S. Geological Survey Circular* 1186, no. 79.

Alley, W.M., and S.A. Leake. 2004. The journey from safe yield to sustainability. *Ground Water* 42, no. 1: 12-16.

Chen, W. 1999. Groundwater in Hebei Province. Beijing: Seismological Press.

Chen, M., and F. Ma. 2002. Groundwater Resources and the related Environment in China. Beijing: Earthquake Press. (in Chinese)

Chen, Z., H. Gao, W. Wei, J. Chen, F. Zhang, and Y. Wang. 2009. Groundwater Renewal and Characteristics in the Deep Confined Aquifer in North China Plain. *Resources Science* 31, no. 3: 388-393. (in Chinese with English abstract)

Fei, Y., J. Miao, Z. Zhang, Z. Chen, H. Song, and M. Yang. 2009. Analysis on Evolution of Groundwater Depression Cones and Its Leading Factors in North China Plain. *Resources Science* 31, no. 3: 394-399.

Kendy, E., P. Gérard-Marchant, M.T. Walter, Y. Zhang, C. Liu, and T.S. Steenhuis. 2003. A soil-water-balance approach to quantify groundwater recharge from irrigated cropland in the north china plain. *Hydrological Processes* 17, no. 10: 2011-2031.

Li, J. 2009. An analysis of the coefficient of replenishment from infiltration of precipitation. *Hydrogeology & Engineering Geology* 2: 29-33.

Liu, C., and Z. Wei. 1989. Agricultural Hydrology and Water Resources in the North China Plain. Beijing: Science Press. (in Chinese)

Liu, C., J. Yu, and E. Kendy. 2001. Groundwater exploitation and its impact on the environment in the north china plain. *Water International* 26, no. 2: 265-272.

Liu, H., G. Wang, and Y. Zhu. 2004. A discussion of methods of investigation and check of groundwater withdrawal. *Hydrogeology and Engineering Geology* 5: 109-111.

Liu, J., C. Zheng, L. Zheng, and Y. Lei. 2008. Ground water sustainability: methodology and application to the north china plain. *Ground Water* 46, no. 6: 897-909.

Lu, X., M. Jin, M.T. van Genuchten, and B. Wang. 2011. Groundwater Recharge at Five Representative Sites in the Hebei Plain, China. *Ground Water* 49, no. 2: 286-294.

Sophocleous, M. 2005. Groundwater recharge and sustainability in the high plains aquifer in kansas, usa. *Hydrogeology Journal* 13, no. 2: 351-365.

Theis, C.V. 1940. The source of water derived from wells. *Civil Engineering* 10, no. 5: 277-280.

von Rohden, C., A. Kreuzer, Z. Chen, R. Kipfer, and W. Aeschbach-Hertig. 2010. Characterizing the recharge regime of the strongly exploited aquifers of the North China Plain by environmental tracers. *Water Resources Research* 46, no. 5: W5511.

Wu, A., C. Li, Y. Xu, J. Liu, and G. Luo. 2010. Key Issues Influencing Sustainable Groundwater Utilization and Its Countermeasures in North China Plain. *South-to-North Water Transfers and Water Science & Technology* 6: 110-113.

Wu, Z., X. Chen, and Q. Xu. 1992. Natural environment evolution on the North China Plain over past 40000 years. Beijing: China Science & Technology Press. (in Chinese)

Zhang, R. 2003. Characteristics of groundwater resources and their reasonable development. *Hydrogeology and Engineering Geology* 6: 1-5. (in Chinese with English abstract)

Zhang, G., Y. Fei, J. Shen, and L. Yang. 2007. Influence of unsaturated zone thickness on precipitation infiltration for recharge of groundwater. *Journal of Hydraulic Engineering* 38, no. 5: 611-617. (in Chinese with English abstract)

Zhang, R., X. Liang, and M. Jin. 2004. On researches and practices in hydrogeology and environmental geology for sustainable development. *Hydrogeology and Engineering Geology* 1: 82-86. (in Chinese with English abstract)

Zhou, Y. 2009. A critical review of groundwater budget myth, safe yield and sustainability. *Journal of Hydrology* 370, no. 1-4: 207-213.

Zhu, Y., and S. Liu. 1995. Groundwater dynamic environment evolution and its constraints in hebie plain. *Journal of China University of Geosciences* 4: 433-437. (in Chinese with English abstract)

Zhang, Z., G. Luo, Z. Wang, C. Liu, Y. LI, and X. Jiang. 2009. Studyon Sustainable Utilization of Groundwater in North China Plain. *Resources Science* 3: 355-360. (in Chinese with English abastract)

CHAPTER 2

USE OF GROUNDWATER MODELING TO ASSESS SUSTAINABILITY OF GROUNDWATER RESOURCES IN THE NORTH CHINA PLAIN

Abstract

Intensive groundwater development across the Quaternary aquifer of the North China Plain (NCP) has caused a general, long-term trend of depletion in groundwater storage in both shallow unconfined and deep confined aquifer zones, adversely affecting the environment and ecosystems, including drying-up of rivers, land subsidence, seawater intrusion, and groundwater quality deterioration. The concern is that the severe groundwater depletion will diminish groundwater supplies and then impact the regional economy and social development. The objective of this study was to evaluate spatial and temporal variability in groundwater depletion using groundwater modeling. This study is a major component of a comprehensive regional groundwater depletion analysis and quality evolution in the NCP with the purpose understanding long term effects of human activates and alternative land use on groundwater changes. A numerical groundwater flow model was developed for the NCP and was calibrated for both predevelopment (1960s) and post-development (1960s–2008) conditions. Initial recharge estimates and hydraulic parameters were derived from the literature and recharge was modified through calibration. Steady state flow model presenting the natural condition was calibrated using water level contours in 1959. Transient flow model for the post-development period was calibrated using water level contours in 1975, 1984, 2001 and 105 and 72 annual water level time series from 1993 through 2008 in the shallow and deep aquifers, respectively. Model output

indicates that mean groundwater depletion was ~4 km^3/yr from 1970 through 2008. Mean annual groundwater depletion was ~2.5 in the 1970s, and increased to ~4.0 km^3 in the 1980s. The mean depletion rate was ~2.0 km^3/yr in 1990-1996; in this period the precipitation show an increasing trend. The mean depletion rate was ~5.0 km^3/yr in 1997–2008, which is the period with smallest precipitation. Groundwater level hydrograph data from 117 time series were used to detect the seasonal variation in groundwater storage, and indicate that aquifer depletion occurs mostly in the spring. Mean annual simulated recharge is ~120 mm/yr and is focused in the Piedmont plain (200–350 mm/yr) and much lower in the central and coastal plain areas (50–100 mm/yr). Integrating all available data through groundwater modeling provides a comprehensive approach to evaluate sustainability of groundwater resources, and the model constructed can be used to examine potential sustainability strategies to be conducted in the NCP.

2.1. Introduction

Groundwater is a crucial source of water for agricultural, industrial and environmental uses as well as for drinking water supply due to its generally good quality and widespread occurrence. At present, groundwater contributes about 20% of people's fresh water globally (Kinzelbach et al., 2003), and estimated total groundwater withdrawals range from ~750 to 800 km^3/year (Shah et al., 2000). Groundwater exploitation has facilitated economic development and food production. For example, from 1961 to 2004, global crop yield per area increased by a factor of 2.3 and total crop yield increased by a factor of 2.4 (Oki and Kanae, 2006); these increases would not have been possible without major increases in irrigation, a significant share of which came from groundwater. However, the severe consequences of over exploitation of groundwater are well known, e.g. groundwater depletion, groundwater quality deterioration,

ecosystem degradation, and in some cases land subsidence or sea water intrusion (Sophocleous, 2002; Konikow and Kendy, 2005; Fogg and LaBolle, 2006). During the past 50 years, excessive groundwater depletion has become a global problem, affecting major regions of North Africa, the Middle East, South and Central Asia, North China, North America, and Australia (Shah et al., 2000; Shah et al., 2003; Konikow and Kendy, 2005). The North China Plain is one of the prime examples of this problem (Alley et al., 2002).

Groundwater sustainability is commonly defined as groundwater development in a manner that can be maintained for an indefinite time without causing unacceptable environmental, economic, or social consequences (Alley et al., 1999). Groundwater depletion refers to sustained loss of groundwater from storage (Hurd et al., 1999; Kinzelbach et al., 2003). As discussed by Theis (1940), some loss of water from aquifer storage always occurs in response to any increase in withdrawal from wells. If pumping is initiated in a previously untapped aquifer, the storage loss will continue until the natural discharge from the aquifer is decreased, and/or the original recharge rate to the aquifer is increased, by amounts which sum to the total pumping. At that point a new equilibrium prevails, in which the pumping replaces the natural discharge that has been lost and accounts as well for any increase in recharge that has occurred. If the aquifer is initially in use but the pumping rate is increased, the same principle apply, except that a new equilibrium will not be attained until the total initial discharge has decreased and/or the recharge has increased, by amounts which sum to the increase in pumping. Should the pumping be increased by an amount which exceeds the sum of the total reduction in initial discharge and the total increase in recharge which can be achieved, storage loss will continue until ultimately falling water levels will force a reduction in pumping rate.

Persistent, multi-year declines of water level are usually an indication that pumping has in fact reached levels that cannot be balanced by the increases in recharge and decreases in prior discharge which are possible in the aquifer, and thus that the level of pumping is not sustainable. However, careful analysis of the initial flow regime, the changes imposed to date by pumping, and the changes likely under continued pumping are generally needed to confirm this interpretation. These analyses are usually done with the help of flow simulation. Reasonable information on the components of the water budget and the characteristics of the flow regime at the various stages of aquifer utilization can only be gained through flow simulation. Sustainability assessments depend on such information, and must consider areas and periods of unevenly distributed pumping and recharge fluctuation with time (Alley et al., 1999, 2004; Foster, 2000). Given the complexity and heterogeneity of aquifer systems, and the ability of numerical modeling to integrate different data and to evaluate regional groundwater dynamics, simulation is clearly an excellent tool for use in sustainability assessments (Luckey and Becker, 1999; Kinzelbach et al., 2003; Konikow and Kendy, 2005; Welsh, 2006).

In the North China Plain (NCP), several numerical models have been built to evaluate groundwater resources and flow dynamics. However, none of these models appears suitable for evaluation of the water balance and the impact of groundwater development across the entire NCP. Some were developed to assess groundwater budget during predevelopment (Zhang et al., 2008), or to evaluate flow dynamics over a relatively short period after the groundwater had been highly developed (Wang et al., 2007, 2008; Shao et al., 2009). Those models that did have relatively long simulation periods focused primarily on the shallow part of the aquifer system (Zhang, 2007; Cui et al., 2009; Xue et al., 2010); however, the deep part of the aquifer system plays an important role in water supply. Additionally, many of the existing models were

restricted to local areas of the NCP (Jia and Liu, 2002; Xie et al., 2002; He et al., 2003; Shao et al., 2003; Hu et al., 2010).

A further limitation of most existing models is that groundwater recharge is calculated by multiplying precipitation by a coefficient which is taken constant over time; this approach does not allow simulation of the impacts of water level decline on recharge. The objective of this study was to develop a numerical groundwater flow model for the entire NCP for both predevelopment (1960s) and post-development (1960s–2008) conditions. Groundwater recharge was varied to match steady state and transient groundwater level data. The calibrated flow model provides a tool for comprehensive assessment of long-term large-scale groundwater balance and sustainability issues.

2.2. Study Site and Hydraulic Data

2.2.1. Study Site

The North China Plain (NCP) as defined in this study ranges the Yanshan Mountains in the north, the Bohai Sea on the east, the Yellow River in the south and the Taihang Mountains on the west (Figure 2.1). Some studies define the NCP as extending to the Huaihe River in the south (Song et al., 2010). The total area of the NCP as defined is ~140,000 km^2. The NCP covers the entire plains of Beijing Municipality, Tianjin Municipality and Hebei Province, and the northern parts of plains of the Shandong and Henan Provinces. The population of the NCP, based on 2000 county census data, is ~105 million (National Bureau of Statistics of China, 2003). The average population density is ~800 persons per km^2, ranging from to ~ 400 persons per km^2 in rural areas to ~12,000 persons per km^2 in the Beijing City urban area. The region accounts for ~15% of

China's total gross domestic product (GDP) and ~ 10% of total grain production based on the 2009 statistical data (China Statistical Yearbook, 2010).

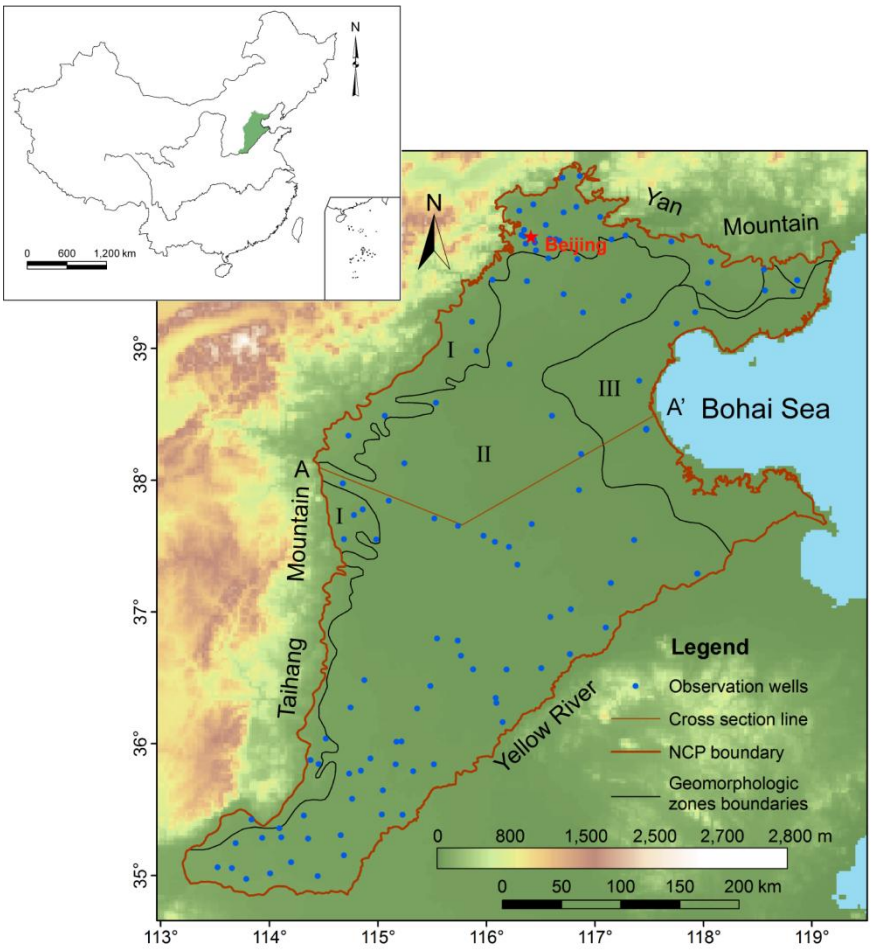

Figure 2.1. Location and topograph of the North China Plain. (1) Boundaries of geomorphologic zones (Wu et al., 1996) of (I) piedmont plain; (II) alluvial fan and flood plain and (III) coastal plain. (2) A-A' line of cross section in Figure 2.2; and (3) Locations of observations wells used in water level analysis model calibration.

The NCP is divided into four main hydrogeological zones from the Taihang Mountains on the west to the Bohai Sea on the east; these zones are based on the geomorphology of

palaeochannels, in the sense that geomorphology has defined their sedimentary character and relative geographic positions, as piedmont plain, alluvial fan, alluvial plain, and coastal plain (Wu et al., 1996). In turn the sedimentary character and geographic position have determined the geohydrologic rules of the four zones: mountain and piedmont plain as the groundwater recharge zone, parts of the alluvial plain and coastal plain as the regional groundwater discharge zone, and the alluvial fan and part of the alluvial plain as an intermediate zone (Chen et al., 2004). The alluvial fan and alluvial plain, which were formed through the depositional process of the Yellow River, Haihe River, Luanhe River and their tributaries (Wu et al., 1996; Xu et al., 1996) constitute the main part of the NCP. The topography is relatively flat with an average elevation of ~ 30 m a.s.l and slopes from ~100 m a.s.l, at the base of the Taihang Mountians in the west, to sea level at the coast (Figure 2.1). The piedmont are is the primary area of grain production in the NCP, where the percentage of wheat cultivation area is much higher than the mean value across the NCP and most of irrigation is from groundwater (Zhang et al., 2010). According to data on crop water deficit from 1990 to 2000, the volumes of groundwater consumed by the wheat and maize are ~5,000 and ~3,000 m^3/ha in the piedmont plain and central plain, respectively (Xu et al., 2005).

The climate in the NCP is continental semi-arid, with mean annual temperature of 12–13 ℃ and mean annual precipitation of 400-700 mm (Chen, 2003). Precipitation, influenced by the East Asia monsoon, decreases from southeast to northwest, and ~70–80% of precipitation occurs during the monsoon season from June through September (Chen, 1999). Mean annual precipitation was ~560 mm from 1951 to 2008, and decreased from ~600 mm in the 1950s to ~500 mm in 2000s based on the precipitation at 23 meteorological stations available from the China Meteorological Administration (http://cdc.cma.gov.cn, accessed in January 2011). Mean

annual pan evaporation ranges from 1,100 to 2,000 mm (Chen, 2005), as measured using 20 cm diameter evaporation pans.

Winter wheat and summer maize are the main crops in the NCP rotation system, accounting for ~80% of total cultivated area and ~90% of grain yield based on statistical data from 2009 (China Statistical Yearbook, 2010). Winter wheat is sown at the beginning of October and harvested in mid-June the following year, and summer maize is planted immediately after wheat harvest and harvested at the end of September the same year. Long-term lysimeter measurements show that annual water consumption of the two crops without water deficit exceeds precipitation by ~300 mm in the Piedmont area (Liu et al., 2002). The monsoon season coincides with the growing season of maize, whereas only 20–30 % of annual precipitation falls during the wheat growing season (Liu et al., 2001). As a result, supplemental irrigation is required for the two crops, especially for production of winter wheat. In recent years, groundwater has provided ~70% of the total water supply to support grain production and ~50% of the total urban water supply (Han, 1998); 70–80 % of groundwater exploitation is used for irrigation (Zhang et al., 2009, 2010).

The Quaternary aquifer of the NCP is traditionally divided into two aquifer zones referred as the “shallow” and “deep” (Fei, 1988). Extensive groundwater exploitation from the two aquifer zones has greatly impacted the hydrodynamic and hydrogeochemical system and caused many environmental problems, such as groundwater depletion, groundwater contamination and salinization, and land subsidence (Liu et al., 2001). Among these problems, continuing groundwater depletion in both shallow and deep aquifer zones is a common concern. Recent field investigations and water level monitoring data have shown that: (a) the maximum water table depth in the shallow aquifer has reached 65 m, and the area with the water table

declines ≥10 m below the land surface is ~62,000 km^2, or ~45% of the entire plain; and (b) the maximum depth to potentiometric surface in the deep aquifer has increased to 110 m, and the area with the water table or potentiometric surface elevation less than the sea level is ~ 88,000 km^2, covering ~70% of the entire plain (Fei et al., 2009).

2.2.2. Hydraulic Data

Data availability in the study area was an important consideration in the selection of methods to evaluate sustainability of groundwater resources in the NCP. The most direct approach to the monitoring of groundwater storage change is to use groundwater level monitoring data, multiplying the water table elevation change by the specific yield and the map area affected (Konikow and Kendy, 2005). Historical groundwater level data were collected by the China Institute of Geo-Environmental Monitoring (CIGEM). The data set includes 230 monthly water level monitoring time series from 1993 to 2008 obtained from 178 monitoring wells (in which 38 wells are multilevel) belonging to the national groundwater level monitoring network (http://www.cigem.gov.cn, accessed in January 2011). The distribution of wells monitored in this study was fairly sparse, especially in some parts of the central plain and coastal plain, where there are relatively few wells in the shallow aquifer zone because shallow groundwater is brackish and not potable.

In addition to the groundwater level monitoring data set, several series of historical water level contour maps were available from the China Geological Survey (CGS): maps of the shallow aquifer zone were available for 1959, 1984, 2001, 2002 (Zhang and Fei, 2009); maps of the deep aquifer zone were available for 1980, 2001, 2002,2003,2004 (Zhang and Fei, 2009); maps of each aquifer zone in the Hebei Plain were available for 1959, 1975, 1985, 1992 (Zhang et al., 2000); and a map of the deep aquifer zone in the Hebei Plain was available for 1969

(http://water.cgs.gov.cn, accessed in January 2011). The groundwater level monitoring data set and these historical ground water level contour maps were used to estimate groundwater storage change and to calibrate the flow model. Although the available water level monitoring time series did not cover the entire period since the beginning of groundwater development, they were the best available data at measurement frequencies sufficient for the estimation of monthly and seasonal changes in groundwater storage, and were therefore utilized for that purpose.

Hydraulic conductivity, specific yield, and storage coefficient are the principal hydraulic parameters in the NCP. Investigation work to estimate the hydraulic parameters across the NCP began in the 1970s, and most of parameters were estimated in the 1980s (Chen, 1990). The hydraulic conductivity, specific yield, and storage coefficients were estimated using pumping test data. No detailed information from these pumping tests was collected in this study, but values of these hydraulic parameters were summarized for the different lithologies across the NCP by Chen (1999) and Zhang et al. (2009). Horizontal hydraulic conductivity of gravel generally ranges from 150–700 m/d and 50–100 m/d in the shallow and deep aquifer zones, respectively. Horizontal hydraulic conductivity of sand generally ranges from 5–200 m/d and 5–60 m/d in the shallow and deep aquifer zones, respectively. Specific yield ranges from ~3 % for clay to ~30 % for gravel. Storage coefficient in the deep aquifer zone decrease from 0.001–0.008 in the alluvial plain to 0.0004–0.0005 in the coastal plain. Horizontal hydraulic conductivity, specific yield, and storage coefficients were mapped across the entire NCP by the CGS (Zhang et al., 2009). The mapped hydraulic parameters had been verified by several modeling studies in the NCP (Wang et al., 2007, 2008; Shao et al., 2009; Zhang et al., 2009), and were not adjusted during model calibration in this study.

2.3. Groundwater Storage Change from Water Level Change

The groundwater level contour map for 1959 was used to calculate the initial groundwater in storage in the NCP. The bottom elevation of the Quaternary aquifer across the NCP is not clearly defined because most boreholes do not penetrate the entire section of Quaternary strata (Zhang et al., 2009). The saturated thickness used to estimate the initial storage was calculated by subtracting a contour map interpolated from the bottom elevation of the boreholes from the water level contour map. All historical water level contour maps were digitized and then converted to a grid using 2 ×2 km cells, which is the same grid scale as was used in the flow model. Groundwater level changes in the shallow aquifer zone were converted to storage changes by multiplying by the specific yield across the NCP (Zhang et al., 2009). Cumulative groundwater storage change and changes were then estimated using historical water level contour maps and the more recent monitoring time series.

The primary challenge for estimating groundwater storage changes using water level changes directly in the NCP is accounting for significant gaps in the groundwater level monitoring time series. The estimated storage change would be highly questionable if these gaps were retained in the calculation process. Preliminary tests showed that different gap filling regression methods resulted in large variations in estimated groundwater depletion. In this study, instead of using a regression method to fill the gaps, two groundwater level contour maps were first generated by inverse distance weighting (IDW) interpolation using monitoring locations where both monitoring data in the two date sets were available, then the groundwater level change was calculated. Based on the data obtained from 22 pumping tests, the mean storage coefficients of the deep aquifer is 0.00125, which is approximately 2% of the area weighted specific yield of the shallow aquifer (Chen, 1999). Therefore, the amount of groundwater

depletion in the deep aquifers is much less than that in the shallow aquifer, and is ignored in the storage change calculation. A total of 117 monitoring wells located in the shallow aquifer were used to calculate groundwater storage change.

2.4. Simulation of the Groundwater Flow System

2.4.1. Conceptual Model of the Groundwater Flow System

In the first regional hydrogeological survey conducted in 1970s (Hebei Bureau of Geology and Mineral, 1977), the Quaternary aquifers in the NCP were divided into four major aquifer units (I, II, III and IV; Figure 2.2). The geologic units corresponding to these aquifers are Holocene series (Q_4), and late (Q_3), middle (Q_2) and early (Q_1) Pleistocene series (Zhang et al., 2009; Foster, 2004). The shallow aquifer zone, as used in this study, corresponds to the first and second aquifer units as defined in the earlier work; the deep aquifer zone, as used here, corresponds to the third and fourth units of the earlier classification. A total of 38 multilevel monitoring wells in the CIGEM monitoring nests show a pervasive downward hydraulic gradient and a generally increasing trend in the magnitude of that gradient with time. The magnitude of the vertical hydraulic gradient ranges from a minimum of 0.04 in areas with little pumping to a maximum of 0.3 within cones of depression. No detailed information on depths of pumping wells is available for the NCP. To simplify model construction, groundwater flow was assumed to be horizontal in each separate aquifer, and rates of flow exchange between aquifers were simulated explicitly by the model.

Precipitation is the dominant source of groundwater recharge in the NCP; other sources of natural recharge include lateral flow from the Taihang and Yan mountains and leakage from the lower reach of the Yellow River. Mountain front lateral flow is a significant source of

recharge, but is not well understood or quantified (Kendy et al., 2003). Recharge rates from lateral flow, used in previous regional water resource evaluations, ranged from 1.0 to 2.0 km^3/yr (Zhu et al., Assessment of Groundwater Source in North China Plain, unpublished report, 1990; Zhang et al., 2009), and were assumed to be restricted to the shallow aquifer (Liu and Wei, 1989). Some researchers made measurements of percolation rates at a number of selected sites along the Taihang Mountain front (Chen et al., 2003; Li et al., 2007; Song et al., 2007). A limitation of the approach is that the total surface area undergoing recharge must be estimated to calculate regional recharge rates. The amount of lateral flow from the mountain area depends on the horizontal permeability, thickness of the saturated zone, and local hydraulic gradient. Estimated mountain front recharge using Darcy's law based on water level contour maps in this study is 2.8, 2.1 and 3.1 km^3 in 1959, 1984, and 2001, respectively.

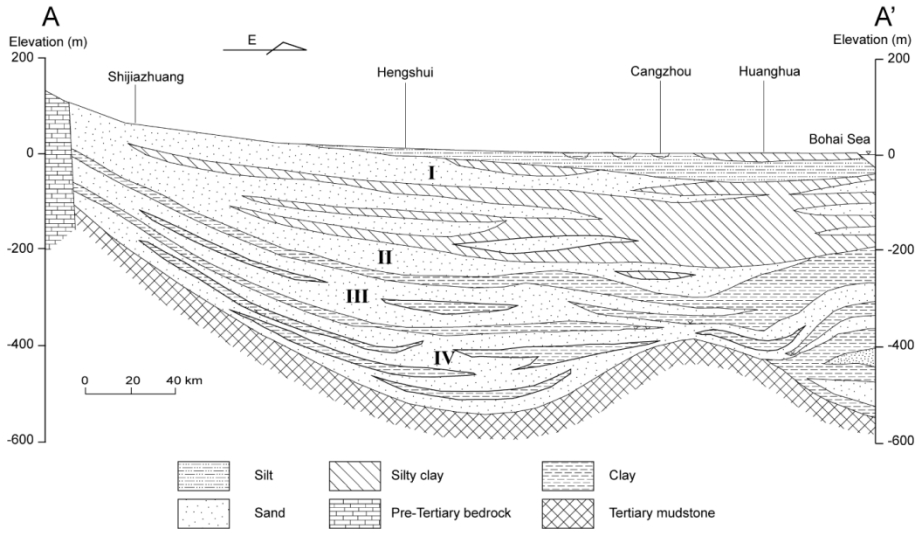

Figure 2.2. Hydrogeological cross section of the NCP along A-A' in Figure 2.1 (modified from Chen et al., 2005).

The lower reach of the Yellow River, flowing from the Taohuayu to the Bohai Sea, serves as the south boundary of the NCP defined in this study. In this section, accumulated sediment deposits have raised the riverbed several meters higher than the grounds, forming "above-ground river". Leakage from this reach of the Yellow River to the NCP was estimated to have decreased from ~0.6 km^3/yr in the 1980s to ~0.4 km^3/yr in the 1990s (Jiao et al., 2005; Ma et al., 2005) because of the severe cutoff of the lower reach in the 1990s (Cai and Rosegrant, 2004; Liu and Xia, 2004). Analyses of groundwater dynamics and isotope data indicate that the area affected by seepage from the Yellow River is limited to 10–20 km wide (Zhao et al., 2003). More than 1,000 reservoirs have been constructed in the NCP since 1950s; these reservoirs control over 90% of the upstream area. Due to overdevelopment of surface water and precipitation decreasing, the runoff in the NCP has shrunk significantly and the leakage to groundwater is limited.

Groundwater is the primary source of water for irrigation in this area (Zhang et al., 2003), and the area irrigated by groundwater accounts for ~70% of the total irrigation area (Liu et al., 2004). The other ~30% irrigation water is derived from upstream reservoirs and the Yellow River by canals. Irrigation return flow is significant because furrow irrigation and flood irrigation are still the primary irrigation techniques applied both for irrigated area using surface water and area using groundwater (Jiang et al., 2009). Detailed information about irrigation areas and applied amount is not available. In this study, natural recharge from precipitation and recharge from irrigation return flow was estimated as total recharge through model calibration. Therefore, the results should reflect recharge from the sum of precipitation and total irrigation, whether the irrigation is originally derived from surface water or groundwater. Using classical groundwater model calibration or inverse modeling to estimate recharge from information on water levels and

hydraulic conductivity may lead to non-unique results (Scanlon et al., 2002) due to the high correlation between recharge rate and hydraulic conductivity. In this study, most of the hydraulic conductivities were obtained from pumping tests and had been verified by previous studies. Therefore, the hydraulic parameters were assumed to be representative, and recharge rates were the primary calibration parameters.

Natural discharge from the NCP aquifer occurs as discharge to streams, evapotranspiration from the water table in areas of shallow depth and diffuse groundwater flow across the eastern boundary of the shallow aquifer zone to the Bohai Sea. Runoff data are unavailable for streams during predevelopment. In the steady state flow model constructed for the predevelopment by Zhang et al. (2008), river (RIV) package of MODFLOW was used to estimate the discharge to streams by mean monthly stream stages in 1965. Natural discharge to streams during predevelopment was estimated ~9.0 km^3/yr by this method; this estimate provided water budget information helping to calibrate the steady state model in this study. Little is known about the discharge to the Bohai Sea, but the amount is thought to be small because the hydraulic conductivity is relatively small for the coastal aquifer and because the horizontal hydraulic gradient in the coastal plain is quite low.

Artificial discharge from the aquifers in the NCP occurs as pumping by numerous wells. The volumes of groundwater discharge through pumping are shown in Figure 2.5. The 1970s was the time of most rapid agricultural development in the NCP, and is the period of most rapidly increasing groundwater pumpage. In the 1980s and 1990s, groundwater pumping still increased, but at a relatively slow rate, as agricultural and industrial development continued. Since the beginning of 2000, environmental problems caused by excessive exploitation of groundwater have focused attention on environmental problems, and agricultural water saving

measures have been promoted; as a result, groundwater pumping has shown a slight decreasing trend (Zhang et al., 2009).

2.4.2. Flow Model Construction

A multi-layer, heterogeneous and anisotropic model was built to simulate the flow system in the NCP using MODFLOW-2000 (Harbaugh et al., 2000). The SRTM (Shuttle Radar Topography Mission) (Rabus et al., 2003) elevation data at 90 m resolution were aggregated to the model grid and used as the model top elevation. Borehole data were not obtained in this study. As an alternative, four aquifer units' bottom elevation contour maps were digitized and then interpolated into the model grid as needed by the layer-property flow (LPF) package (Harbaugh et al., 2000) of MODFLOW.

The finite discrete grid consisted of 325 rows and 300 columns, with a regular cell size of 2 ×2 km. In the three-dimensional reconstruction of the aquifer system, the model grid was discretized into three layers, rather than into the four layers as identified in the conceptual model. Aquifer units I and II were combined and represented by the first layer of the grid. One reason for doing this is that aquifer units I and II are highly connected hydrologically in the piedmont area and in depression cones due to pumping wells' penetrating the two units. Moreover, during the post-development period, parts of aquifer unit I in the piedmont area became dry. If a separate layer had been used to represent this unit, MODFLOW would have made the wells located in this layer invalid automatically, and the distribution of total pumping would be problematic. A different number of active cells were used in each layer to represent their distinct areal extent. Layer 1 (shallow aquifer zone) has 34329 active cells, layers 2 and 3 (deep aquifer zone) 32451 cells each. The flow model first simulated steady state flow based on the 1959 water level data set and then simulated post-development from 1960 through 2008. The transient model

was divided into 49 stress periods of one year each. Pumpage and other source/sink terms were considered to be constant in each stress period.

The definition of a set of appropriate boundary conditions (BCs) for each layer was part of the model calibration process considering the actual magnitude and direction of flow across the boundaries. Combinations of specified-head and specified-flow boundaries were set for layer 1. A specified-head boundary was defined along the eastern boundary, coincident with the coastline of the Bohai Sea, assuming the shallow aquifer zone is hydraulically connected with the sea. Specified-flow was used in all parts of the boundary between the mountain area and the plain to represent the lateral flow from the Yan and Taihang Mountains assuming that lateral flow only occurs in the shallow aquifer zone. To simplify the process of model construction and calibration and considering the available data, the southeast boundary along the Yellow River was also defined as a specified-flow boundary. Boundaries for layer 2 and 3 were assumed no-flow.

The spatial distribution and application times of irrigation were unknown. Considering that the total recharge is the primary concern and goal of this study, as mentioned previously, recharge from precipitation and irrigation return flow (including irrigation from surface water and groundwater) were combined to represent the total areal recharge. At present, more than 40% of the river channels have dried up or become seasonal streams, and the area of wetlands has shrunk from 10,000 km^2 in 1950s to ~ 2,000 km^2 (Xia, 2006). Mean annual discharge to the rivers from 1980 to 2000 is ~0.032 km^3 (Ren, 2007), which is much less than pumpage. Therefore, rivers were not simulated explicitly in this study, and discharge rates were combined with the pumpage.

Statistical pumpage data were available from 1980 through 2008 (Hai River Water Resources Commission (HWCC), Haihe Basin Water Sources Bulletin 1998-2008, http://www.hwcc.gov.cn, accessed in January 2011; Beijing Water Authority, Beijing Water Sources Bulletin 2003-2008, http://www.bjwater.gov.cn, accessed in January 2011; Tian Water Authority, Tianjin Water Sources Bulletin 2002-2008, http://www.tjsw.gov.cn, accessed in January 2011; Water Resources Department of Hebei Province, Hebei Water Sources Bulletin 2000-2007, http://www.hbsw.net, accessed in January 2011; Water Resources Department of Shandong Province, Shandong Water Sources Bulletin 2003-2008, http://www.sdwr.gov.cn, accessed in January 2011; *Ren*, 2007; *Zhang et al*., 2009). In the NCP, the volume of groundwater pumped for irrigation per metric ton of grain production was approximately 450 m^3 based on total groundwater pumpage and total grain yield statistical data from 1980 through 2008. Total groundwater pumpage before 1980 was estimated based on total grain yield assuming that number to be applicable over the entire NCP. The groundwater exploitation data collected in this study were annual pumpage figures at province-level; thus it was necessary to redistribute this pumpage data to active cells of the model. The planting area for wheat and corn covers approximately 50% of the total land area and 70% of the total cultivated area (Xu et al., 2005; Han et al., 2008). In 2000, a total number of 835,370 wells were used over the Hebei Province, which means ~ 4.4 wells/km^2 (Zhang and Li, 2005); thus the withdrawal from each model cell should represent the discharge from more than 16 pumping wells. This was achieved in the simulation by locating one "virtual" pumping well in each active model cell, which accounted for all the simulated withdrawal in that cell. To simplify the model input process, all recharge terms in each cell in layer 1 were converted into volume rates and combined together

with the pumping in that layer into one term; this term and pumping in the other two layers were input into the model through the well (WEL) package.

Evaporation from the water table was simulated by the linear segmented evapotranspiration (ETS) package which uses a user-defined segment line to conceptualize the relationship between water table evaporation and hydraulic head (Banta, 2000). Compared with the evapotranspiration (EVT) package, the ETS package can more closely represent the actual nonlinear relationship between evapotranspiration and water table depth (Doble et al., 2009). Evaporation extinction depth was assigned to 4 m uniformly across the plain, and the potential evapotranspiration calculated using the Pemnan-Monteith equation (Yang et al., 2009) is converted to the maximum evapotranspiration rate needed by ETS. The segmentation is decided according the field measurements of evaporation at different water table depth in the NCP (Li, 2008).

2.4.3. Model Calibration

The calibration process was divided into three parts: calibration of the steady state model; calibration from 1960 through 1992 only using historic water level contour maps and detailed calibration from 1993 through 2008 of the transient model. The steady state model representing predevelopment was calibrated using the groundwater level contour map across the NCP for the shallow aquifer zone and the potentiometric surface map across the Hebei Plain for the deep aquifer zone in 1959. Combinations of trial-and-error method and inverse modeling using PEST (Doherty, 2003) parameter estimation package were implemented in the calibration process of the steady state model. The total areal recharge in each county administrative region was the primary calibration parameter. The ratio between vertical and horizontal hydraulic conductivity (K_h/K_v) was also adjusted in calibration and a uniform value of 10,000 was estimated. Given the

horizontal hydraulic conductivity of 3–200 m/d with previously reported vertical hydraulic conductivity of 0.00003–0.0003 m/d for clay, and 0.005–0.007 m/d for the sand (Chen, 1990) in the NCP, this K_h/K_v ratio is representative.

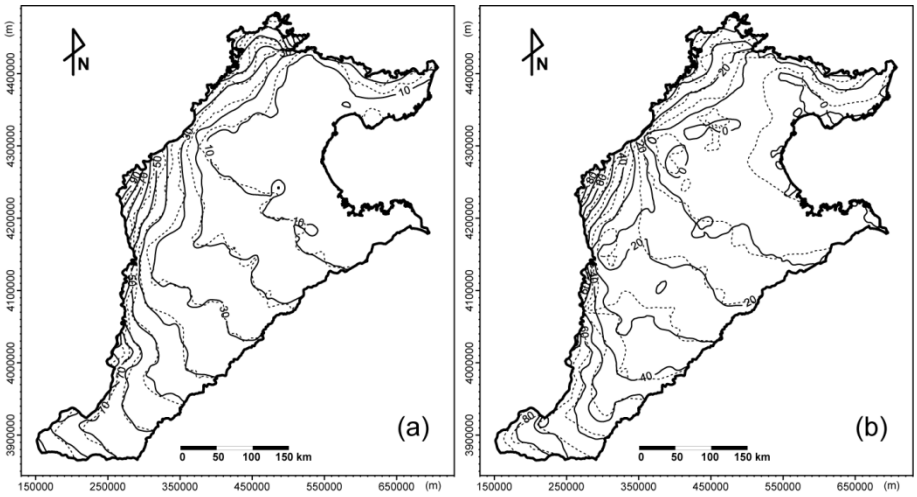

Figure 2.3. Comparison of observed and simulated water level contours in the shallow aquifer zone in (a) 1959 and (b) 1984.

Using the water level distributions as the initial condition for the transient flow model, the transient model was first roughly calibrated to 1992 data only using water level contour maps in 1975, 1984, and 1992 (Zhang, 2000; Zhang et al., 2009), and then calibrated from 1993 through 2008 using monitoring water level time series. In this two part calibration process, total areal recharge in each county administrative region was the primary calibration parameter, and the spatial distribution of pumping was also adjusted through the trial-and-error calibration process. Because the majority of wells were monitored manually, the water level monitoring time series data were pre-filtered to remove obvious erroneous data prior to being used for model calibration. Due to lack of detailed information on the distribution of irrigated fields or an

irrigation density map, the province-level pumpage was first redistributed by county by comparing simulated with measured water level changes, and then was divided equally into each active cell in the county.

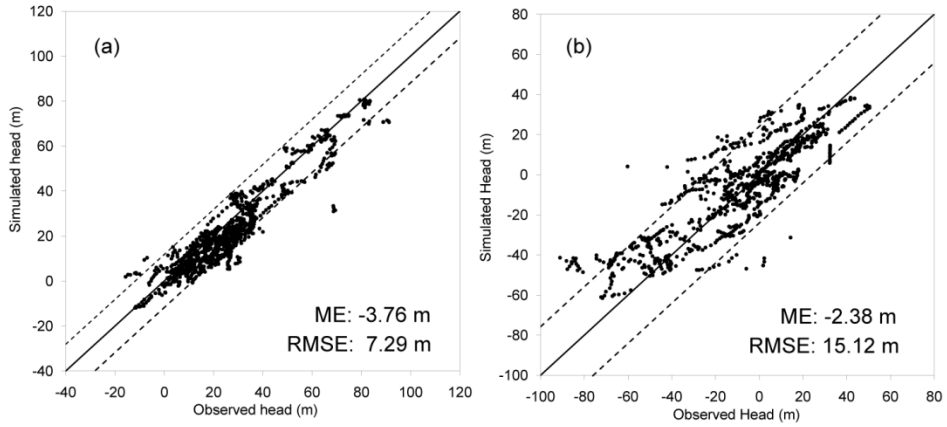

Figure 2.4. Comparison between observed and simulated annual water levels from 1993 through 2008 at (a) 105 shallow observation wells (in model layer 1), total 1231 observations, and (b) 72 deep observation wells (in model layer 2 and 3), total 871 observations. Dotted lines indicate the 95% prediction intervals.

Figure 2.3 shows simulated and measured annual average groundwater level contours in 1959 and 1984 in the NCP. The goodness of fit between simulated and measured water levels in the monitoring wells from 1991 through 2008 is presented in Figure 2.4. The mean error (ME) between simulated and measured water levels was -3.76 m and the root mean square error (RMSE) was 7.29 m for the 105 shallow observation wells (in model layer 1). The ME and RMSE were -2.38 m and 15.12 m, respectively, for 72 deep observation wells (in model layer 2 and 3), total 871 observations.

2.5. Results and Discussion

The calibrated steady-state distribution of hydraulic head representing the water table in pre-development is shown in Figure 2.3a. The simulated water table decreases gradually from 90 m depth in the piedmont area of the Taihang Mountain to ~5 m depth in the coastal plain. Hydraulic gradients are up to 30% in the piedmont area of Taihang and Yan Mountains and relatively flat in the central and east part of the plain. The flat hydraulic gradient in the coastal plain means that the amount of water discharged into the Bohai Sea is limited, and groundwater is discharged mainly through ET and leakage to rivers. In plain view, groundwater flowed into the plain from the mountain area and then discharged to the Bohai Sea. Vertically, the deep aquifer zone received leakage from the shallow aquifer zone in the piedmont area and then discharged to the shallow aquifer in the central and coastal plains. In 1959 and 1960s, the depth to the water table was 0–3 m below the land surface in most places. Increasing groundwater withdrawals since the 1970s caused continuing decline of groundwater levels (Figure 2.5). Simulated annual water table depth shows a nearly linear declining trend (R=0.97). The slope of the trend line shows an annual water table decline of 0.3 m. Most of the cones of depression in the shallow aquifer zone were beneath cities in the piedmont districts east of the Taihang and Yan Mountains. The depression cones in the deep aquifer beneath the eastern part of the plain merged together and formed an extensive, regional cone of depression.

Figure 2.6 shows the monthly and seasonal groundwater storage changes calculated using water level change data. Groundwater storage is lowest in spring (March–May) corresponding to the grain-filling stage of winter wheat (April and May) in the NCP. Groundwater is replenished mostly during the summer/rainy season (July–September), which corresponds to the maize cropping season. Generally, maize cultivation does not have much impact on groundwater

depletion except during drought years, such as 1997, 1999 and 2002, when average annual precipitation was less than 400 mm. From October to the beginning of winter wheat irrigation in the following March, which is the cultivation and vernalization period of next season's winter wheat, groundwater storage gradually increases.

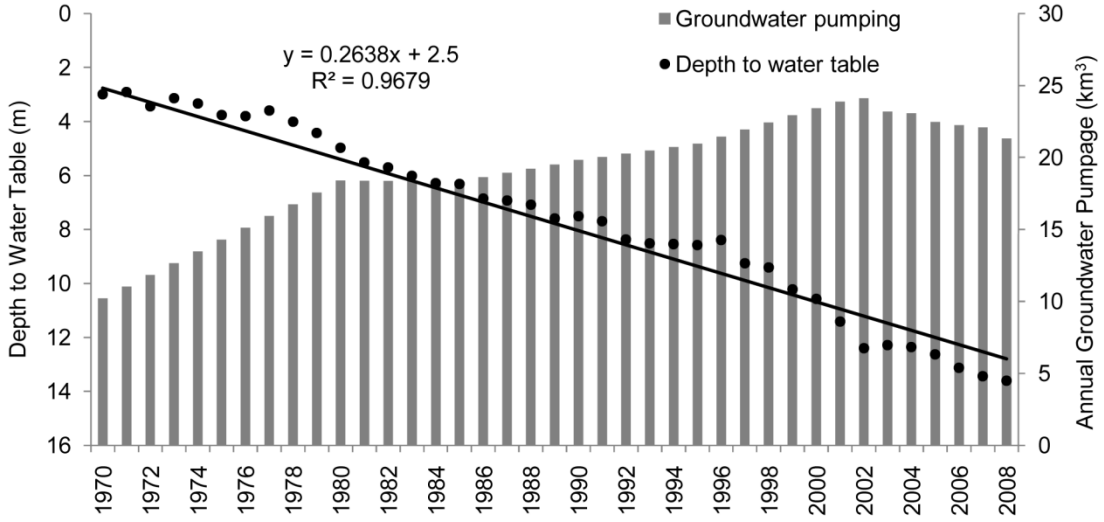

Figure 2.5. Total groundwater pumping and simulated annual averaged water table depth in the NCP. The annual groundwater pumpage before 1980 was estimated.

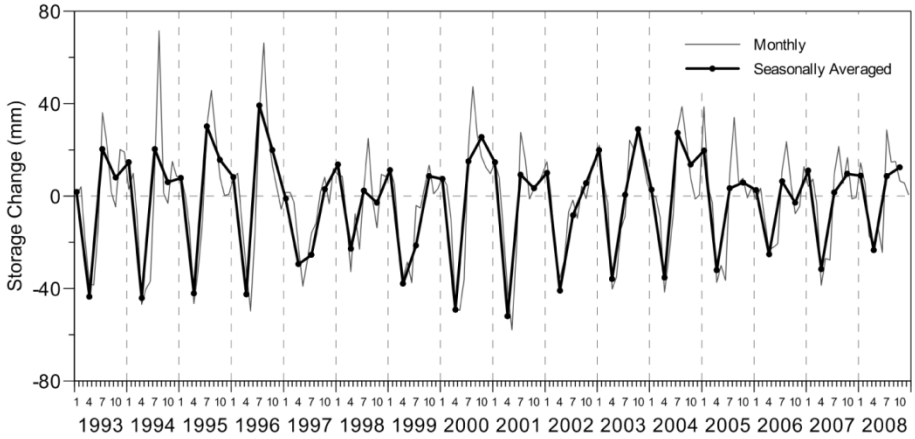

Figure 2.6. Monthly and seasonally averaged groundwater storage change in the NCP calculated using water level changes data.

The trend in simulated groundwater storage change from 1970 through 2008 is shown in Figure 2.7 and Figure 2.8. Because in the NCP where water levels are influenced by precipitation, well pumping and return flow due to applied irrigation, aquifer storage cannot be estimated accurately through by water level change analysis. Moreover, only 130 monitoring wells were chosen to be used for storage estimation, which accounts for approximately one well per 1,000 km^2. These explain the bias that exists between storage variation calculated by water level change and simulated by the model in Figure 2.7. By the end of 2008, the simulated total groundwater storage depletion is ~130 km^3, which is ~3.5% of total initial groundwater storage. Estimated annual groundwater depletion is ~4.0 km^3, which corresponds to an average of 0.3 m/yr decrease in groundwater levels across the entire NCP with area weighted specific yield of 0.075. The results showed an overall depletion trend except in 1973, 1977 and 1990 when annual precipitation exceeded 700 mm and in 1996 when the NCP was affected by a severe flood event. Mean annual groundwater depletion was ~2.5 in 1970s, and increased to ~4.0 km^3 in 1980s. The mean depletion rate was ~2.0 km^3/yr in 1990-1996; in this period the precipitation show an increasing trend. The mean depletion rate was ~5.0 km^3/yr in 1997–2008, which is the period with smallest precipitation. Model estimated annual groundwater storage change was highly correlated with precipitation (R=0.92) and was not well correlated with total pumpage (R=-0.38).

Groundwater budgets in the shallow and deep aquifer zones were calculated separately using Zonebudget (Harbaugh, 1990) to separate depletion from the two zones. Average groundwater depletion between 1970 and 2008 was 28 mm/yr in the shallow aquifer and 2.6 mm/yr in the deep aquifer. The approximately 10 times difference in depletion between the shallow and deep aquifer zones indicates that groundwater exploitation from the shallow aquifer zone was the main driving force of the groundwater depletion in the NCP. The depression cones

in the deep aquifer beneath the eastern part of the plain were mainly caused by extensive groundwater pumping for industrial and urban use. With development of the deep groundwater, leakage from the shallow aquifer zone had been facilitated. In 2008, calculated leakage from the shallow aquifer zone accounted for more than 90% of total pumpage from the deep aquifer zone. This is consistent with water levels in the shallow aquifer zone becoming generally higher than those in the deep aquifer zone.

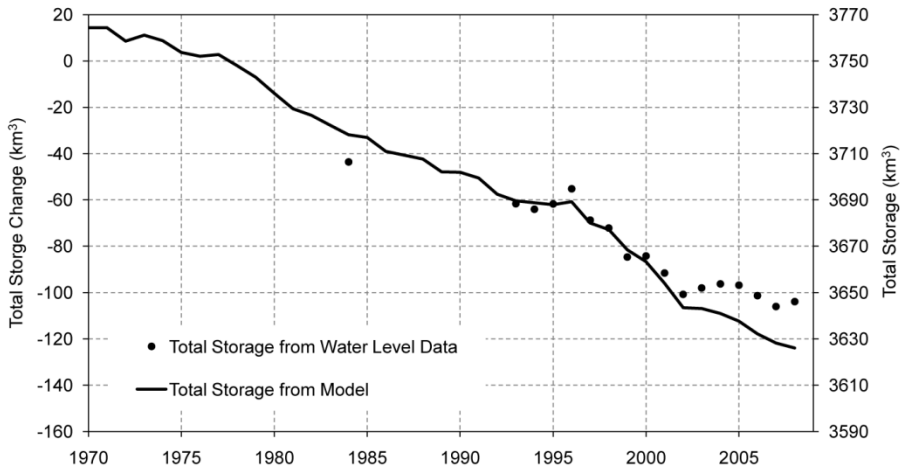

Figure 2.7. Cumulative storage change with 1959 as the base year calculated using water level changes data (dots) and simulated by the model (line) and corresponding change of total groundwater storage in the NCP.

The calibrated mean annual spatially averaged groundwater recharge across the NCP was 130 mm including 120 mm from precipitation and irrigation and 10 mm from mountain front recharge and leakage from the Yellow River. The calibrated average groundwater recharge is consistent with previous point measurements and model results (Kendy et al., 2004; Lu et al., 2010; Wang et al., 2008). Lower recharge corresponds to large droughts in 1972, 1980 and

higher recharge rates correspond to extensive flooding in 1996. Temporal variations in irrigation, precipitation, and model-calibrated groundwater recharge are presented in Figure 2.9. Applied irrigaiton in the NCP has been fairly constant since 1980. The trend of rechage variation shows a similar pattern to the temporal distribution of annual precipitation in the NCP. The linear correlation coefficient between model-calibrated annual groundwater recharge and annual precipitation plus irrigation is 0.86; the results, imply that 21% of the total precipitation and irrigation reach the aquifer as recharge.

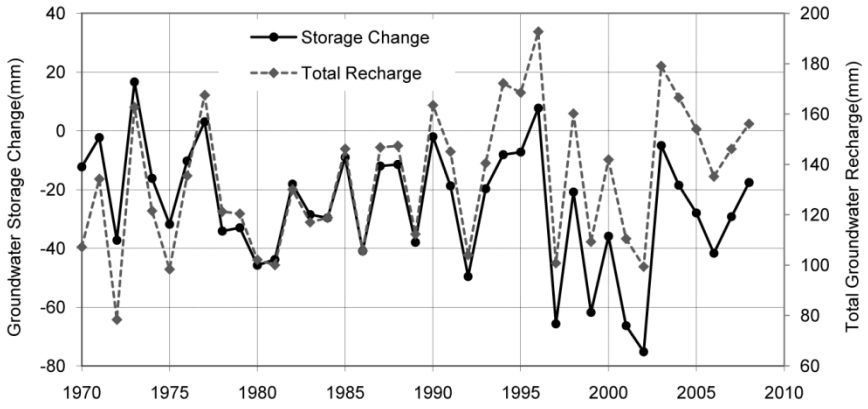

Figure 2.8. Model simulated groundwater storage change and total groundwater recharge trend from 1970 to 2008.

There is considerable spatial variability in pumpage and calibrated recharge over the NCP (Figure 2.10). Calibrated recharge is highest (200–350 mm/yr) in the piedmont area, and decreased to 50-100 mm in the central and coastal plains ares. Disagreement between the overall patterns of groundwater recharge and spatial distribution of mean annual precipitation indicates that surface boundary conditions, such as soil properties may also be a controlling factor on spatial distribution of groundwater recharge. Uneven distribution of groundwater pumpage is

mainly caused by considerable variations in the density of grain crop cultivation as cultivated area per unit land area. According to the 2008 statistical data (Hebei Statistical Yearbook, 2009), grain crop cultivation density in the Hebei Plain ranges from ~15 to ~110 ha/ km^2, and the majority of the counties with higher density than the mean value (70 ha/km^2) are located in the piedmont area. The pattern of groundwater extraction reflects an overall pattern of groundwater storage change and water table depth (Figure 2.11): largest storage depletion in the piedmont area and central plain. It then suggests that groundwater storage depletion in the NCP is generally driven by groundwater pumping for irrigation.

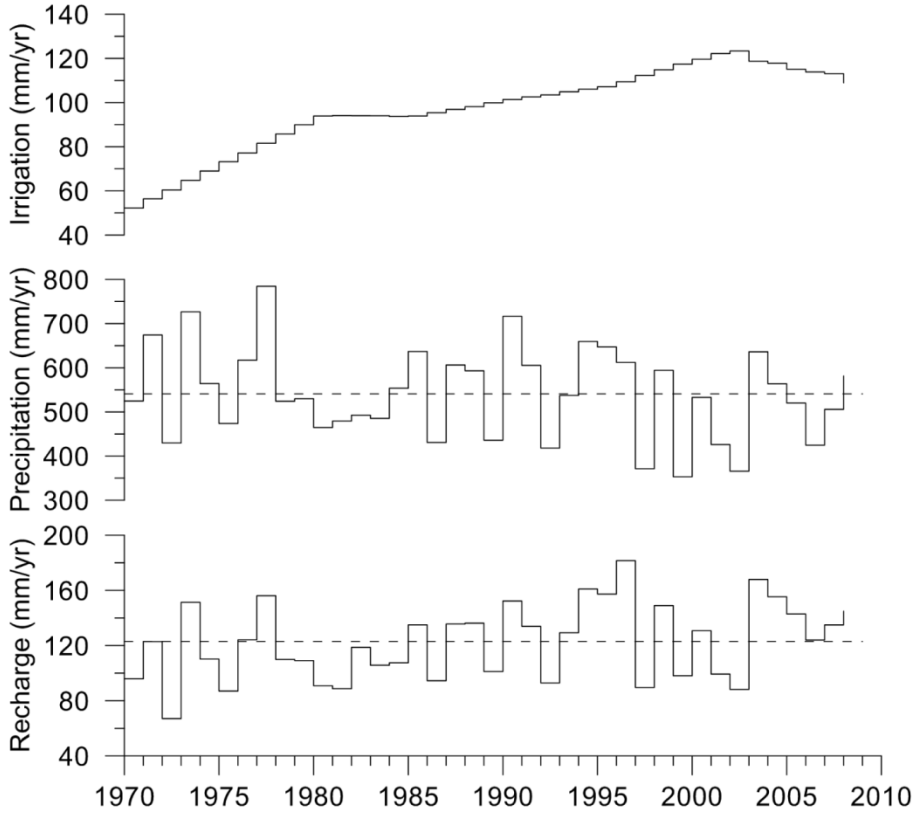

Figure 2.9. Temporal variation of irrigation (assuming irrigation accounting for 70% of total pumpage), precipitation and model-calibrated groundwater from 1970 through 2008.

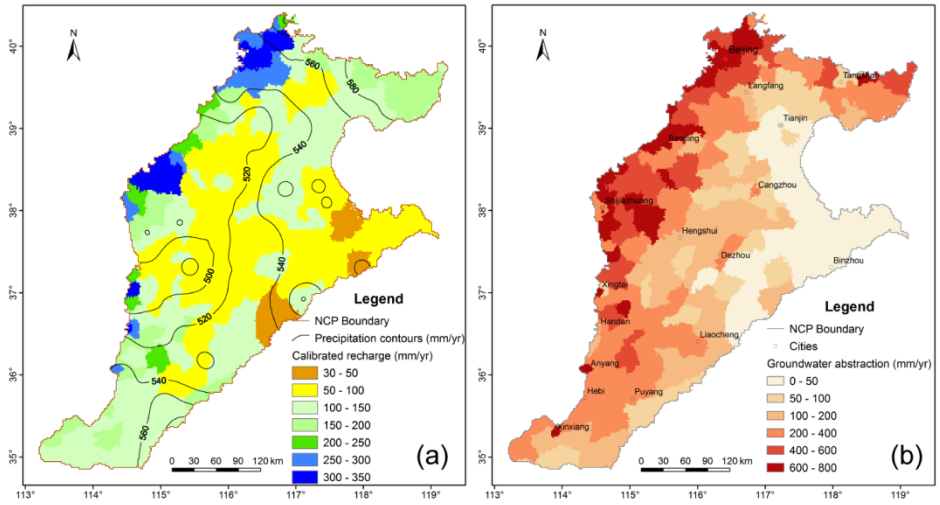

Figure 2.10. Spatial distribution of (a) calibrated averaged annual recharge and precipitation contours interpolated using 23 meteorological stations, and (b) averaged annual total groundwater abstraction from both shallow and deep aquifers for the period from 1970 through 2008.

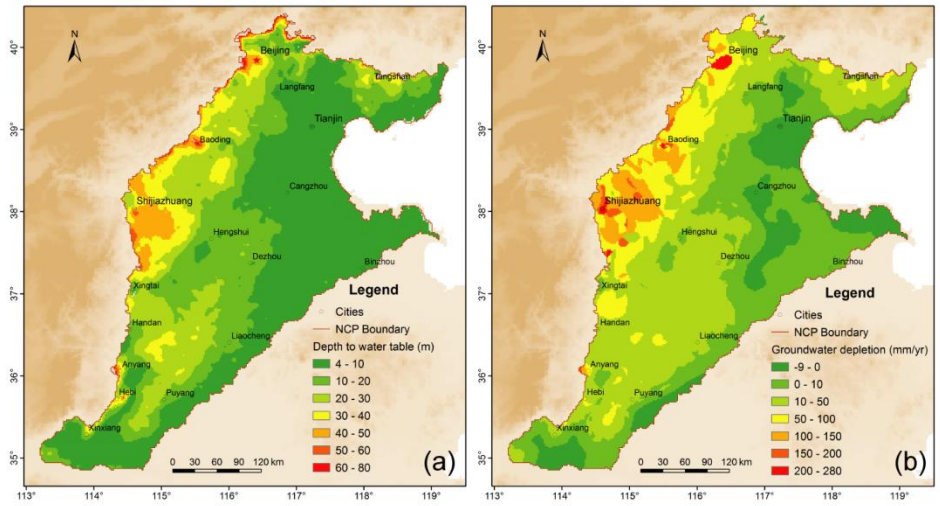

Figure 2.11. Spatial distribution of (a) simulated water table depth in 2008 and (b) average annual groundwater depletion from 1970 through 2008.

2.6. Strategies for Sustainability

It is clear that the current level of groundwater in the NCP is unsustainable, and numerous studies have been conducted to explore effective and feasible approaches to mitigate groundwater depletion. Some of these studies are reviewed by Zheng et al. (2010) and Liu et al. (2010).

Considering that groundwater depletion is caused mainly by winter wheat production, the most effective means of reducing irrigation demand is by reducing irrigated acres of winter wheat. However, over 70% of the food supply for local farmers is currently from wheat (Yang et al., 2002). Importing food from outside is impractical. Moreover, considering that the wheat is self-sufficient while the maize supply has relied on in part on importation, substantial reduction of wheat acreage would conflict with the Chinese government's emphasis on food security; moreover, a simple change in agricultural crop rotation would be difficult. The most reasonable strategies involve the augmentation and conservation of water resources.

Historically, a common response to flood and droughts in the NCP is to construct reservoirs. The construction of reservoirs in the Hebei Province started in the 1950s. By the end of 1988, there were total 1176 reservoirs in Hebei including 17 large reservoirs with single storage capacity larger than 0.1 km^3 (Hebei Water Conservancy, 1995). Majority of the large reservoirs are located in the mountain front area of the Taihang and Yan Mountains, and control over 90% of the upstream area. The recharge from the rivers has become seasonal. The central plain has no suitable locations for dams and reservoirs. Depleted aquifers can be transformed into underground "reservoirs" by artificially recharging excess runoff when available.

In the NCP, the brackish water with locates below most of the middle and coastal plain, where fresh water are pumped from the deep aquifer zone. At present, pumpage from the deep

aquifer zone account for approximate 40% of total groundwater withdrawals in the NCP. Pumpage from the deep aquifer has caused severe land subsidence with total area of 33,000 km^2 of cumulative subsidence greater than 500 mm by the end of 2005. On the other hand, the area of simulated water table depth less than 10 m is 58,000 km^2 in the 2008, most of which covers the brackish water region. The simulated annual evaporation from the shallow groundwater in this region is more than 1.6 billion m^3. Pumping shallow brackish water as replacement of deep fresh groundwater for irrigation will mitigate the overexploitation of the deep aquifer zone, and slow down the rate of the downward migration of the brackish/fresh water interface (Foster et al., 2004).

Agriculture is the largest water user in the NCP. Therefore, increasing the efficiency of agricultural water is a major focus of water conservation efforts. Although the water use efficiency (WUE) for wheat and maize on well managed experimental sites can reach to 1.0–1.9 kg/m^3, which is comparable with global average value, the WUE in farmers' field is much lower than on the experimental sites (Fang et al., 2010). Therefore, the most effective means to the WUE is by replacing the flood irrigation with water saving irrigation techniques, such as border irrigation, low pressure pipe irrigation and sprinkler irrigation (Blanke et al., 2007). The area with water saving techniques applied just accounted approximate 40% of total irrigation area based on the statistic data for the Hebei Province in 2007 (Hebei Agricultural Statistical Yearbook, 2008). Reusing of reclaimed water in urban area and for industry is another option to improve water conservation. At present, ~ 60% of the wastewater from cities in the NCP is treated based on statistic data in 2007 (China Urban Construction Statistical Yearbook, 2007). On the other hand, the coverage of wastewater collection and treatment system is still very low

in majority of counties and towns (Wang et al., 2006). Therefore, there is significant potential for agricultural water conservation.

Use source of water other than local groundwater, import surface water from outside river basin. The Chinese government is heavily relying on the South-to-North Water Diversion (SNWD) project designed to transfer water from the water-rich south, mainly the Yangtze River, to the drought-prone north. It consists of three routes: the eastern, the central, and the western, among which the middle and eastern routes will impact the NCP (Liu and Zheng, 2002). Construction on the central route began in 2003, and 0.3 and 0.26 billion m^3 of water had been transferred from reservoirs in the Hebei Province to Beijing in 2008 and 2009, respectively. The first phase of the SNWD was scheduled to be completed in 2010, but environmental concerns and resettlement issues have pushed the completion date to 2014.

2.7. Conclusions

A multilayer, heterogeneous and anisotropic groundwater flow model was built for the pre-development and post development conditions of the NCP. In the absence of flow rate data of the interception between the steams and the groundwater in the study area, recharge rates were calibrated by water levels. The values of hydraulic conductivity, specific yield and specific storage parameters used in the model were obtained from a reasonable number of pumping tests and had been verified by previous model studies. Therefore, in spite of the fact that no accurate long-term data are available for the recharge from the mountain area and from the leakage of the Yellow River, the calibration was considered acceptable and within practice standard. Mean annual spatially averaged total recharge from precipitation and irrigation calibrated through the model was 130 mm which was ~21% of precipitation and applied irrigation.

The flow model produced the development history of the groundwater system, and the output of the model provided the annual groundwater depletion rates. A monthly series of groundwater storage change was also obtained independently from water level change data and specific yield across the NCP. Given the fact that the distributions monitoring wells available in this study are sparse and uneven, the agreement between the storage change from the model and that estimated by the water level change data are acceptable. The calibrated flow model revealed an average of ~30 mm/yr of groundwater depletion rate. The regional transient groundwater flow model provides a useful tool for reproducing groundwater dynamic field and monitoring groundwater depletion in those areas such as the NCP especially when available water level monitoring data is sparse. Moreover, since no strategy alone can solve the groundwater depletion in the NCP, the groundwater model then can be integrated with climate change model, agricultural model and economic dynamic model to analyze various groundwater development and management scenarios and develop effective management strategies that ensure long-term and stable groundwater supplies while mitigating negative environmental consequences.

Both the temporal and spatial storage change distribution pattern indicated that the main driving factor of groundwater depletion in the NCP is the groundwater exploitation to maintain agriculture. The seriousness of groundwater depletion in the NCP is self-explanatory problem which restrict the development of regional economic. Although evaluating of different management responses of groundwater depletion in the NCP exceeded this study, those sustainable management strategies of groundwater resources in the NCP is not only needed for mitigating the water depletion problem, but is also instructive for many similar places with facing the same problem and looking for solutions.

Acknowledgements

This work was supported by the National Basic Research Program of China (grant #2006CB403404) and National Natural Science Foundation of China (grant #40911130505). We appreciate the data support from China Geological Survey and China Institute of Water Resources and Hydropower Research.

References

Alley, W. M., T. E. Reilly, and O. L. Franke. 1999. Sustainability of ground-water resources, U.S. Geological Survey Circular 1186, U.S. Geological Survey, Denver, CO.

Alley, W. M., R. W. Healy, J. W. LaBaugh, and T. E. Reilly. 2002. Flow and storage in groundwater systems. *Science* 296, no. 5575: 1985-1990.

Alley, W. M., and S. A. Leake. 2004, The journey from safe yield to sustainability. *Ground Water* 42, no.1: 12-16.

Banta, E. R. 2000. Modflow-2000, the US Geological survey modular ground-water model-documentation of packages for simulating evapotranspiration with a segmented function (ETS1) and drains with return flow (DRT1).

Blanke, A., S. Rozelle, B. Lohmar, J. Wang, and J. Huang. 2007. Water saving technology and saving water in China. *Agricultural Water Management* 87, no. 2: 139-150.

Cai, X., and M. W. Rosegrant. 2004. Optional water development strategies for the Yellow River Basin: Balancing agricultural and ecological water demands. *Water Resource Research* 40, no. 8: W4S-W8S. doi:10.1029/2003WR002488.

Chen, J.Y., C.Y. Tang, Y.J. Shen, Y. Sakura, A. Kondoh, and J. Shimada. 2003. Use of water balance calculation and tritium to examine the dropdown of groundwater table in the piedmont of the North China Plain (NCP). *Environmental Geology* 44, no. 5: 564-571.

Chen, J., C. Tang, Y. Sakura, A. Kondoh, J. Yu, J. Shimada, and T. Tanaka. 2004. Spatial geochemical and isotopic characteristics associated with groundwater flow in the North China Plain. *Hydrological Processes* 18, no. 16: 3133-3146.

Chen, W. 1990. Evaluation of water resources and hydraulic parameters for the shallow groundwater in the Hebei Plain. *Hydrogeology and Engineering Geology* 6: 19-22. (in Chinese)

Chen, Z.Y., J.X. Qi, J.M. Xu, J.M. Xu, H. Ye, and Y.J. Nan. 2003. Paleoclimatic interpretation of the past 30 ka from isotopic studies of the deep confined aquifer of the North China plain. *Applied Geochemistry* 18, no. 7: 997-1009.

Chen, Z., Z. Nie, Z. Zhang, J. Qi, and Y. Nan. 2005. Isotopes and sustainability of ground water resources, North China Plain. *Ground Water* 43, no. 4: 485-493.

Cui, Y., Y. Wang, J. Shao, Y. Chi, and L. Lin. 2009. Research on Groundwater Regulation and Recoveryin North China Plain after the Implementation of South-to-North Water Transfer. *Resources Science* 31, no. 3: 382-387. (in Chinese with English abstract)

Doble, R.C., C.T. Simmons, and G.R. Walker. 2009. Using MODFLOW 2000 to Model ET and Recharge for Shallow Ground Water Problems. *Ground Water* 47, no. 1: 129-135.

Doherty, J. 2003. Version 5 of PEST Manual, Watermark Numerical Computing, Brisbane Australia. Downloadable from: http://www. sspa. com/pest.

Fang, Q.X., L. Ma, T.R. Green, Q. Yu, T.D. Wang, and L.R. Ahuja. 2010. Water resources and water use efficiency in the North China Plain: Current status and agronomic management options. *Agricultural Water Management* 97, no. 8: 1102-1116.

Fei, J. 1988. Groundwater resources in the north china plain. *Environmental Geology and Water Sciences* 12, no. 1: 63-67.

Fei, Y., J. Miao, Z. Zhang, Z. Chen, H. Song, and M. Yang. 2009. Analysis on Evolution of Groundwater Depression Cones and Its Leading Factors in North China Plain. *Resources Science* 31, no. 3: 394-399. (in Chinese with English abstract)

Fogg, G.E., and E.M. LaBolle. 2006. Motivation of synthesis, with an example on groundwater quality sustainability. *Water Resources Research* 42, no. 3: W3S-W5S.

Foster, S. 2000. Sustainable Groundwater Exploitation for Agriculture. Current Issues and Recent Initiatives in the Developing World. Papeles del proyecto aguas subterráneas.

Foster, S., H. Garduno, R. Evans, D. Olson, Y. Tian, W. Zhang, and Z. Han. 2004. Quaternary aquifer of the North China Plain—assessing and achieving groundwater resource sustainability. *Hydrogeology Journal* 12, no. 1: 81-93.

Haihe River Water Resources Commission of the Ministry of Water Resources of China. Haihe River Basin Water Resources Bulletin 1998-2008.

Han, Z. S. 1998. Groundwater for urban water supplies in northern China-An overview. *Hydrogeology Journal* 6, no. 3: 416-420.

Harbaugh, A. W. 1990. A computer program for calculating subregional water budgets using results from the US Geological Survey modular three-dimensional finite-difference ground-water flow model, Open-File Report 90-392, U.S. Geological Survey, Reston, Virginia.

Harbaugh, A. W., E. R. Banta, M. C. Hill, and M. G. McDonald. 2000. MODFLOW-2000, The U. S. Geological Survey Modular Ground-Water Model-User Guide to Modularization Concepts and the Ground-Water Flow Process, Open-File Report 00-92, U.S. Geological Survey, Reston, Virginia.

He, G., J. L. Shao, Y. L. Cui, and D. Zhang. 2003. Application of FEFLOW to Groundwater Flow Simulation. Journal of Chengdu University Technology (Sci. Tech. Ed.), 4, 356-361. (in Chinese)

Hebei Bureau of Geology and Mineral. 1977. Evaluation and Rational Development and Utilization of Groundwater Resources in the Hebei Plain (Heilonggang Plain) (in Chinese).

Hebei Provincial Bureau of Statistics. 2009. Hebei Agricultural Statistical Yearbook 2008. Beijing: China Statistics Press.

Hebei Department of Water Resources. 1995. Hebei Water Conservancy (in Chinese). Shijiazhuang: Hebei People's Publishing House.

Hu, Y.K., J.P. Moiwo, Y.H. Yang, S.M. Han, and Y.M. Yang. 2010. Agricultural water-saving and sustainable groundwater management in Shijiazhuang Irrigation District, North China Plain. *Journal of Hydrology* 393, no. 3-4: 219-232.

Hurd, B., N. Leary, R. Jones, and J. Smith. 1999. Relative regional vulnerability of water resources to climate change. *Journal of the American Water Resources Association* 35, no. 6: 1399-1409.

Jia, J., and C. Liu. 2002. Groundwater Dynamic Drift and Response to Different Exploitation in the North China Plain: A Case Study of Luancheng County, Hebei Province. *Acta Geographica Sinica* 57, no. 2: 201-209. (in Chinese with English abstract)

Jiang, X., H. Li, S. Cai, L. Ji, T. Cheng, and N. Xu. 2009. Investigation and analysis of farmers'irrigation actions in the North China Plain well irrigation district. *Anhui Agricultural Science Bulletin* 15, no. 11: 152-154. (in Chinese with English abstract)

Jiao, H., Y. Duan. 2005. Sustainable utilization of groundwater resource in the Yubei Plain. *Hydrogeology and Engineering Geology* 1: 61-66. (in Chinese)

Kendy, E., Y. Zhang, C. Liu, J. Wang, and T. Steenhuis. 2004. Groundwater recharge from irrigated cropland in the North China Plain: case study of Luancheng County, Hebei Province, 1949-2000. *Hydrological Processes* 18, no. 12: 2289-2302.

Kinzelbach, W., P. Bauer, T. Siegfried, and P. Brunner. 2003. Sustainable groundwater management--Problems and scientific tool. *Episodes* 26, no. 4: 279-284.

Konikow, L.F., and E. Kendy. 2005. Groundwater depletion: A global problem. *Hydrogeology Journal* 13, no. 1: 317-320.

Li, F.D., X.F. Song, C.Y. Tang, C.M. Liu, J.J. Yu, and W.J. Zhang. 2007. Tracing infiltration and recharge using stable isotope in taihang Mt., north China. *Environmental Geology* 53, no. 3: 687-696.

LI, J. 2008. The synthesize analysis of the diving evaporation coefficient. *Ground Water* 06: 27-30. (in Chinese)

Liu, C., J. Yu, and E. Kendy. 2001. Groundwater exploitation and its impact on the environment in the North China Plain. *Water International* 26, no. 2: 265-272.

Liu, C., et al. (2002), Determination of daily evaporation and evapotranspiration of winter wheat and maize by large-scale weighing lysimeter and micro-lysimeter, Agr. Forest Meteorol., 111(2), 109-120.

Liu, C., X. Zhang, and Y. Zhang. 2002. Determination of daily evaporation and evapotranspiration of winter wheat and maize by large-scale weighing lysimeter and micro-lysimeter. *Agricultural and Forest Meteorology* 111, no. 2: 109-120.

Liu, C., and J. Xia. 2004. Water problems and hydrological research in the Yellow River and the Huai and Hai River basins of China. *Hydrological Processes* 18, no. 12: 2197-2210.

Liu, C., J. Chen, and J. Qiao. 2004. A survey of irrigation status in the well irrigation distict in the North Chian Plain. *Water Resources Development Research* 10: 38-41.

Liu, J., C.M. Zheng, L. Zheng, and Y.P. Lei. 2008. Ground Water Sustainability: Methodology and Application to the North China Plain. *Ground Water* 46, no. 6: 897-909.

Liu, J., C.M. Zheng, L. Zheng, and Y.P. Lei. 2008. Ground Water Sustainability: Methodology and Application to the North China Plain. *Ground Water* 46, no. 6: 897-909.

Lo áciga, H. 2002. *Sustainable ground-water exploitation*. *International Geology Review* 44, no. 12: 1115-1121.

Lu, X., M. Jin, M.T. van Genuchten, and B. Wang. 2011. Groundwater Recharge at Five Representative Sites in the Hebei Plain, China. *Ground Water* 49, no. 2: 286-294.

Luckey, R. L., and M. F. Becker. 1999. Hydrogeology, water use, and simulation of flow in the High Plains aquifer in northwestern Oklahoma, southeastern Colorado, southwestern Kansas, northeastern New Mexico, and northwestern Texas, Water-Resources Inv. Rep. 99-4104, U.S. Geological Survey.

Ma, Z., et al. 2005. Sustainable utilization of groundwater resource in the Lubei plain of Shandong Province. *Hydrogeology and Engineering Geology* 2: 1-10. (in Chinese)

Ministry of Housing and Urban-Rural Development of China. 2007. China Urban Construction Statistical Yearbook 2007, China Construction Press, Beijing.

National Bureau of Statistics of China. 2010. China Statistical Yearbook 2010, China Statistics Press, Beijing.

National Bureau of Statistics of China. 2003. China Population County Census Data 2000, China Statistics Press, Beijing.

Oki, T., and S. Kanae. 2006. Global hydrological cycles and world water resources. *Science* 313, no. 5790: 1068-1072.

Rabus, B., M. Eineder, A. Roth, and R. Bamler. 2003. The shuttle radar topography mission--a new class of digital elevation models acquired by spaceborne radar. *Isprs Journal of Photogrammetry and Remote Sensing* 57, no. 4: 241-262.

Shah, T., D. Molden, R. Sakthivadivel, and D. Seckler. 2000. The global groundwater situation: overview of opportunities and challenges. *International Water Management Institute. Sri Lanka*

Shah, T., A.D. Roy, A.S. Qureshi, and J. Wang. 2003. Sustaining Asia's groundwater boom: An overview of issues and evidence. *Natural Resources Forum* 27, no. 130-141.

Shao, J., Y. Cui, Y. Zhao, and G. He. 2003. Groundwater Numerical Modeling And Its Application in Affected Zone of The Down-yellow River (Henan Section). *Journal of Changchun University of Science and Technology* 33, no. 1: 51-55. (in Chinese)

Shao, J., Z. Zhao, Y. Cui, R. Wang, C. Li, and Q. Yang. 2009. Application of Groundwater Modeling Systemto the Evaluation of Groundwater Resources in North China Plain. *Resources Science* 31, no. 3: 361-367. (in Chinese with English abstract)

Song, X., F. Li, C. Liu, C. Tang, Q. Zhang, and W. Zhang. 2007. Water Cycle in Taihang Mountain and Its Recharge to Groundwater in the North China Plain. *Journal of Natural Resources* 22, no. 3: 398-408. (in Chinese with English abstract)

Song, Z.W., H.L. Zhang, R.L. Snyder, F.E. Anderson, and F. Chen. 2010. Distribution and Trends in Reference Evapotranspiration in the North China Plain. *Journal of Irrigation and Drainage Engineering-Asce* 136, no. 4: 240-247.

Wang, B.G., M.G. Jin, J.R. Nimmo, L. Yang, and W.F. Wang. 2008. Estimating groundwater recharge in Hebei Plain, China under varying land use practices using tritium and bromide tracers. *Journal of Hydrology* 356, no. 1-2: 209-222.

Wang, S., J. Shao, X. Song, X. Zhou, and Z. Huo. 2007. The application of groundwater model,MODFLOW,and GIS technology in the dynamic evaluation of groundwater resource in North China Plain. *Geographical Research* 26, no. 5: 975-983.

Wang, S.Q., J.L. Shao, X.F. Song, Y.B. Zhang, Z.B. Huo, and X.Y. Zhou. 2008. Application of MODFLOW and geographic information system to groundwater flow simulation in North China Plain, China. *Environmental Geology* 55, no. 7: 1449-1462.

Wang, X.C., P.K. Jin, and X.C. Wang. 2006. Water shortage and needs for wastewater re-use in the north China. *Water Science & Technology* 53, no. 9: 35-44.

Welsh, W. D. 2006. Great Artesian Basin transient groundwater model, Bureau of Rural Sciences, Department of Agriculture, Fisheries and Forestry, Australia.

Wu, C., Q.H. Xu, X.Q. Zhang, and Y.H. Ma. 1996. Palaeochannels on the North China Plain: Types and distributions. *Geomorphology* 18, no. 1: 5-14.

Xia, J. 2006. Water Security and Ground Water Problem to Changing Environment in North China, paper presented at International Symposium on Groundwater Sustainability, Alicante, Spain.

Xie, X., H. Guo, K. Tang, and M. Yin. 2002. Dual coupled model for integrated assessment of surface water and groundwater in North China Plain. *Journal of Hydraulic Engineering* 12: 95-100.

Xu, Q.H., C. Wu, X.Q. Zhu, and X.L. Yang. 1996. Palaeochannels on the North China Plain: Stage division and palaeoenvironments. *Geomorphology* 18, no. 1: 15-25.

Xu, Y., X. Mo, Y. Cai, and X. Li. 2005. Analysis on groundwater table drawdown by land use and the quest for sustainable water use in the Hebei Plain in China. *Agricultural Water Management* 75, no. 1: 38-53.

Yang, Y.H., M. Watanabe, Y. Sakura, C.Y. Tang, and S. Hayashi. 2002. Groundwater-table and recharge changes in the Piedmont region of Taihang Mountain in Gaocheng City and its relation to agricultural water use. *Water Sa* 28, no. 2: 171-178.

Yang, G., Z. Wang, H. Wang, and Y. Jia. 2009. Potential evapotranspiration evolution rule and its sensitivity analysis in Haihe River basin. *Advances in Water Science* 20, no. 3: 409-415. (in Chinese)

Zhang, G., Y. Fei, M. Yang, Z. Liu, and J. Wang. 2009. Impact of irrigating farmland increase production with water save on groundwater exploitation in the plain of Hutuo River basin. *Advances in Water Science* 20, no. 3: 350-355. (in Chinese with English abstract)

Zhang, G., Z. Liu, Y. Fei, Y. Lian, and M. Yan. 2010. The relationship between the distribution of irrigated crops and the supply capability of regional water. *Acta Geoscientica Sinica* 31, no. 1: 17-22. (in Chinese with English abstract)

Zhang, X., L. Xue, Q. Zhang, and J. Li. 2008. Simulation of Groundwater Exploitation at Early Stage and Analysis on Water Budget in Haihe River Basin. *Journal of Arid Land Resources and Environment* 09: 102-107. (in Chinese)

Zhang, X. 2007. Numerical simulation of the shallow groundwater in the Haihe Basin. *Haihe Water Resources* 03: 52-54. (in Chinese)

Zhang, S., and L. Li. 2005. Water Resouces in China. Sino Maps Press, Beijing. (in Chinese)

Zhang, X.Y., D. Pei, and C.S. Hu. 2003. Conserving groundwater for irrigation in the North China Plain. *Irrigation Science* 21, no. 4: 159-166.

Zhang, X., L. Xue, Q. Zhang, and J. Li. 2008. Simulation of Groundwater Exploitation at Early Stage and Analysis on Water Budget in Haihe River Basin. *Journal of Arid Land Resources and Environment* 09: 102-107. (in Chinese)

Zhang, Z., Z. Shen, Y. Xue, and F. Ren. 2000. Groundwater environment evolution in the North China Plain. Beijing: Geological Publishing House. (in Chinese)

Zhang, Z., Y. Fei, Z. Chen, et al. 2009. Investigation and Assessment of Sustainable Utilization of Groundwater Resources in the North China Plain. Geological Publishing House, Beijing. (in Chinese)

Zhang, Z. and Y. Fei. 2009. Atlas of Groundwater Sustainable Utilization in the North China Plain. SinoMaps Press, Beijing. (in Chinese with English Preface)

Zheng, C., J. Liu, G. Cao, E. Kendy, H. Wang, and Y. Jia. 2010. Can China Cope with Its Water Crisis?-Perspectives from the North China Plain. *Ground Water* 48, no. 3: 350-354.

CHAPTER 3

INTEGRATION OF SOIL WATER BALANCE AND UNSATURATED FLOW MODEL FOR ESTIMATING REGIONAL GROUNDWATER RECHARGE IN THE NORTH CHINA PLAIN

Abstract

Accurate estimation of groundwater recharge is important for sustainable groundwater exploitation, and proper management and protection of groundwater resources. Groundwater recharge remains one of the principal uncertainties in the water balance of the North China Plain (NCP). Understanding impacts of climate, surface conditions such as soil properties and land use, and groundwater withdrawal on groundwater recharge is essential for estimating groundwater recharge. In this study, spatial and temporal variability in recharge were evaluated by integrating a soil water balance and one-dimensional unsaturated flow models. Estimated recharge was verified using a saturated zone flow model. Soil hydraulic parameters were estimated using pedotransfer functions. Simulation of 12 years (1993–2008) was performed across the NCP. Simulated mean annual recharge is ~150 mm across the NCP, representing 18% of mean annual precipitation + irrigation, and ranging from ≤ 360 mm in the piedmont area to ≤ 260 mm in the middle and coastal plain. Variability of soil texture from clay to loamy sand resulted in a large range in recharge rates. Increasing thickness of the unsaturated zone has little effect on the long term mean annual recharge. This work provides useful information toward a comprehensive assessment of groundwater recharge in the NCP and identifies important parameters controlling recharge.

3.1. Introduction

In arid and semiarid regions where agriculture relies on irrigation, accurate estimation of groundwater recharge and evapotranspiration (ET) is extremely important for sustainable exploitation of groundwater. However, recharge is difficult to estimate because of spatial variability in soil texture, vegetation, and temporal and spatial variations in climatic factors such as precipitation and ET (Wang et al., 2009). It may be complicated further by irrigation (Gee and Hillel, 1988). Traditional physical methods to estimate recharge and measure ET directly and empirical models require large field measurements, and yet are still limited to local scales. Different approaches can be used to estimate groundwater recharge, including water-balance, water table fluctuation, chemical and isotopic tracers, and numerical simulations (Simmers, 1987; Scanlon et al., 2002; Xu and Beekman, 2003). It is difficult to assess the accuracy of any method, and thus it is highly beneficial to apply multiple methods of estimation to constrain uncertainties (Healy and Cook, 2002; Scanlon et al., 2002). Furthermore, extrapolating local measurements to regional scales can be problematic due to variations in climatic, physical and biological characteristics of the land and subsurface (Scanlon et al., 2002). The optimal choice of methods depends on the spatial and temporal scales required for the study and data availability at the study site (Scanlon et al., 2002; Delin et al., 2007).

A primary category of approach for regional groundwater recharge estimation is soil water balance, which estimates groundwater recharge as the amount of water percolating beneath the root zone (net infiltration or potential recharge). There are numerous examples of groundwater recharge estimation using this method such as the U.S. Geological Survey (USGS) INFIL model (USGS, 2008), BALAN (Samper and Garc á-Vera, 1992) and the U.S. Environmental Protection Agency (U.S. EPA) HELP model (Schroeder et al., 1994). Although

these models can easily and quickly produce reasonable regional groundwater recharge distributions where the water table is below the base of the root zone, the water flow process in the unsaturated zone from the base of the root zone to the water table is ignored. Neglecting unsaturated zone process is inappropriate where the thickness of the unsaturated zone is significant for storing and transferring water (Harter and Hopmans, 2004; Hunt et al., 2008).

Unsaturated flow modeling is becoming a common tool for evaluating groundwater recharge ant its spatial and temporal distribution (e.g., Keese et al., 2005; Small, 2005; Liggett et al., 2009). Although these models, such as DAISY(Hansen et al., 1990), UNSAT-H (Fayer, 2000), SWAP (Kroes and van Dam, 2003) and HYDRUS -1D (Šimůnek et al., 2005) can simulate unsaturated flow and estimate recharge and ET, the impact of climate, vegetation, and soil properties on groundwater dynamics cannot be evaluated directly without simulation of the saturated zone process. Models recently developed integrating groundwater flow in the saturated zone with variably saturated flow such as HYDRUS-3D (Šimůnek, 2006), MODFLOW-VSF (Thom et al., 2006), MODFLOW-SURFACT (Panday and Huyakorn, 2008) and HydroGeoSphere (Therrien et al., 2005) are better at simulating both unsaturated and saturated flow to estimate the recharge and discharge. However, they are all based on the use of the three-dimensional Richards' equation, and their application is heavily constrained by computational resources (van Walsum and Groenendijk, 2008). For basin-scale simulation, the assumption of one-dimensional flow is thought to be reasonable (Harter and Hopmans, 2004). Consequently, models such as MIKE-SHE (Refsgaard et al., 1995) and MODFLOW-UZF (Niswonger et al., 2005) coupled one-dimensional vertical flow in the unsaturated zone with three-dimensional flow in saturated zone for simplicity and greater computational efficiency. In MIKE SHE and MODFLOW-UZF, the one-dimensional form of Richards' equation is approximated by a

kinematic-wave equation solved by the method of characteristics, which precludes the need to develop a structured grid for the unsaturated zone (Niswonger et al., 2005).

Primary difficulties in application of process-based vadose zone modeling for recharge estimation are data requirements and model input parameters such as soil hydraulic characteristics. Harter and Hopmans (2004) provided an excellent review of various methods based on geostatistical techniques used in upscaling soil hydraulic parameters. Instead of measuring in situ soil hydraulic characteristics, a simpler alternative is developing a set of so-called pedotransfer functions (PTFs) (Wösten, 2001) to estimate those unsaturated zone hydraulic characteristics from more readily measured or basic soil properties in the attribute database of a digital soil survey map (Li et al., 2007). Many of the available and well-established PTFs for the prediction of soil hydraulic properties from continuous soil properties are based on statistical regressions (Pachepsky and Rawls, 2004). Most of PTFs were developed to estimate the soil water retention and saturated hydraulic conductivity (Nemes et al., 2003), and soil texture, bulk density and organic matter content are most commonly used in developing PTFs. Most of the models simulating variably saturated flow were developed primarily for application in agricultural research, and require considerable information on vegetation parameters. Information on vegetation distribution and land use is often readily available, and remote sensing data can also aid in determination of vegetation parameters. However, for study areas where vegetation types are relatively homogeneous and the land use remains largely unchanged during the simulation period, it is preferable to limit the number of model input parameters to reduce estimation uncertainty and minimize calibration non-uniqueness.

ET, as a primary discharge term in the soil water budget, strongly affects the accuracy of recharge estimation. The methods for calculating ET in different codes also vary. The most

commonly used method is to calculate the potential or reference ET (ET_p) first using meteorological data (Lu et al., 2005), and then calculate the potential bare soil evaporation and plant transpiration separately using empirical equations. The actual evaporation and transpiration are determined based on vegetation and soil moisture conditions and are summed to the actual ET (ET_a). This approach often requires small time scales, i.e., generally daily meteorological data. Therefore, time steps in the saturated zone flow model should be small, which is usually unnecessary and infeasible for regional simulation. As a remedy, time sub-steps might be used as in the HYDRUS package for MODFLOW (Seo et al., 2007).

Methods employing the complementary relationship of ET (Bouchet, 1963) are popular for estimating regional ET because they permit regional ET_a to be estimated solely from routine meteorological data, and do not need extremely detailed data describing the near-surface boundary. The models avoid the complexity of the soil-plant system and thus do not require data on soil moisture or vegetation parameters (Hobbins et al., 2001). Good agreement has been shown between the ET estimates from this type of models and those from the regional water balance calculation (e.g., Hobbins et al., 2001; Xu and Singh, 2005).

Coupling a root zone soil water balance and a simplified unsaturated zone flow model can combine the benefit of different methods for ET estimation and are feasible for regional scale application and model calibration. The purpose of this study was to determine the effects of soil type and variation in unsaturated zone thickness on regional groundwater recharge estimation from precipitation and irrigation based on data from the North China Plain (NCP). A soil water balance model coupled with the MODFLOW code and the UZF package was used in this study to construct a regional flow model considering unsaturated flow process explicitly. Those characteristics of the PTFs and the available data make this method the most reasonable

and practical one for developing regional unsaturated model in the NCP to simulate the true behavior of the aquifer in transient state. Although model calibration is beyond the scope of this study, the simulated groundwater recharge is validated with water level observations.

3.2. Materials and Methods

3.2.1. Study Site

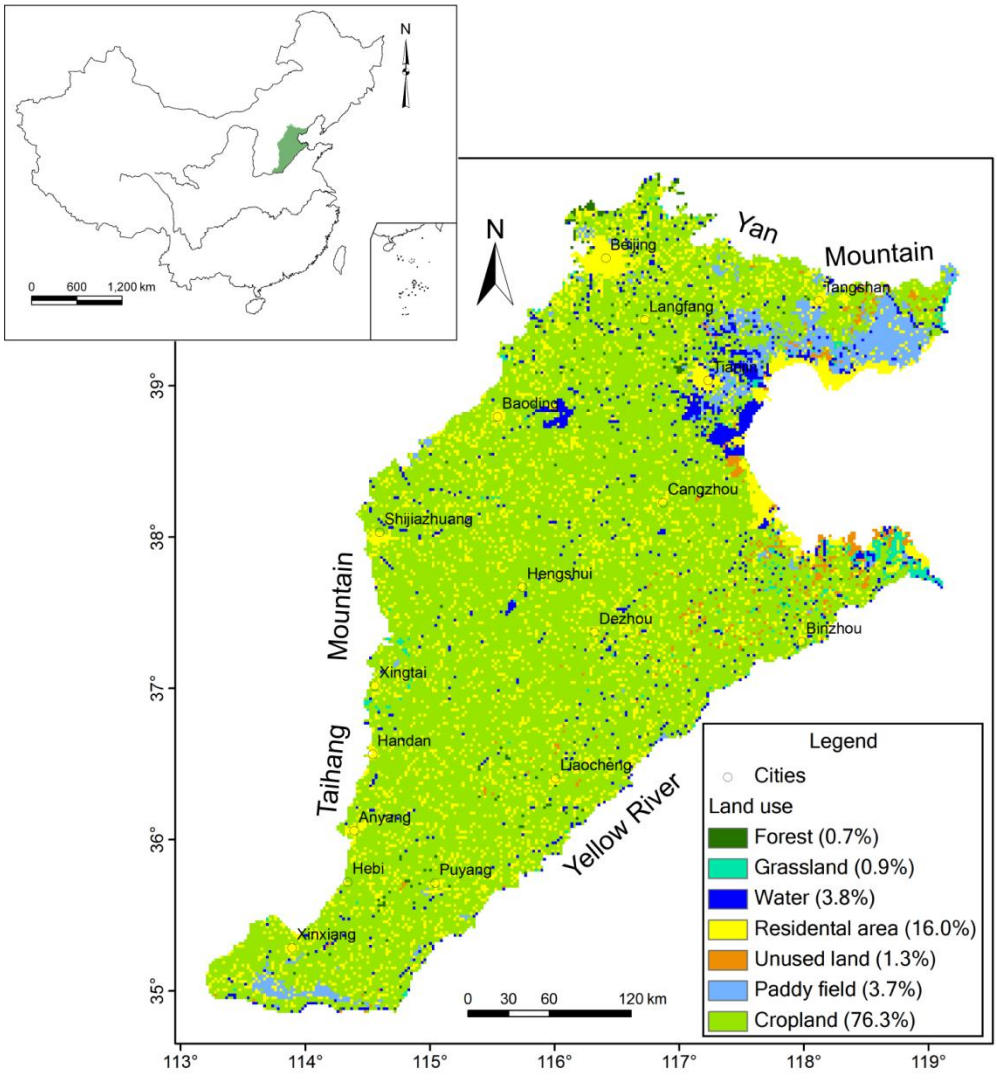

Figure 3.1. Location of the North China Plain and land use in 2000.

The North China Plain (NCP) (~140,000 km^2) refers to the plain with altitude of <100 m above mean sea level bordered on the north by the Yanshan Mountains, on the east by the Bohai Sea, on the south by the Yellow River and on the west by the Taihang Mountains in northeast China (Figure 3.1). The NCP covers the entire plains of Hebei Province, Beijing Municipality, Tianjin Municipality and the northern parts of plains of the Shandong and Henan Provinces. The population of the NCP, based on 2000 county census data, is ~105 million (National Bureau of Statistics of China, 2003) with a population density of ~800 persons per km^2. The NCP is the dominant national center of wheat and maize production and an extremely important economic, political and cultural region of China, producing ~15% of China's total gross domestic product (GDP) and ~ 10% of total grain production based on the 2009 statistical data (China Statistical Yearbook, 2010).

Recharge from infiltration of precipitation accounts for approximately 70–80 % of total natural groundwater recharge in the NCP (Chen, 1999; Chen and Ma, 2002). Most previous recharge estimates were used in groundwater resources evaluation as a water balance term. A common approach used in these estimates was to assume that a certain fraction of precipitation and irrigation percolates to groundwater, regardless of the quantity of water applied (Kendy et al., 2003). This fraction is represented by the infiltration recharge coefficient (usually expressed as α), and is multiplied by mean annual precipitation and/or irrigation to calculate mean annual groundwater recharge. Areal groundwater annual recharge estimation based on this method ranges from 70 to 180 mm/yr (Zhu and Zheng, 1983; Liu and Wei, 1989; Chen, 1999; Water Resources Department of the Hebei Province, 2003; Ren, 2007). Because the value of recharge coefficients depends on soil properties, unsaturated zone thickness, and precipitation amount, it varies spatially and temporally (Li, 2009). These recharge estimates represent long-term average

values for different periods and did not provide information on temporal variability in recharge rates. Some researchers have estimated local groundwater recharge in the NCP. Although there are numerous previous studies of local recharge using environmental tracer methods (Wang et al., 2008; Liu et al., 2009; Song et al., 2009; von Rohden et al., 2010) and unsaturated zone flow models (Kendy et al., 2004; Lu et al., 2011), a critical challenge is up scaling those typically local-scale estimates or model parameters to regional scales. Generally, a large amount of data, including thickness and hydraulic properties of the unsaturated zone, rainfall patterns, irrigation types and regime, land use and ET is required to regionalize point measurements of groundwater recharge to obtain regional recharge estimates. Considering the available data in the NCP, regionalizing point recharge estimates to regional rates seems unpractical.

A key factor affecting recharge estimation in the NCP is the increase in unsaturated zone thickness. Because of the long period of overexploitation of groundwater in the NCP, the thickness of the unsaturated zone has increased from 2–15 m in the 1970s to 8–30 m, even up to 30–56 m in some local areas (Zhang et al., 2004). Ignoring unsaturated zone processes could be problematic for analysis of groundwater recharge changes, especially for assessment of further groundwater quality evolution and development of groundwater protection strategies. Although the impact of the unsaturated zone thickness on infiltration has been evaluated by field soil moisture and potential monitoring and analysis (Zhang, 1992; Zhang et al., 2007), the impact of the unsaturated zone on groundwater recharge at regional scale has generally not been addressed.

3.2.2. Root Zone Soil Water Balance

The water balance for the soil root zone, in the absence of significant runoff, is represented by:

$$R_p = P + I_r - ET_a - \Delta\theta \tag{3.1}$$

where R_p is potential recharge, P is precipitation, I_r is irrigation, ET_a is actual ET, and $\Delta\theta$ is change of soil water storage.

The complementary relationship between actual (ET_a) and potential ET (ET_p) (Bouchet, 1963) is

$$ET_a + ET_p = 2ET_w \tag{3.2}$$

where ET_a, ET_p, and ET_w are actual, potential and wet environment ET, respectively.

The complementary relation areal ET (CRAE) method (Morton, 1983; Morton et al., 1985) calculates ET_p and ET_w as follows:

$$\lambda \mathrm{ET_p} = Q_n - \left[\gamma f_T + 4\varepsilon\sigma T_p^3\right]\left(T_p - T\right) \tag{3.3}$$

$$\lambda \mathrm{ET_w} = b_1 + b_2 \frac{\Delta_p}{\Delta_p + \gamma} Q_{TP} = b_1 + b_2 \frac{\Delta_p}{\Delta_p + \gamma}\left[Q_n - 4\varepsilon\sigma T_p^3\left(T_p - T_a\right)\right] \tag{3.4}$$

where, λ is latent heat flux, γ is psychrometirc constant, and Q_n is net available energy at the surface, usually approximated by net absorbed radiation at the surface minus diffusive ground heat flux, R_n - G. T_p and T are equilibrium and air temperature, respectively; ε is surface emissivity; σ is Stefan-Boltzman constant, and f_T is vapor transfer coefficient. where Δ_p and Q_{TP} are slope of the saturated vapor pressure curve and net available energy adjusted to equilibrium temperature.

Actual ET is calculated as a residual in (3.2). The model requires data on average temperature, wind speed, elevation, and dew point.

3.2.3. Regional Flow Model Description

Vertical flow through a homogeneous unsaturated zone can be described by the one-dimensional Richards' equation as:

$$\frac{\partial \theta}{\partial t} = \frac{\partial}{\partial z}\left[K(\theta)\frac{\partial h}{\partial z} - K(\theta) \right] - S \tag{3.5}$$

where θ is volumetric water content; S is ET rate per unit length; $K(\theta)$ is unsaturated hydraulic conductivity as a function of water content; z is elevation in the vertical direction; and t is time.

The UZF package developed for coupling to the MODFLOW code (Niswonger et al., 2006) simplifies equation (3.5) by removing the diffusive term, assuming that the vertical flux is only driven by gravitational forces. The equation solved by UZF using the method of characteristic is:

$$\frac{\partial \theta}{\partial t} + \frac{\partial K(\theta)}{\partial z} + S = 0 \tag{3.6}$$

In general, unsaturated flow modeling using Richards' equation directly requires fine grids and is notable for the large computational efforts required and associated long runtimes (Hunt et al., 2008). Moreover, the required data for the soil-water constitutive relationships are often not readily available for basin scale models. For realistic basin scale simulations, closed-form solutions for simulating unsaturated flow are highly advantageous because there are no restrictions for numerical stability. The kinematic wave approximation of the one-dimensional Richards' equation through a homogeneous unsaturated zone as used in the UZF package provides an alternative that is well suited to large-scale models (Niswonger et al., 2006).

The Brooks and Corey (1964) formula is used to relate unsaturated hydraulic conductivity to water content in the UZF code:

$$K(\theta) = K_s \left(\frac{\theta - \theta_r}{\theta_s - \theta_r} \right)^{\varepsilon} \tag{3.7}$$

where Ks is saturated hydraulic conductivity; θ_r is residual water content; θ_s is saturated water content; and ε is Brooks-Corey exponent used in the UZF code.

Due to the general absence of data that characterize sediment heterogeneity within the unsaturated zone, the assumption of homogeneous unsaturated zone is reasonable in basin scale models (Niswonger and Prudic, 2009). The main model parameters needed by the UZF package include infiltration rate (FINF), vertical saturated hydraulic conductivity (VKS), saturated water content (THTS) and a Brooks-Corey coefficient, epsilon (EPS), which relates conductivity and water content (Table 3.1). Infiltration rate is input as positive values of the R_p obtained from the water balance model for the root zone. The negative flux rate of R_p is simulated as evaporation in the UZF package.

Table 3.1. MODFLOW Input Parameters Used in Text.

Name	Package Used	Description
VKS	UZF	Saturated hydraulic conductivity of soil
EPS	UZF	Brooks-Corey epsilon
FINF	UZF	Infiltration rate
THTS	UZF	Saturated water content
THTI	UZF	Initial water content
S_y	LPF	Specific yield

3.3. Data Sets on Climate, Soils, and Irrigation

Precipitation, temperature, wind speed, solar radiation, and relative humidity data were obtained from China's Monthly Surface Climate Data Set (http://cdc.cma.gov.cn/), which is maintained by China Meteorological Administration (CMA). The data record for most stations started in 1957 and is updated continuously. The meteorological data set is in discrete format, i.e., point values with 23 station locations available in the NCP. To generate estimates of areal ET, point values of these variables were interpolated to a grid with the same cell size as the regional flow model, and ET_a was calculated at each resulting grid cell. Because the station networks in

this study cannot support the semivariogram estimation required by kriging, an inverse distance weighted (IDW) scheme was used in the interpolation procedure.

Monthly mean data values were estimated as the mean of the average monthly maximum and minimum values. Dew point temperature (T_{dew}) was calculated using temperature and relative humidity (Allen, 1998):

$$T_{dew} = \frac{237.7\gamma(T, RH)}{17.27 - \gamma(T, RH)} \tag{3.8}$$

$$\gamma(T, RH) = \frac{17.27T}{237.7 + T} + \ln(RH / 100) \tag{3.9}$$

where T is air temperature in degrees Celsius; and RH is the relative humidity.

NASA's Shuttle Radar Topography Mapping (SRTM) mission (Rabus et al., 2003) produced digital elevation data at 90 m resolution and these data were aggregated to the model grid and used as the elevation input for the ET_a estimation.

Soil texture (including sand, silt and clay contents) and bulk density were obtained from the 1:1,000,000 scale the Chinese Soil Data Set (Institute of Soil Science, Chinese Academy of Sciences). The data set, which is in raster format at 1 km resolution, was aggregated to the grid used in this study. Seven soil hydraulic parameters (θ_s, θ_r, α, n, K_s, K_0, L) in van Genuchten (1980) model were calculated using PTFs developed by Schaap (2001). θ_s and K_s was input in the UZF as VKS and THTS, respectively. The Brooks-Corey epsilon (EPS) in the UZF was calculated as the modified expression derived by Morel-Seytoux et al. (1996) as:

$$\varepsilon = 1 + 2/(1 - 1/n) \tag{3.10}$$

Soil moisture data were obtained from China's Crop Growth Data Set (http://cdc.cma.gov.cn/) maintained by CMA. The dataset contains 104 monitoring stations in the NCP. The data record for most stations starts in 1993 and is updated continuously. The data set

contains water content measured at depths of 10, 20 and 50 cm on the 8th, 18th and 28th day of each month. The soil moisture data in this data set are Relative Gravimetric Water Content (the ratio of water content and field capacity), and the bulk density and field capacity obtained from the soil data set were used to convert the gravimetric water content to volumetric water content.

No accurate irrigation data were available for the NCP. Generally irrigation is applied four or five times during the wheat growing season, and there or four times during the maize growing season and the total irrigation amount for the double crop system is ~4,200 m^3/ha (Liu et al., 2004). In the models, it was assumed that irrigation takes place seven times: five times from March to July, once in September and October, respectively, with 60 mm of irrigation each time.

3.4. Model Setup

As previously noted, a three-layer model was used in this study. In the upper layer soil water is extracted by evaporation and transpiration and groundwater recharge was calculated from equation (1). Percolation water from the upper layer is transmitted through the middle layer to the water table by UZF package. The bottom layer is the saturated zone with flow simulated using MODFLOW.

The simulation period extended from January, 1993 through December, 2008 with 192 monthly stress periods. The spatial discretization of the variably saturated model is the same as that for the regional flow model previously discussed in Chapter 2. The initial condition was inherited from the simulated water level distribution in 1992 from the previous model. Because no detailed monthly water supply data are available, annual pumping data in the previous model were redistributed into each month assuming the irrigation accounts for 70% of annul

exploitation applied in March-July, September, and October with the same irrigation volume for each month. Groundwater withdrawal for industrial and domestic use, which account for 30% of the total exploitation, is distributed into each month equally.

3.5. Results and Discussion

3.5.1. Calculated Evapotranspiration Rates

Temporal variations in ET_a and ET_p are generally consistent with those of precipitation (Figure 3.2). ET_a rates are lowest in winter (November–January) with monthly ET_a rates ranging from 3 to 13 mm. ET_a rates begin to increase in March, when the winter wheat in the NCP turns green, and reaches its highest value up to ~150 mm in July and August. Precipitation is generally lower than estimated ET_a rates, except during the monsoon season when precipitation is similar or a little higher than estimated ET_a rates. Annual ET_a rates obtained by accumulating monthly values range from 520 to 680 mm in 1993 through 2008 (Figure 3.2) and show a similar pattern to annual precipitation. The spatial distribution of ET_a indicates that ET_a decreases from 520–580 mm/yr in the west and north piedmont area to 670-740 mm in the southern NCP (Figure 3.4).

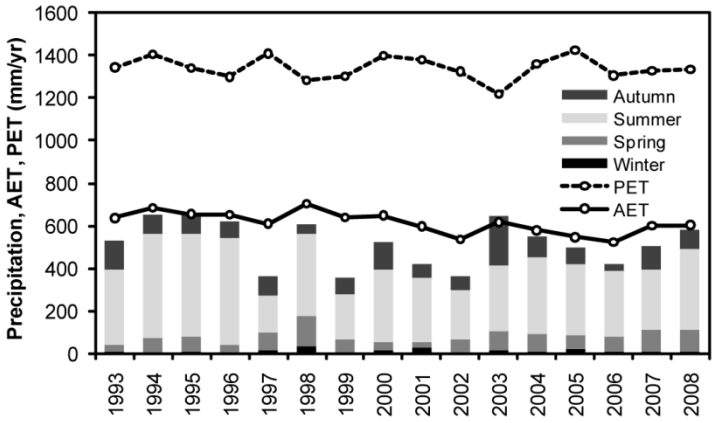

Figure 3.2. Spatially averaged annual PET (dashed line); annual AET (solid line); and seasonal precipitation (stack): winter (December-February), spring (March-May), summer (June-August) and autumn (September-November) from 1993 to 2008 in the NCP.

Recent ET research in the NCP has focused on the spatial distribution of ET_p rates (Mo et al., 2005; Yang et al., 2009; Song et al., 2010). No spatially distributed measured ET_a was obtained in this study to evaluate the estimation error directly. The ranges of estimated ET_p used other methods (Table 3.2) are first converted to ET_a and then are used for comparison. The estimated ET_a in the piedmont area underestimates by ~300 mm/yr compared the measured ET_a by lysimeter. However, measured ET_a is under experimental site condition without water supply restrictions. Due to various irrigation conditions and farmers practice, water demand of the wheat and corn double cropping system cannot be met, the situation that simulated ET_a is less than that measured by the lysimeter at the experimental station is expected. The spatially averaged mean annual ET_a is estimated as ~620 mm/yr, which is close to those estimated by the remote sensing methods.

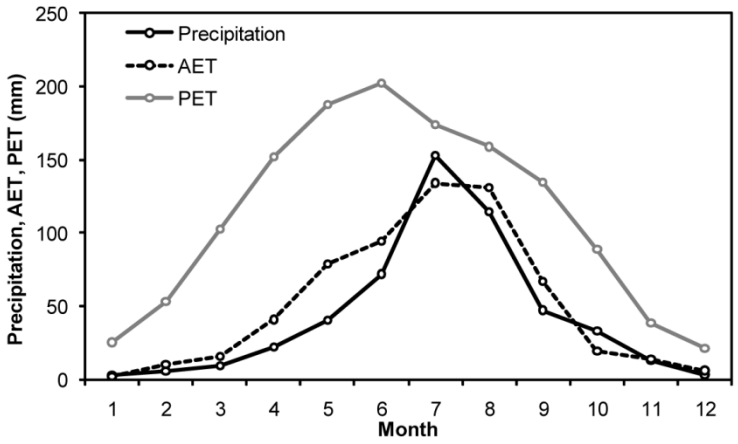

Figure 3.3. Spatially averaged monthly precipitation, AET and PET in the NCP.

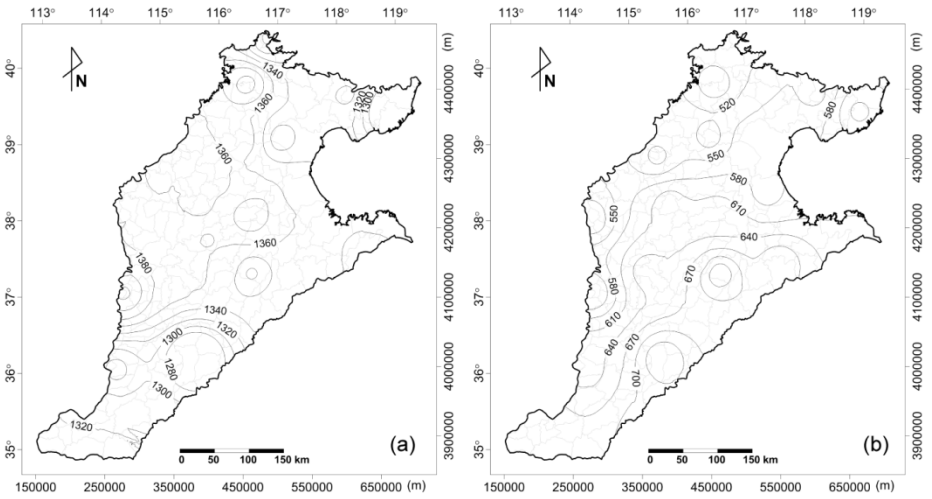

Figure 3.4. Spatial distribution of mean annual (a) potential evaportranspiration and (b) actual evaportranspiration , 1993to2008.

Table 3.2. Annul ET estimated used those estimated using other methods in the NCP.

ET	Method	Period	Source[a]
700-800	SEBS	2002-2003	1
420-932	SVAT	1981-2001	2
880-1100[b]	K_c*ET_0	1961-2006	3,4
870-930	Lysimeter	1995-2000	4
380-850	α*ET_{pan}	2005	5

[a]Source are as follows:1, Zhao et al.(2009); 2, Mo et al.(2005); 3,Song et al.(2010); 4, Liu et al.(2002).

[b]Calculated based on ET_0 from source 3 and K_c from source 4.

The ~700 mm difference between estimated ET_p and ET_a reflects low water availability, which is associated with the irrigation practice in the NCP. The CRAE model assumes that the integration of atmospheric moisture accounts for all surface hydrology; therefore, its application is unaffected in regions where groundwater pumping is present (Hobbins et al., 2009).

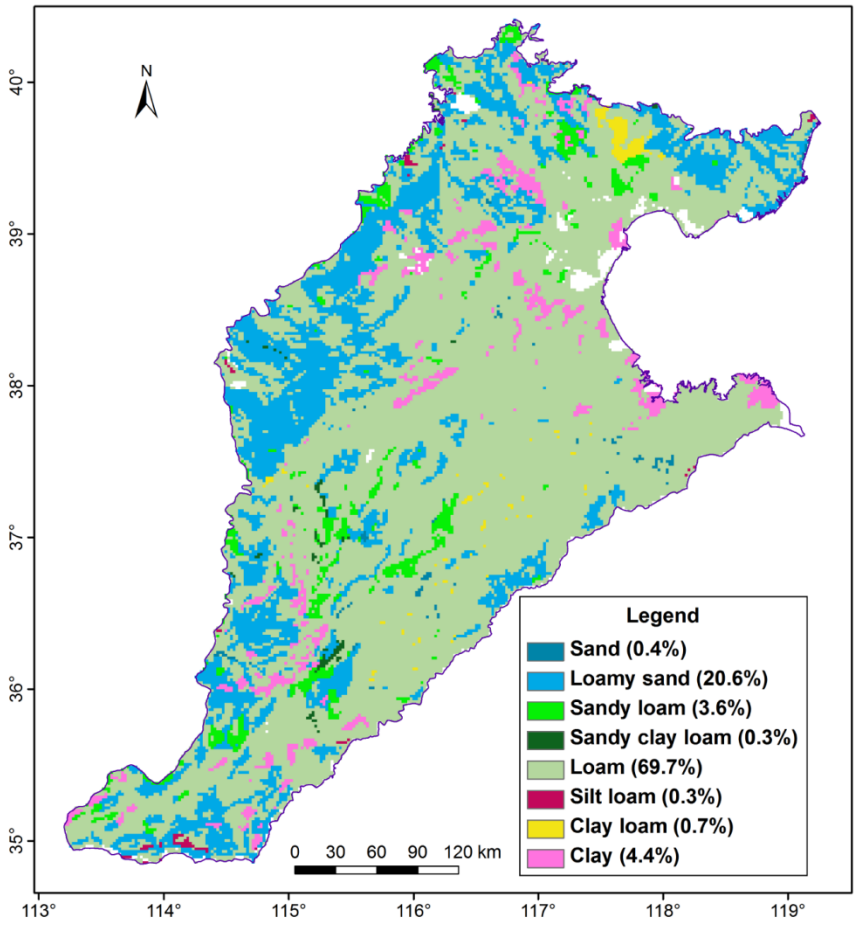

Figure 3.5. USDA (U.S. Department of Agriculture) soil texture types in the NCP, translated from the GSCC (genetic soil classification of China) soil family definitions.

3.5.2. Calculated Recharge Rates

The timing of groundwater recharge depends on temporal distribution of precipitation and irrigation. The magnitude of groundwater recharge depends on precipitation and irrigation, and also ET. Higher groundwater recharge rates occur during the monsoon season from July to September (Figure 3.7). Figure 3.7 also indicates the importance of antecedent soil moisture and timing of rainfall, irrigation and ET in generating recharge. More groundwater recharge is

generated in cold winter season than in spring with more rainfall, irrigation and corresponding higher ET.

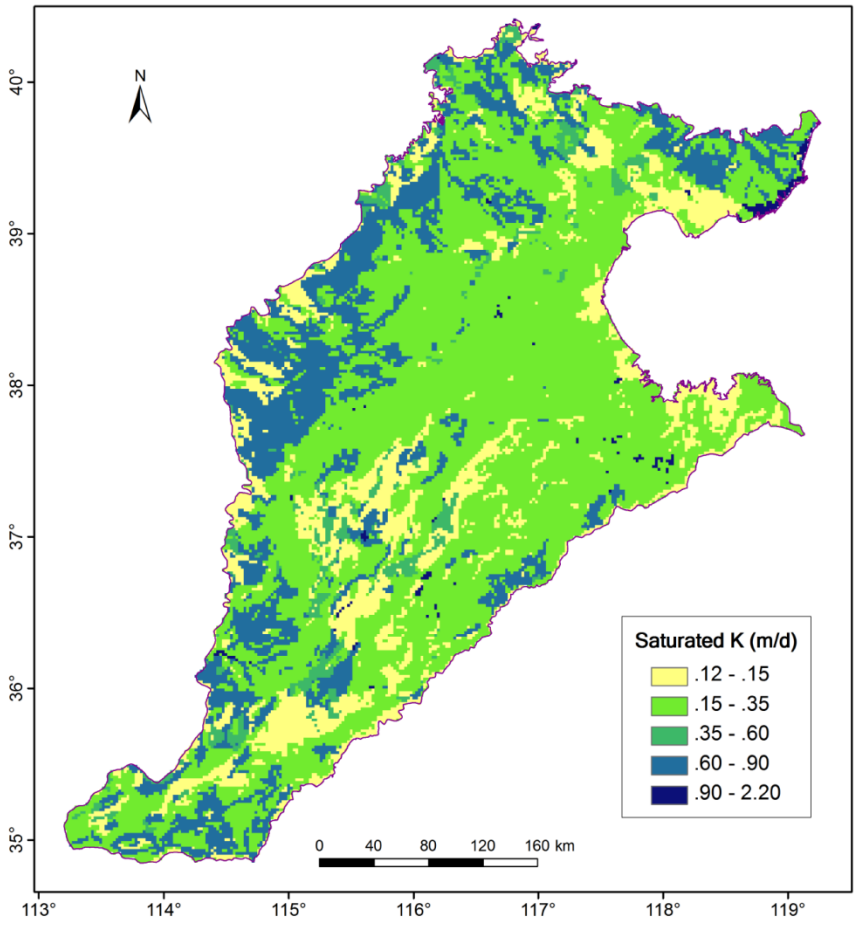

Figure 3.6. Saturated vertical hydraulic conductivity of the soil in the NCP calculated by PTFs developed by Schaap (2001) using soil sand, silt and clay contents, and bulk density.

Simulated mean annual recharge ranges from 0 to 360 mm/yr in the piedmont area (Figure 3.8). This recharge represents up to 44% of the mean annual precipitation plus irrigation. Simulated recharge is high because the recharge is identical to infiltration over the long term. The area with recharge ranging from 0 to 260 mm/yr accounts for 90% of the entire NCP. This recharge represents 30% of mean annual precipitation plus irrigation. Mean annual recharge is

153 mm which represents 18% of the mean annual precipitation plus irrigation. The area with simulated recharge less than mean recharge accounts for ~60% of the entire NCP area and most of it is in the central plain and coastal plain. Mean annual net recharge (recharge minus ET across water table) is 117 mm.

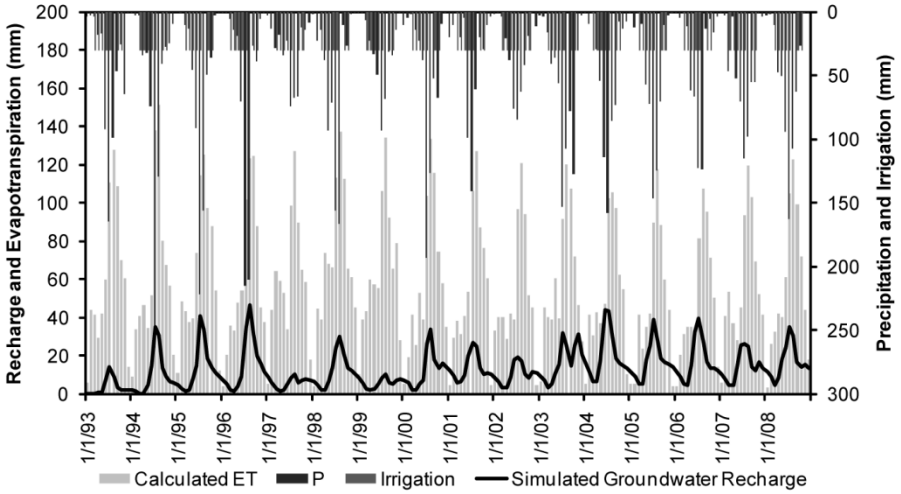

Figure 3.7. Calculated spatially averaged monthly groundwater recharge from 1993 to 2008.

Groundwater recharge for loamy sand ranges from ~9 to ~360 mm/a, i.e., ~1% and ~43% of average annual precipitation plus irrigation, respectively. Groundwater recharge for loam ranges from ~1 to ~270 mm/yr i.e., ~0.1% and ~32%, respectively. Groundwater recharge for clay soils ranges from ~0.1 to ~220 mm/yr, i.e., ~0.01% and ~26%, respectively. Figure 3.9 clearly shows that the groundwater recharge is higher in coarse soils. Due to the uneven distribution of precipitation and irrigation, overlaps in groundwater recharge for loam and clay, loamy sand and loam can also be observed. The range in recharge rates within any soil texture class is greater than that between soil texture classes, suggesting that soil texture is not the primary control on groundwater recharge (Figure 3.9).

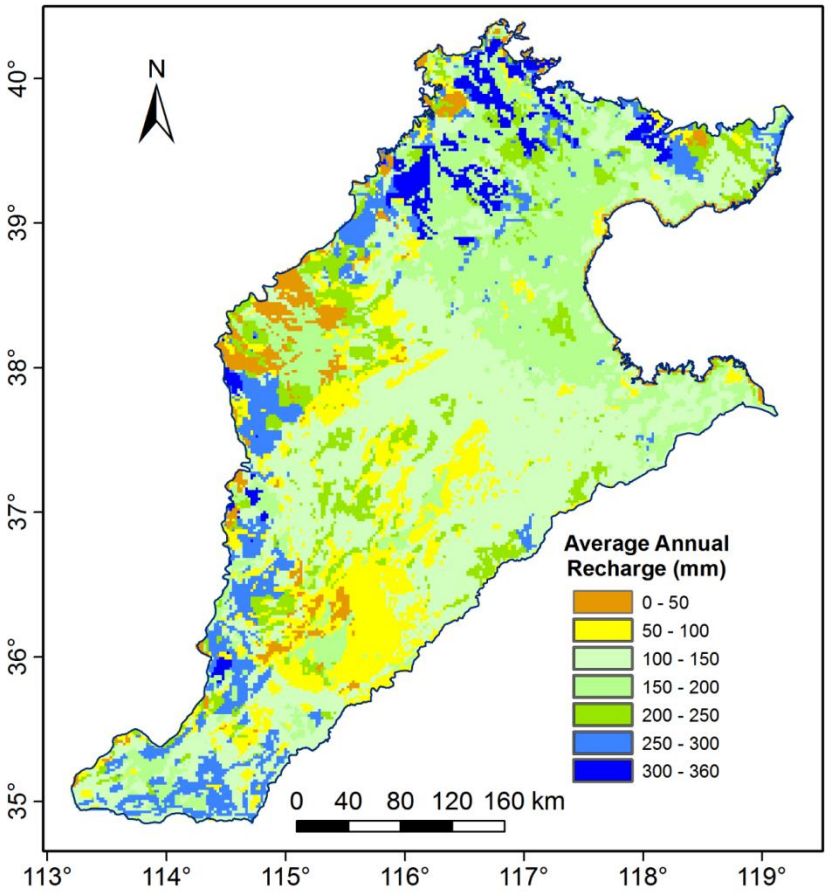

Figure 3.8. Calculated distribution of mean annual groundwater recharge at the water table.

To assess the relationship of recharge with the unsaturated thickness, the recharge coefficient, defined as ratio of mean annual recharge to mean annual precipitation plus irrigation, Rc=R/(P+I), for different unsaturated zone thicknesses is plotted in Figure 3.10. The relation between the recharge coefficient and unsaturated zone thickness indicates that the thickness of unsaturated zone does not affect the recharge over a long time period. The Rc value for the loamy sand is smallest with unsaturated zone thickness less than 2 m, and approaches sable at ~30% with unsaturated zone thickness greater than 2 m. The Rc value for both loam and clay is highest for unsaturated zone thickness of 2–4 m, and decreases with the increasing unsaturated

zone thickness until it reaches some stable value. This kind of relationship between recharge coefficient and unsaturated zone thickness is also observed by the field experiment results in the NCP (Li et al., 2007; Li, 2009). The soil texture is dominated by loamy sand in the entire plain, and therefore generally the unsaturated zone thickness has little impact on the groundwater recharge over the duration of the study period (1993–2008).

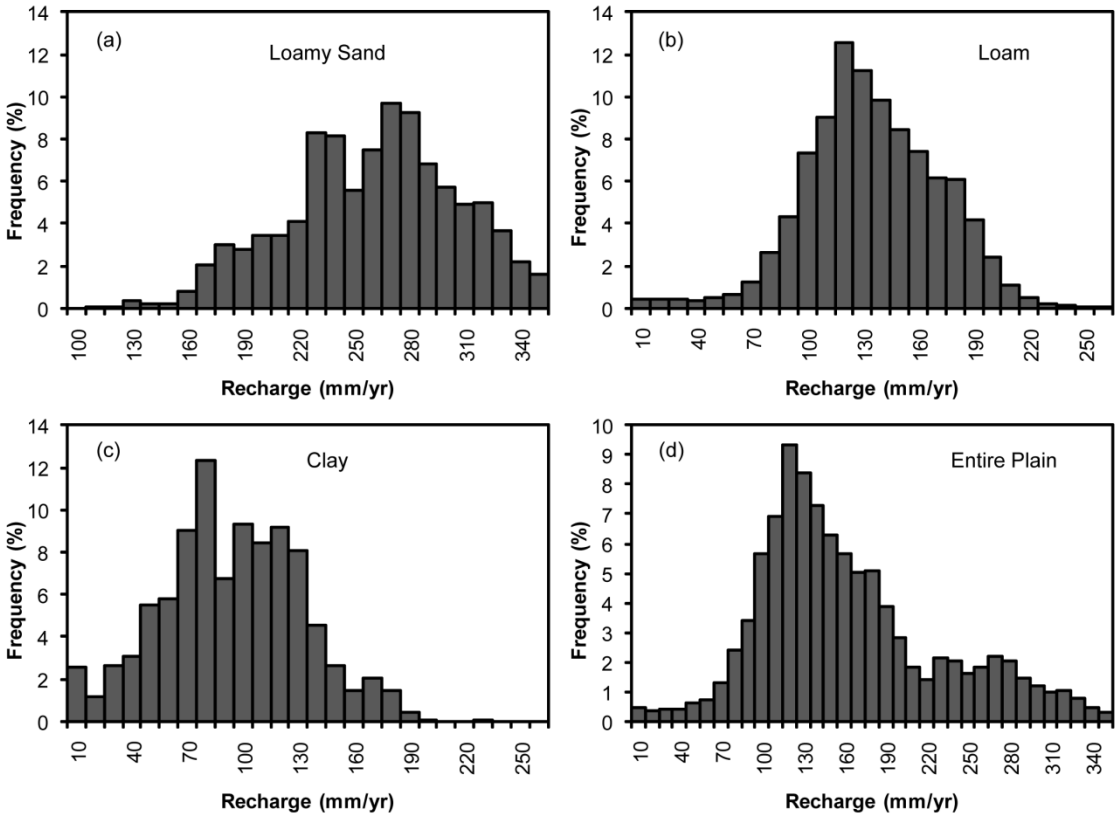

Figure 3.9. Distribution of groundwater recharge for (a) loamy sand, (b) loam, (c) clay and (d) the entire plain.

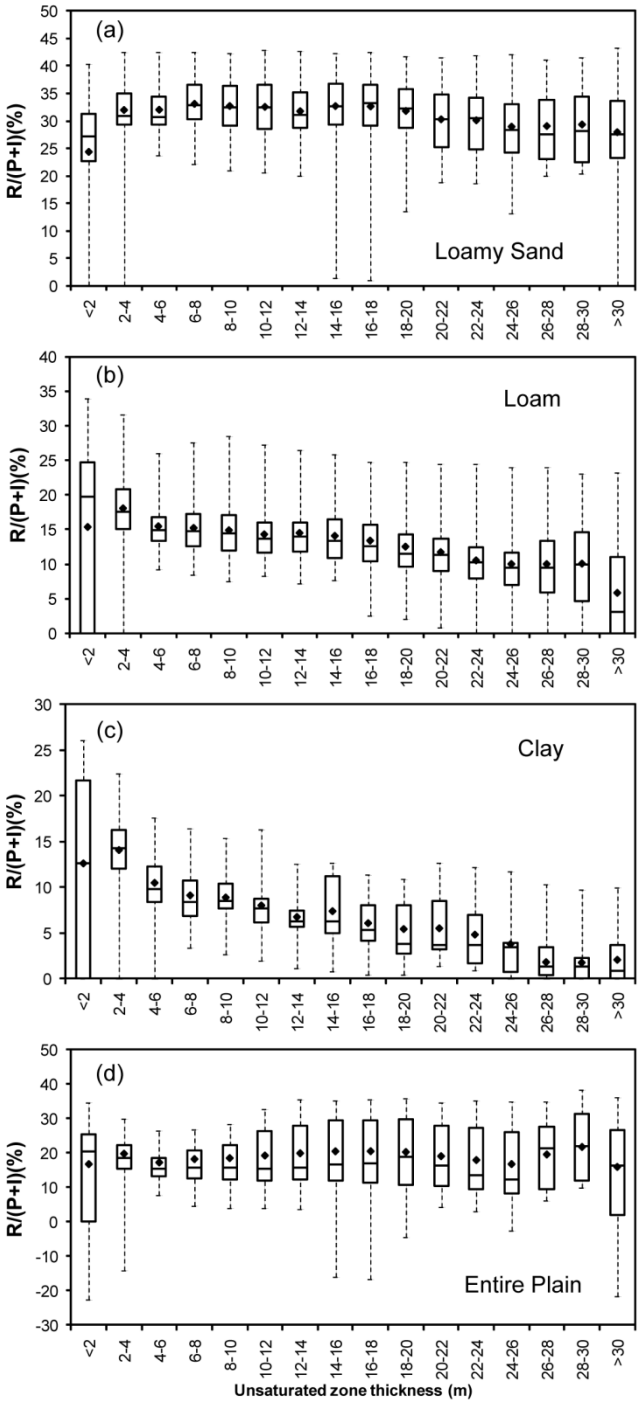

Figure 3.10. Mean annual recharge as a percentage of mean annual precipitation plus irrigation at different unsaturated zone thickness.

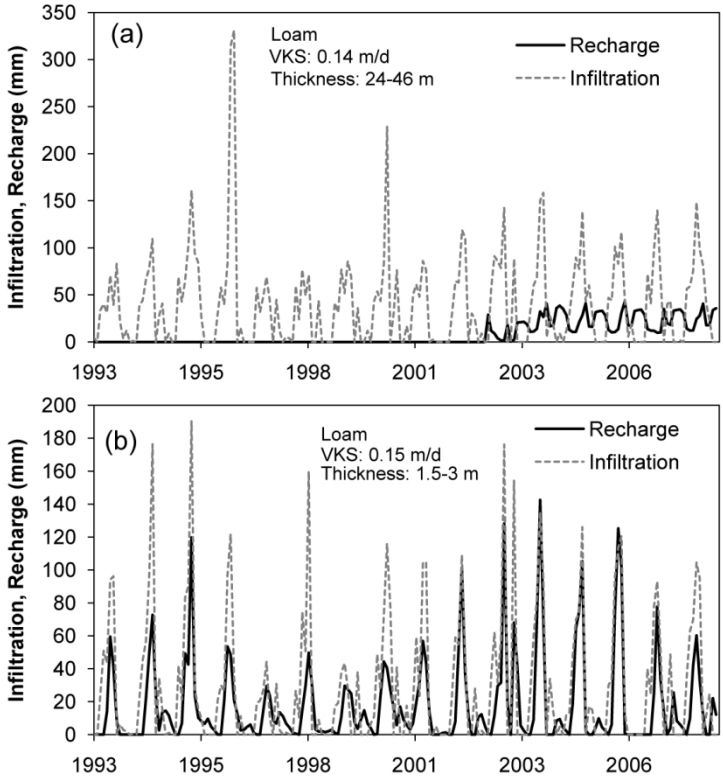

Figure 3.11. Variation of monthly recharge and infiltration with time at two observation locations: (a) in the piedmont area with unsaturated thickness of up to 46 m, and (b) in the central plain with unsaturated zone thickness of up to 3 m.

The simulated monthly recharge variations at two observation model cells located in the piedmont area and central plain are presented in Figure 3.11. The soil texture types at both locations are loam and the calculated vertical hydraulic conductivity are 0.14 and 0.15 m/d, respectively. The thicknesses of unsaturated zone range from 24 to 46 m and 1.5 to 3 m during the simulation period, respectively. It indicates clearly that the unsaturated zone has effect both on temporal distribution and magnitude of the recharge arrival at groundwater table. The thick unsaturated zone not only delayed the arrival time of recharge and smoothed the temporal variations, but also reduced the amount of recharge arriving at the water table. Thus, in thicker

unsaturated zones, both the amount and the timing of the local recharge estimated by the approach which applies the infiltration leaving the root zone to the water table directly will be less realistic.

3.5.3. Sensitivity and Uncertainty Analysis of Calculated Recharge Rates

The ratio of mean annual groundwater recharge to precipitation plus irrigation is used to calculate parameter sensitivity for UZF. A series of simulations were performed in which individual parameters and initial conditions were multiplied by a factor ranging from 0.1 to 2.5 for saturated water content (THTS), 0.5 to 2.5 for initial water content (THTI), and 0.1 to 10 for other parameters (S_y, VKS and EPS), while other parameters and initial conditions were maintained at their base case value (values used in recharge simulation). The effect of changing these parameters on the simulated ratio was analyzed (Figure 3.12). Factors of 0.3 and 0.4 multiplied by the EPS did not converge and could not be used in the evaluation. Initial water content is the most sensitive parameter for the UZF. Increasing the THTI by a factor of 2.5 increases recharge by up to a factor of 10. This also indicates that antecedent soil moisture is of great importance in groundwater recharge. Recharge rates are also highly sensitive to specific yield (S_y). In addition to using S_y to calculate water storage change in the saturated zone, UZF additionally use S_y to calculate wetting front velocity and amount of water available to be captured by a rising water table. Groundwater recharge is inversely related to EPS which is also has highly sensitive to THTS and VKS. EPS is the only parameter with higher sensitivity than other parameters when decreasing.

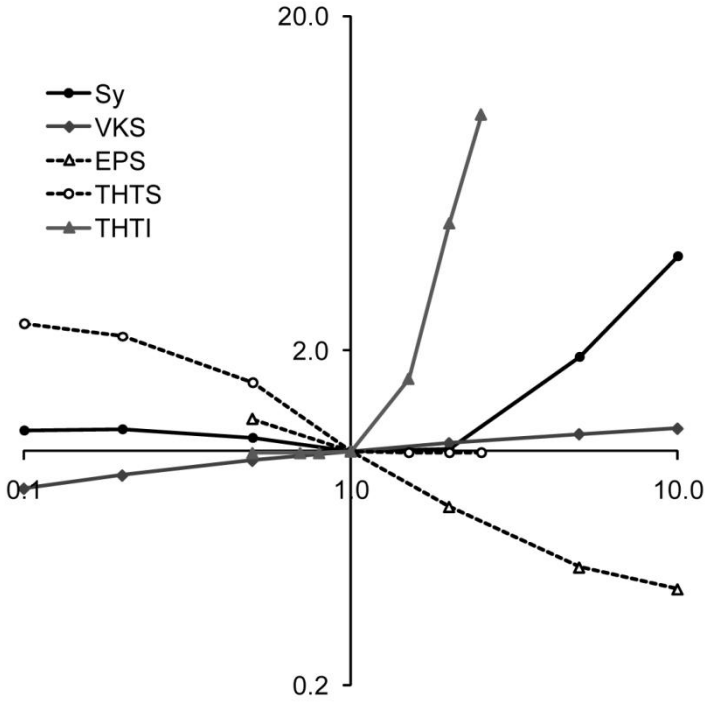

Figure 3.12. Effect of model parameters and initial conditions (expressed as a fraction of base case) on the computed recharge (expressed as the ratio of mean annual recharge to precipitation plus irrigation).

3.5.4. Arrival Time of Percolating Water to Groundwater

The time required for downward flux to travel from the base of the root zone to the water table is referred as water travel time in this paper. In the UZF model, it is calculated as the time when water reaches the water table. To study the effects of groundwater table depth and soil hydraulic properties on travel time distribution, the statistic criterion of the initial time lag (e.g., the time delay between beginning of infiltration and first arrival of recharge at the water table) for different soil textures with varying unsaturated zone thicknesses is plotted in Figure 3.13. Due to continuous decline of the water table in the NCP, the travel time is expected increase with time. The initial time lag is insensitive to unsaturated zone thickness for the loamy sand. The

mean time lag increases from 0.6 years for unsaturated zone thickness of less than 2 m to 3 years for greater than 30 m. The range in time lags remains relatively low. A clear non linear positive relationship between lag time and unsaturated zone thickness is revealed for loam. The mean time lag increases from 0.4 years for unsaturated zone thickness of less than 2 m to 8 years for greater than 30 m, and the time lag variation also increases with unsaturated zone thickness. For clay, the time lag increases with unsaturated zone thickness of less than 10 m, and remains at nearly the same value with unsaturated zone thickness from 10 to 26 m, and shows an increasing trend again with unsaturated zone thickness greater than 26 m.

3.5.5. Validation of Calculated Recharge Rates

The comparison of the simulated water level and measured water levels in the 105 observations wells, total 13900 observation values, is presented in Figure 3.14. The root mean square error (RMSE) is ~10 m. This result is acceptable regarding the variation range of water levels (-18.2 to 92.5 m).

An effective recharge of 117 mm/yr is quite high compared to mean annual precipitation of ~520 mm. Because the fraction of precipitation that contributes to recharge ranges from ~1% to ~20% (Chen, 1999) this result suggests that a part of the recharge comes from the irrigation derived from the groundwater pumping. The deficit between pumping (~160 mm/yr) and net recharge of ~40 mm/yr, divided by the area weighted specific yield of 0.075 results in a water table decline rate of ~0.5 m/yr.

The groundwater recharge rate estimated by other methods is listed in Table 3.3, and all estimates had account for the effect of irrigation. Although the range of estimated recharge rates is quite wide using different methods, estimated groundwater recharge rates are comparable with

those estimated by other techniques. Moreover, the estimated recharge in this study is validated by the saturated zone flow modeling, and should be more reliable.

Table 3.3. Annul local and regional recharge rates estimated used other methods in the NCP.

Region	R (mm/yr)	Method[a]	Source[b]
Piedmont Area	150-292	GD	1
	170-180	UFM	2
	10-200	CMB	3
	50-1090	UFM	4
	300	GD	7
Alluvial Plain	0-238	GD	1
	140-155	UFM	2
Coastal Plain	106-113	GD	1
	89	UFM	2
Entire Plain	147	FPI	5
	103	FPI	6

[a]Estimation methods include: UFM, unsaturated flow simulation; CMB, chloride mass balance; GD, groundwater dating, age gradient derived from tracers (e.g., Tritium and bromide); FPI, fraction of precipitation and irrigation.

[b]Source are as follows:1, Wang et al., (2008); 2, Lu et al., (2011); 3,Liu et al., (2009); 4, Kendy et al., (2004); 5, Chen, (1999); 6, Ren, (2007); and 7, von Rohden et al., (2010).

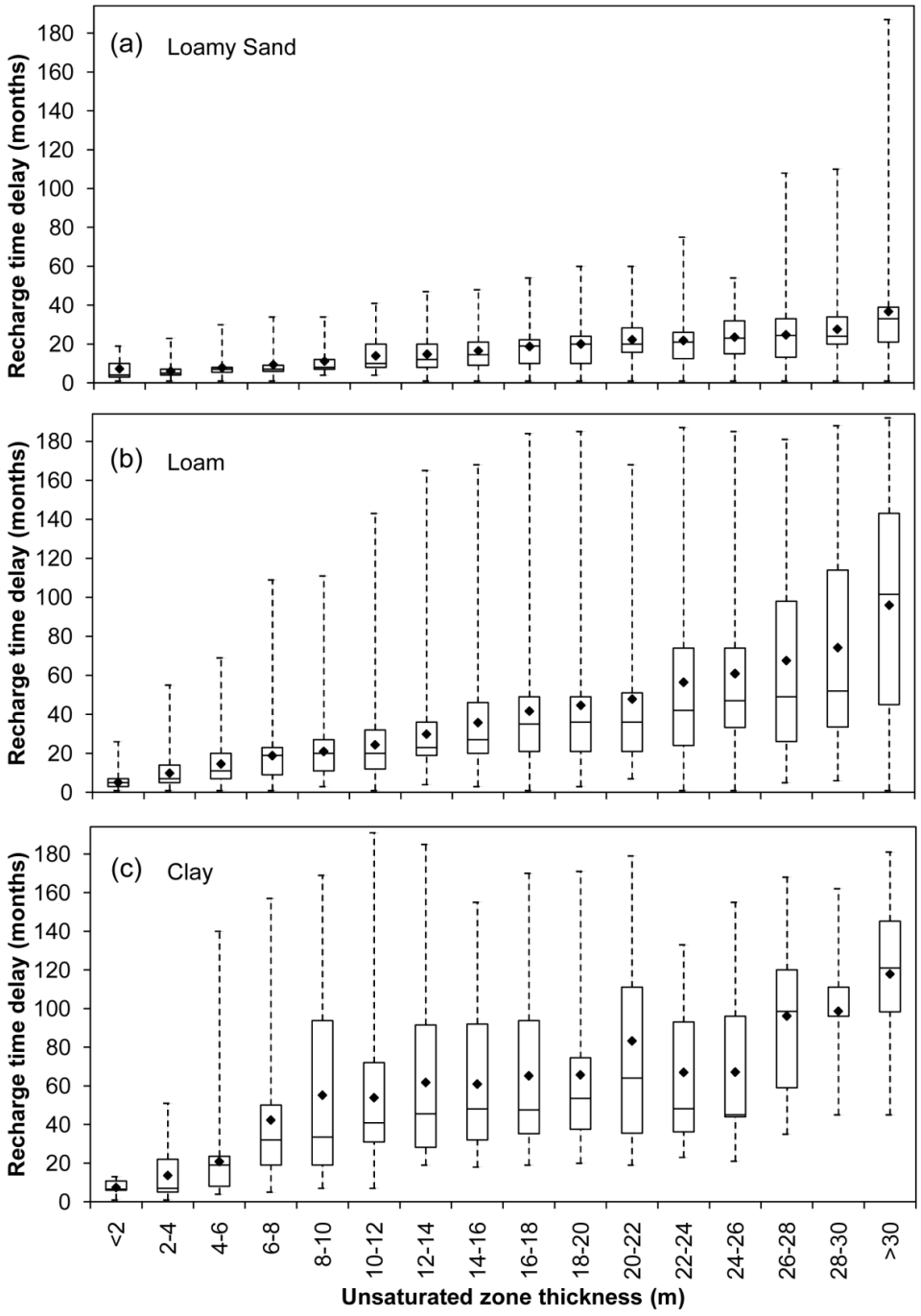

Figure 3.13. Statistical distribution of time delay of recharge reaching the water table for (a) Loamy sand, (b) Loam and (c) Clay at different unsaturated zone thicknesses.

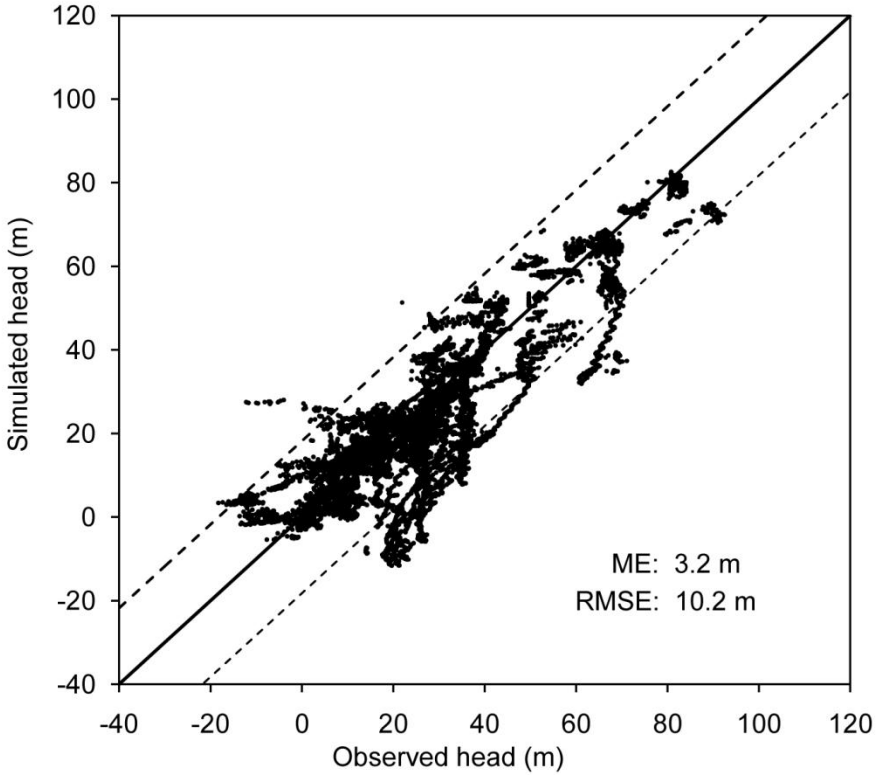

Figure 3.14. Comparison of calculated and observed water levels from 1993 through 2008 at 105 observations wells, a total of 13900 monthly observation values in model layer 1, which represents the shallow aquifer zone. Dotted lines indicate 95% prediction intervals.

3.6. Conclusion

A soil water balance model coupled with a variably saturated flow models is used to estimate the groundwater recharge in the NCP. The estimated recharge rates in the NCP range from up to 360 mm in the piedmont area to up to 260 mm in the middle and coastal plain. The estimated average mean annual groundwater recharge is 153 mm, which represent 18% of the average annual precipitation plus irrigation. The net recharge (recharge minus evaporation from the water table) is 117 mm/yr.

The model results indicate clearly that the unsaturated zone has affect on both temporal distribution and magnitude of the recharge arrival at groundwater table. The time lag of the groundwater recharge in the NCP ranges 0 to 10 years where the current unsaturated zone thickness is greater than 30 m.

The fundamental cause of water depletion in the NCP is the higher water demand of the wheat and maize double cropping system than the precipitation allows. The groundwater system is in a net discharge state because the total pumping exceeds the effective recharge rate. The deficit results in an annual water table decline of 0.5 m from 1993 to 2008, the duration analyzed in this study.

Acknowledgements

This work was supported by the National Basic Research Program of China (grant #2006CB403404) and National Natural Science Foundation of China (grant #40911130505). We appreciate the data support from China Geological Survey and China Institute of Water Resources and Hydropower Research.

References

Bouchet, R.J. 1963. Evapotranspiration réelle et potentielle, signification climatique. IAHS Publ 62, no. 134-142.

Brooks, R.H., A.T. Corey, and S.U. Colorado. 1964. Hydraulic properties of porous media.

Chen, W. 1999. Groundwater in Hebei Province. Beijing: Seismological Press. (in Chinese)

Chen, M., and F. Ma. 2002. Groundwater Resources and the related Environment in China. Beijing: Earthquake Press. (in Chinese)

Delin, G.N., R.W. Healy, D.L. Lorenz, and J.R. Nimmo. 2007. Comparison of local- to regional-scale estimates of ground-water recharge in Minnesota, USA. *Journal of Hydrology* 334, no. 1-2: 231-249.

Gee, G.W., and D. Hillel. 1988. Groundwater recharge in arid regions: Review and critique of estimation methods. Hydrological Processes 2, no. 3: 255-266.

Hansen, S., H.E. Jensen, N.E. Nielsen, and H. Svendsen. 1990. DAISY-Soil plant atmosphere system model, The National Agency for Environmental Protection, Copenhagen, Denmark.

Healy, R.W., and P.G. Cook. 2002. Using groundwater levels to estimate recharge. *Hydrogeology Journal* 10, no. 1: 91-109.

Hobbins, M.T., J.A. Ramírez, T.C. Brown, and L.H.J.M. Claessens. 2001. The complementary relationship in estimation of regional evapotranspiration: The complementary relationship areal evapotranspiration and advection-aridity models. *Water Resources Research* 37, no. 5: 1367-1387.

Hunt, R.J., D.E. Prudic, J.F. Walker, and M.P. Anderson. 2008. Importance of unsaturated zone flow for simulating recharge in a humid climate. *Ground Water* 46, no. 4: 551-560.

Kendy, E., P. Gérard-Marchant, M.T. Walter, Y. Zhang, C. Liu, and T.S. Steenhuis. 2003. A soil-water-balance approach to quantify groundwater recharge from irrigated cropland in the North China Plain. *Hydrological Processes* 17, no. 10: 2011-2031.

Kendy, E., Y. Zhang, C. Liu, J. Wang, and T. Steenhuis. 2004. Groundwater recharge from irrigated cropland in the North China Plain: case study of Luancheng County, Hebei Province, 1949-2000. *Hydrological Processes* 18, no. 12: 2289-2302.

Keese, K.E., B.R. Scanlon, and R.C. Reedy. 2005. Assessing controls on diffuse groundwater recharge using unsaturated flow modeling. *Water Resources Research* 41, W6010.

Li, Y., and X. Li. 2007. Study on Precipitation Infiltration Recharge with Groundwater Depth Variation. *Journal of China Hydrology* 5: 58-60. (in Chinese with English abstract)

Li, J. 2009. An analysis of the coefficient of replenishment from infiltration of precipitation. *Hydrogeology & Engineering Geology* 2: 29-33. (in Chinese with English abstract)

Liggett, J., and D. Allen. 2009. Comparing approaches for modeling spatially distributed direct recharge in a semi-arid region (Okanagan Basin, Canada). Hydrogeology Journal.

Liggett, J., and D. Allen. 2010. Comparing approaches for modeling spatially distributed direct recharge in a semi-arid region (Okanagan Basin, Canada). *Hydrogeology Journal* 18, no. 2: 339.

Lin, W., H. Dong, G. Wang, Z. Su, and L. Chen. 2008. Regional evapotranspiration estimation in hebei plain based on remote sensing. *Remote Sensing for Land & Resources* 1: 86-90. (in Chinese with English abstract)

Liu, C., X. Zhang, and Y. Zhang. 2002. Determination of daily evaporation and evapotranspiration of winter wheat and maize by large-scale weighing lysimeter and micro-lysimeter. Agricultural And Forest Meteorology 111, no. 2: 109-120.

Liu, J., Z. Chen, Z. Zhang, Y. Fei, F. Zhang, J. Chen, and Z. Wang. 2009. Estimation of Natural Groundwater Recharge in the Hutuo River Alluvial-Proluvial Fan Using Environmental Tracers. *Geological Science and Technology Information* 6: 114-118. (in Chinese with English abstract)

Liu, C., and Z. Wei. 1989. Agricultural Hydrology and Water Resources in the North China Plain. Beijing: Science Press. (in Chinese)

Liu, C., J. Chen, and J. Qiao. 2004. A survey of irrigation status in the well irrigation distict in the North Chian Plain. *Water Resources Development Research* 10: 38-41 (in Chinese).

Liu, S., R. Sun, Z. Sun, X. Li, and C. Liu. 2004. Comparison of Different Complementary Relationship Models for Regional Evapotranspiration Estimation. *Acta Geographica Sinica* 59, no. 3: 331-340. (in Chinese with English abstract)

Lu, X., M. Jin, M.T. van Genuchten, and B. Wang. 2011. Groundwater Recharge at Five Representative Sites in the Hebei Plain, China. *Ground Water* 49, no. 2: 286-294.

Mo, X., L. Xue, and Z. Lin. 2005. Spatio-temporal Distribution of Crop Evapotranspiration from 1981-2001 over the North China Plain. *Journal of Natural Resources* 20, no. 2: 181-187. (in Chinese with English abstract)

Morel-Seytoux, H.J., P.D. Meyer, M. Nachabe, and J. Touma. 1996. Parameter equivalence for the Brooks-Corey and van Genuchten soil characteristics: Preserving the effective capillary drive. *Water Resources Research* 32, no. 5: 1251-1258.

Morton, F.I. 1983. Operational estimates of areal evapotranspiration and their significance to the science and practice of hydrology. *Journal of Hydrology* 66, no. 1-4: 1-76.

Morton, F.I., F. Ricard, and S. Fogarasi. 1985. Operational estimates of areal evapotranspiration and lake evaporation: Program WREVAP. Inland Waters Directorate, National Hydrology Research Institute, Environment Canada. Ottawa, Ont.

Niswonger, R.G., D.E. Prudic, and R.S. Regan. 2006. Documen- tation of the Unsaturated-Zone Flow (UZF1) Package for modeling unsaturated flow between the land surface and the water table with MODFLOW-2005. U.S. Geological Survey Techniques and Methods 6-A19.

Niswonger, R.G., and D.E. Prudic. 2009. Comment on" Evaluating Interactions between Groundwater and Vadose Zone Using the HYDRUS-Based Flow Package for MODFLOW" by Navin Kumar C. Twarakavi, Jirka Simunek, and Sophia Seo. *Vadose Zone Journal* 8, no. 3: 818.

Pachepsky, Y., and W.J. Rawls. 2004. *Development of pedotransfer functions in soil hydrology*, Elsevier.

Panday, S., and P.S. Huyakorn. 2008. MODFLOW SURFACT: a state-of-the-art use of vadose zone flow and transport equations and numerical techniques for environmental evaluations. *Vadose Zone Journal* 7, no. 2: 610.

Poulovassilis, A., M. Anadranistakis, A. Liakatas, S. Alexandris, and P. Kerkides. 2001. Semi-empirical approach for estimating actual evapotranspiration in Greece. *Agricultural Water Management* 51, no. 2: 143-152.

Refsgaard, J.C., B. Storm, and V.P. Singh. 1995. MIKE SHE. In *Computer Models of Watershed Hydrology*, ed. Singh, V.P. Highlands Ranch, Colorado: Water Resources Publications.

Samper, F.J., and M.A. Garc A-Vera. 1992. BALAN v. 10: program for calculating water and salt balances in soil. Departamento de Ingenier á del Terreno. Universidad Polit écnica de Catalu ña, Spain.

Scanlon, B.R., R.W. Healy, and P.G. Cook. 2002. Choosing appropriate techniques for quantifying groundwater recharge. *Hydrogeology Journal* 10, no. 1: 18-39.

Schaap, M.G., F.J. Leij, and M.T. van Genuchten. 2001. ROSETTA: a computer program for estimating soil hydraulic parameters with hierarchical pedotransfer functions. *Journal of Hydrology* 251, no. 3-4: 163-176.

Schroeder, P.R., T.S. Dozier, P.A. Zappi, B.M. McEnroe, J.W. Sjostrom, and R.L. Peyton. 1994. The hydrologic evaluation of landfill performance (HELP) model: user's guide for version 3. EPA/600/R-94/168a. Office of Research and Development, U.S. Environmental Protection Agency, Washington, DC.

Seo, H.S., J. Šimůnek, and E.P. Poeter. 2007. Documentation of the HYDRUS package for MODFLOW-2000, the US Geological Survey modular ground-water model. GWMI 2007-01. Int. Ground Water Modeling Ctr., Colorado School of Mines, Golden.

Shang, S.H., L.Y. Sun, and Z.C. Hao. 2008. Using Complementary Relationship to Estimate Monthly Evapotranspiration in Arid Oasis. *Journal of China Hydrology* 3: 67-69 (in Chinese with English abstract).

Simmers, I. 1987. *Estimation of natural groundwater recharge*, Springer.

Small, E.E. 2005. Climatic controls on diffuse groundwater recharge in semiarid environments of the southwestern United States. *Water Resources Research* 41, W4012.

Song, X.F., S.Q. Wang, G.Q. Xiao, Z.M. Wang, X. Liu, and P. Wang. 2009. A study of soil water movement combining soil water potential with stable isotopes at two sites of shallow groundwater areas in the North China Plain. *Hydrological Processes* 23, no. 9: 1376-1388.

Song, Z.W., H.L. Zhang, R.L. Snyder, F.E. Anderson, and F. Chen. 2010. Distribution and Trends in Reference Evapotranspiration in the North China Plain. *Journal of Irrigation And Drainage Engineering-Asce* 136, no. 4: 240-247.

Sophocleous, M.A. 1991. Combining the soilwater balance and water-level fluctuation methods to estimate natural groundwater recharge: Practical aspects. *Journal of Hydrology* 124, no. 3: 229-241.

Sophocleous, M. 1992. Groundwater recharge estimation and regionalization: the Great Bend Prairie of central Kansas and its recharge statistics. *Journal of Hydrology* 137, no. 1: 113-140.

Thoms, R.B., R.L. Johnson, R.W. Healy, and S.U. Geological. 2006. User's guide to the variably saturated flow (VSF) process for MODFLOW. U.S. Geological Survey Techniques and Methods 6-A18.

U.S. Geological Survey. 2008. Documentation of computer program INFIL 3. 0 - Distributed-parameter watershed model to estimate net infiltration below the root zone. U.S. Geological Survey Scientific Investigations Report 2008-5006.

van Walsum, P.E.V., and P. Groenendijk. 2008. Quasi steady-state simulation of the unsaturated zone in groundwater modeling of lowland regions. *Vadose Zone Journal* 7, no. 2: 769.

von Rohden, C., A. Kreuzer, Z. Chen, R. Kipfer, and W. Aeschbach-Hertig. 2010. Characterizing the recharge regime of the strongly exploited aquifers of the North China Plain by environmental tracers. *Water Resources Research* 46, no. 5: W5511.

Wang, B.G., M.G. Jin, J.R. Nimmo, L. Yang, and W.F. Wang. 2008. Estimating groundwater recharge in Hebei Plain, China under varying land use practices using tritium and bromide tracers. *Journal of Hydrology* 356, no. 1-2: 209-222.

Wang, T., V.A. Zlotnik, J. Imunek, and M.G. Schaap. 2009. Using pedotransfer functions in vadose zone models for estimating groundwater recharge in semiarid regions. *Water Resources Research* 45, no. 4: W4412.

Wösten, J., Y.A. Pachepsky, and W.J. Rawls. 2001. Pedotransfer functions: bridging the gap between available basic soil data and missing soil hydraulic characteristics. *Journal of Hydrology* 251, no. 3-4: 123-150.

Xu, C.Y., and V.P. Singh. 2005. Evaluation of three complementary relationship evapotranspiration models by water balance approach to estimate actual regional evapotranspiration in different climatic regions. *Journal of Hydrology* 308, no. 1-4: 105-121.

Xu, Y., and H.E. Beekman. 2003. Groundwater recharge estimation in Southern Africa. UNESCO IHP Series No. 64.

Yang, G., Z. Wang, H. Wang, and Y. Jia. 2009. Potential evapotranspiration evolution rule and its sensitivity analysis in Haihe River basin. *Advances in Water Science* 20, no. 3: 409-415. (in Chinese with English abstract)

Zhang, G. 1992. Measuring groundwater recharge through thick unsaturate zone. *Ground Water* 2: 81-84. (in Chinese)

Zhang, G., Y. Fei, and K. Liu. 2004. Evolution of and countermeasure for the groundwater in the Haihe Plain. Beijing: Science Press. (in Chinese)

Zhang, G., Y. Fei, J. Shen, and L. Yang. 2007. Influence of unsaturated zone thickness on precipitation infiltration for recharge of groundwater. *Journal of Hydraulic Engineering* 38, no. 5: 611-617. (in Chinese with English abstract)

Zhao, J., J. Shao, Y. Cui, and Z. Xie. 2009. Estimating Regional Evapotranspiration in North China Plain with Remote Sensing Method. *Urban Geology* 4, no. 1: 43-48. (in Chinese with English abstract)

CHAPTER 4

SUSTAINABILITY EVALUATION OF DEEP GROUNDWATER IN THE NORTH CHINA PLAIN BY GROUNDWATER FLOW AND AGE SIMULATION

Abstract

Groundwater in the deep aquifer beneath an intermediate, brackish flow zone across the central and coastal parts of the North China Plain (NCP) is the primary water resource for irrigation and domestic use. Accurate information about the groundwater recharge regime and alternation by extensive groundwater abstraction is necessary for sustainability assessment for the deep groundwater in the NCP. This paper presents the application of direct simulation of groundwater mean ages to the NCP through the use of a solute transport model. This provides an effective means to constrain the regional flow model and improve the estimation of flow parameters, including recharge rates. The simulated age distribution and the calibrated flow model are then used to characterize the flow regime under natural conditions and an altered state by groundwater pumping. The model results indicate that simulated groundwater ages in the NCP are affected by both paleo-hydrologic conditions and extensive groundwater pumping. Flow paths analysis, water budget calculation and simulated groundwater age distribution show that the lateral flow to the deep aquifer in the NCP is limited and that the primary inflow is the downward leakage from the shallow aquifer, which is enhanced by the extensive development of the deep aquifer. Transient flow modeling reflecting the post-development conditions confirms that widely distributed vertical recharge and resulting flow have become the dominant processes shaping the flow patterns both in the shallow and deep aquifers in the NCP.

4.1. Introduction

Understanding groundwater circulation and renewability is essential to evaluate how sustainable groundwater resources are under natural and human-induced conditions in this region. Groundwater age (or residence time) is the average over the water molecules in a sample of the time elapsed since recharge, integrating the effects of advection, hydrodynamic mixing and geochemical reaction along the flow path (Goode, 1996; Bethke and Johnson, 2002a). The groundwater age data can provide highly valuable information about the circulation and historical evolution of the groundwater, such as the recharge rate, flow velocity and flow path (Smethie et al., 1992; Zoellmann et al., 2001; Pint et al., 2003; Xu and Beekman, 2003; Sturchio et al., 2004). Therefore, the groundwater age can be used to help calibrate groundwater flow models, understand the groundwater flow regime, and assess the renewability, and hence the sustainability of the groundwater (Sultan et al., 2000; Zhu, 2000; Sanford et al., 2004; Chen et al., 2005; Bethke et al., 2008).

Although various techniques based on environmental tracers can be used to date groundwater (Clark and Fritz, 1997; Kazemi et al., 2006), they commonly cannot treat the water sample as mixtures or give the age distribution. The spatial distribution of groundwater age is often obtained by interpolation of measured sample ages (Chen, 2001). To quantify the distribution of ages in aquifers, several types of mathematical models have been developed during the past decades. A classical age modeling is lumped-parameter models (Richter et al., 1993; Amin and Campana, 1996). This analytical model assumes that the specific age distributions describing piston flow, exponential mixing or dispersive mixing are known beforehand, and the inverse problem is solved by fitting the model results and measured age. Given a known velocity field, age distribution considering only advection can be calculated by

an analytical method or particle tracking algorithms. However, the resulting advective ages ignore the effect of dilution, dispersion and mixing along the flow path (Bethke and Johnson, 2002a and 2002b). Moreover, the particle tracking method cannot calculate the residence-time distributions, since the moving groundwater volumes are not associated to the simulated ages (Kazemi et al., 2006).

More elaborate methods use the advective-dispersive equation to describe the age transport through aquifers. Goode (1996) derived the transport equation with a source term and with mean age as the primary variable. Engesgaard and Molson (1998) applied the technique to interpret a regional flow system using tritium as tracer and found the simulated age compared well with observed tritium data. Castro and Goblet (2005) found that direct simulation of the mean age filed employing this method yielded the most consistent results when mixing process in a particular groundwater system is not negligible. Varni and Carrera (1998) made further developments using moment analysis and established equations for moments of groundwater age. Bethke and Johnson (2002b) showed that the contribution of aquitards to groundwater age depends only on the ratio of aquitard to aquifer flow volumes and derived an idealized groundwater age equation in aquitard. Ginn (1999) derived a four dimensional (space and age) advection-dispersion governing equation for groundwater age, where transport in the age dimension is with unit velocity and zero dispersion-diffusion, and showed that previous age equations (Goode, 1996; Varni and Carrera, 1998; Bethke and Johnson, 2002b) can be derived from this governing equation (Ginn et al., 2009). These mathematical models have paved the way for regional scale simulation of groundwater age. The link between these efforts and the isotopic age data can then help to verify the model results and to interpret the isotopic ages more confidently.

In the North China Plain, direct measurements of base flow are often not available. It is well known that simulated water levels are only sensitive to the ratios of recharge and hydraulic conductivity, and better model calibration can be performed using known flow rates (e.g. groundwater discharge rate to the surface water). The distribution of groundwater age can be used to constrain flux and hence recharge.

In the NCP, environmental traces have been used to determine the recharge rate (Wang et al., 2008; Liu et al., 2009; von Rohden et al., 2010), and to characterize the groundwater age regime and flow path (Zhang et al., 1987; Zhang et al., 1997; Chen et al., 2005). The principal problem in previous isotopic age studies is the conflict between groundwater age determined by ^{14}C and ^{36}Cl for the deep aquifer in the central plain and coastal plain. Groundwater age obtained based on ^{14}C ranges from 10 to 30 kyr (Zhang et al., 1987; Zhang et al., 2001; Chen et al., 2005; Wu et al., 2007), however, the ^{36}Cl age is old up to 250–300 kyr (Liu et al., 1993; Dong et al., 2002).

The primary goal of this study is to improve the estimates of recharge values used in the flow model which has been developed in the North China Plain. The calibrated flow model is then used to simulate the age distribution in the entire aquifer system, and to characterize the flow regime.

4.2. Materials and Methods

4.2.1. Study Area

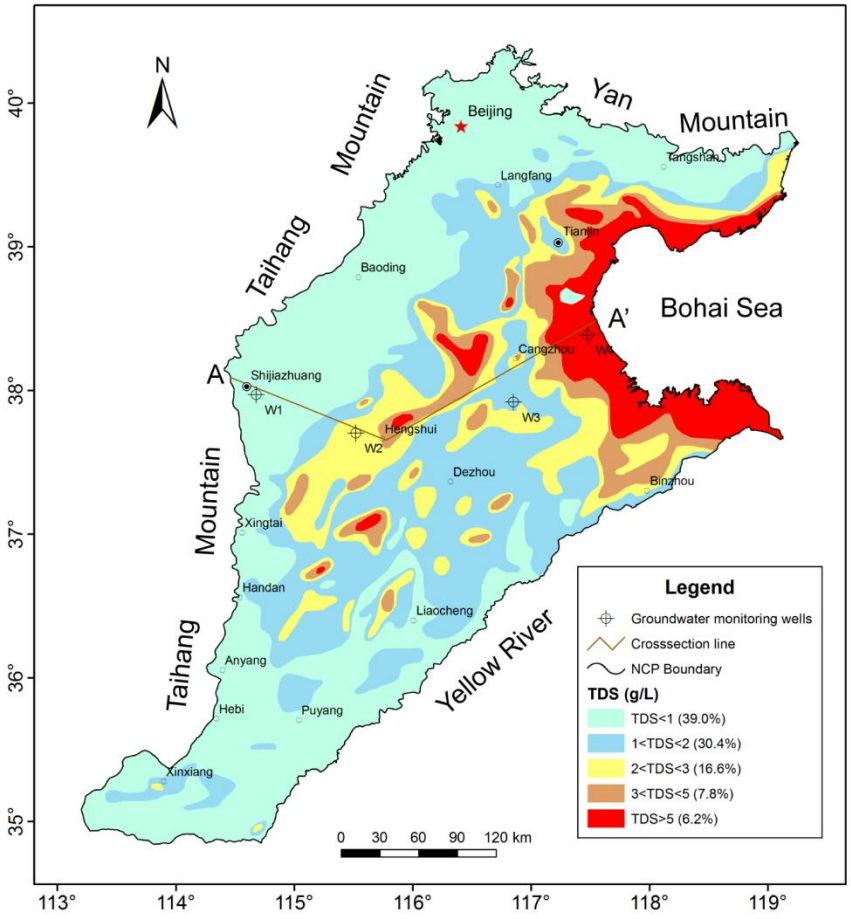

Figure 4.1. Concentration of TDS in the shallow groundwater across the NCP (source: China Geological Survey, http://water.cgs.gov.cn/web/ShowArticle.asp?ArticleID=640, obtained at January, 2010), location of the cross section AA' along which the simulated groundwater age is presented in Figure 4.5 and the locations of wells for vertical hydraulic gradient analysis.

The NCP occupies an area of 140,000 km^2 in northeast china, and is bordered on the north by the Yanshan Mountains, on the east by the Bohai Sea, on the south by the Yellow River and on the west by the Taihang Mountains (Figure 4.1). The plain consists of four main

hydrogeological zones from the Taihang Mountain to the Bohai Sea: piedmont pluvial plain, the central alluvial and flood plains, and the coastal plain (Wu et al., 1996). The population of the NCP, based on 2000 state census data, is approximate 105 million. This region accounts for ~15% of China's total gross domestic product (GDP) and ~10% of total grain production based on the 2009 statistical data (China Statistical Yearbook, 2010). In the North China Plain, approximately 70–80% of the annual water supply comes from groundwater pumping.

The Quaternary aquifers with a thickness ranging from 200 to 600 m in the NCP are traditionally divided into four major aquifer units often referred as aquifer I, II, III and IV. The corresponding geologic units of the aquifers are Holocene series (Q4), and late (Q3), middle (Q2) and early (Q1) Pleistocene series, respectively (Zhu et al., 1995). The NCP aquifer is traditionally divided into two aquifer zones referred as the "shallow" and "deep" (Wu et al., 2010). The first aquifer unit which is unconfined and the second aquifer unit which is semi-confined are together referred as the "shallow" aquifer zone due to the strong hydraulic connection between the two aquifers. The third and fourth aquifer units are confined and are together referred as the "deep" aquifer zone, which is characterized by poor hydraulic connection because the low permeability clay layers inhibit the downward groundwater flow.

In the central and east parts of the NCP, in conjunction with continental salinization and transgression, shallow groundwater is frequently characterized by high mineralization. The area of the saline water with the concentration of total dissolved solids (TDS) >1g/L in the shallow aquifer zone is ~80,000 km^2 (Fang et al., 2003), which accounts for ~60% of the entire plain (Figure 4.1). The primary source of water supply in these regions is the third and fourth aquifer units. Extensive groundwater exploitation from the two aquifer zones has greatly impacted the hydrodynamic and hydrogeochemical characteristics of the flow system and caused many

environmental problems, such as aquifer depletion, groundwater contamination and salinization, and land subsidence (Liu et al., 2001). The recharge rate and its variation caused by the flow regime change in the deep aquifer zone has become a crucial issue for the groundwater sources sustainability evaluation in the NCP (Chen et al., 2009).

4.2.2. Mean Age Transport Model

The transient mean age of groundwater was first derived by Goode (1996) with a mass conservation approach as follows,

$$\frac{\partial A}{\partial t} = \frac{\partial}{\partial x_i}\left(D_{ij} \frac{\partial A}{\partial x_j} \right) - \frac{\partial}{\partial x_i}\left(\frac{q_i}{\theta} A \right) + 1 \quad i,j=1,2,3 \tag{4.1}$$

where A is the mean age, also referred to as the mean residence time. Equation (4.1) can be solved by assigning A=0 as the initial condition. The zeroth-order source term of unity (1) indicates that groundwater is aging at the rate of one unit per unit time. The implementation of the mean age calculation is straightforward and easily simulated by a numerical model code that solves the advection-dispersion equation. The age distribution simulated by (4.1) may be more compatible with field-measured isotope age data, which have integrated the effects of dispersion, diffusion and mixing over the length of flow paths (Cornaton and Perrochet, 2006; Newman et al., 2010).

In simulating the mean groundwater age, we are generally interested in the steady-state distribution by running the age model for a sufficiently long time or by setting the time derivative $\partial A/\partial t = 0$. Thus equation (1) becomes:

$$\frac{\partial}{\partial x_i}\left(D_{ij} \frac{\partial A}{\partial x_j} \right) - \frac{\partial}{\partial x_i}\left(\frac{q_i}{\theta} A \right) + 1 = 0 \quad i,j=1,\ 2\ ,3 \tag{4.2}$$

For the boundary conditions, a no-flow boundary in the flow model become a no "age-mass" boundary in the age transport model. A specified inflow boundary also becomes a no age-mass boundary since the age of any inflow entering the model domain is considered zero. An outflow boundary, on the other hand, is allowed to carry an advective "age-mass" freely out of the model domain.

An important question that should be kept in mind is how the initial-condition affects the current age distribution. Indeed we cannot prove that that the groundwater age distribution is in steady state and the initial condition may matter to the current age distribution. That means simulating groundwater age distributions requires specification of initial conditions that may involve connate waters or other information related to the creation of the actual subsurface (Ginn et al., 2009). However this challenge is from characterization limitations and not from the fundamental models.

4.2.3. Water Level and Groundwater Age Observations

The groundwater flow model set up in this study is to simulate steady-state groundwater flow prior to the development of groundwater in the NCP. The amount of groundwater pumpage was limited prior to the 1960s in the NCP. The water level contour maps can represent the groundwater potential field in the predevelopment period. A total of 289 and 164 locations were digitized from the water level contour maps for model calibration. Water level data were collected at all the multilevel monitoring wells on monthly basis from 1993 to 2008.

Although a significant number of isotopic age data have been acquired by previous studies, to keep the consistency of different data sources, only the carbon-14 activities were collected to be used in this study. Moreover, to remove the effect of mixing with shallow young groundwater, only those samples with ^{3}H content less than 1 TU (tritium unit) were used in the

final data set. Total 97 carbon-14 activities were collected from previous studies (Chen, 2002; IHEG, 2006; Kreuzer et al., 2009; Mao et al., 2010). All these samples have carbon-14 and carbon-13 activity available (Table 4.1).

Table 4.1. Well information, ^{14}C, and ^{13}C concentrations.

Well ID	Well Depth /Aquifer	^{14}C(pmc)	^{13}C(‰)	Year Sampled	^{14}C Analyzed Method[a]	^{14}C Apparent Age(yr)	Pearson Age (yr)	Source[b]
1	500	2.44±0.17	-12.39	1999	LSC	30695	27478	+
2	300	13.47±0.33	-9.76	1999	LSC	16572	11619	+
3	320	9.94±0.17	-9.06	1999	LSC	19084	13601	+
4	310	11.10±0.49	-8.83	1999	LSC	18172	12506	+
5	300	6.85±0.17	-8.54	1999	LSC	22162	16261	+
6	280	11.65±0.27	-5.5	1999	LSC	17772	8890	+
7	370	6.29±0.19	-10.64	1999	LSC	22867	18536	+
8	400	13.56±0.38	-8.73	1999	LSC	16517	10771	+
9	300	12.23±0.24	-8.93	1999	LSC	17371	11784	+
10	280	15.25±0.35	-8.71	1999	LSC	15546	9784	+
11	380	8.03±0.13	-9.36	1999	LSC	20848	15596	+
12	330	12.84±0.38	-10.76	1999	LSC	16968	12718	+
13	380	10.22±0.28	-9.32	1999	LSC	18855	13572	+
14	340	10.93±0.27	-9.85	1999	LSC	18300	13412	+
15	350	18.40±0.42	-9.83	1999	LSC	13994	9092	+
16	265	56.30±4.4	-9.3	1999	LSC	4749	morden	+
17	200	62.4±0.84	-7.45	1999	LSC	3899	morden	+
18	251	24.50±0.46	-7.3	1999	LSC	11627	4636	+
19	300	6.66±0.24	-12.39	1999	LSC	22395	19177	+
20	150	31.35±0.53	-9.26	1999	LSC	9589	4260	+
21	600	1.67±0.08	-9.91	2004	AMS	33830	28986	++
22	180	40.92±0.31	-9.7	2004	AMS	7387	2389	++
23	250	4.17±0.11	-9.35	2004	AMS	26265	21005	++
24	310	2.30±0.09	-9.52	2004	AMS	31184	26053	++
25	320	1.82±0.08	-8.03	2004	AMS	33119	26787	++
26	300	3.96±0.11	-8.75	2004	AMS	26692	20962	++
27	360	0.89±0.07	-9.46	2004	AMS	39033	33856	++
28	480	0.93±0.05	-9.67	2004	AMS	38669	33650	++
29	350	1.25±0.07	-6.04	2004	AMS	36225	27956	++
30	300	1.00±0.07	-7.22	2005	AMS	38069	31003	++
31	390	21.22±0.22	-8.85	2005	AMS	12815	7165	++
32	375	1.53±0.08	-8.34	2005	AMS	34554	28486	++
33	150	48.11±0.36	-8.71	2005	AMS	6049	286	++
34	350	22.89±0.23	-9.17	2005	AMS	12189	6791	++
35	260	14.88±0.19	-8.37	2005	AMS	15749	9707	++
36	240	19.2	-9.3	2002	LSC	13642	8344	+++
37	170	30	-8.6	2002	LSC	9953	4101	+++
38	160	22.9	-11.1	2002	LSC	12185	8162	+++
39	158	9	-9.3	2002	LSC	19906	14608	+++
40	450	9	-12.8	2002	LSC	19906	16928	+++
41	150	32.7	-10.7	2002	LSC	9240	4950	+++
42	265	10	-9.7	2002	LSC	19035	14037	+++
43	150	75.9	-13.4	2002	LSC	2280	morden	+++
44	150	73.1	-11.5	2002	LSC	2590	morden	+++
45	400	4.7	-10.8	2002	LSC	25276	21053	+++
46	400	6	-11.5	2002	LSC	23257	19492	+++
47	300	8.7	-10.1	2002	LSC	20186	15479	+++
48	300	12.1	-9.3	2002	LSC	17459	12161	+++
49	400	11.6	-9.4	2002	LSC	17808	12586	+++
50	500	4.8	-12.5	2002	LSC	25102	21949	+++

Table 4.1 continued.

51	300	10.5	-10.1	2002	LSC	18631	13924	+++
52	400	16.4	-11.2	2002	LSC	14945	10987	+++
53	400	7.9	-10.2	2002	LSC	20983	16347	+++
54	500	11.3	-11.1	2002	LSC	18024	14001	+++
55	300	12.1	-9.7	2002	LSC	17459	12462	+++
56	200	60.3	-11.9	2002	LSC	4182	667	+++
57	260	6.4	-14	2002	LSC	22724	20413	+++
58	260	5.2	-10.1	2002	LSC	24440	19733	+++
59	380	7.7	-10.5	2002	LSC	21195	16768	+++
60	380	6	-12.3	2002	LSC	23257	19986	+++
61	500	10.4	-11.9	2002	LSC	18710	15196	+++
62	300	8.7	-7.9	2002	LSC	20186	13740	+++
63	280	10.8	-9.9	2002	LSC	18398	13547	+++
64	III	51.75	-9.36	-	LSC	5446	193	++++
65	III	81.07	-9.11	-	LSC	1735	morden	++++
66	III	48.8	-9.55	-	LSC	5931	822	++++
67	III	30.52	-9.55	-	LSC	9811	4702	++++
68	III	12.92	-9.68	-	LSC	16917	11905	++++
69	III	1.45	-7.11	-	LSC	34998	27826	++++
70	III	1.01	-6.14	-	LSC	37987	29828	++++
71	III	3.73	-8.09	-	LSC	27187	20907	++++
72	III	4.69	-8.75	-	LSC	25294	19564	++++
73	III	17.84	-8.2	-	LSC	14249	8064	++++
74	III	7.25	-6.04	-	LSC	21693	13425	++++
75	III	10.04	-6.93	-	LSC	19002	11656	++++
76	III	52.87	-10.51	-	LSC	5269	849	++++
77	III	25.48	-8.42	-	LSC	11303	5302	++++
78	III	45.46	-9.15	-	LSC	6517	1103	++++
79	III	10.54	-9.38	-	LSC	18600	13363	++++
80	III	15.13	-9.87	-	LSC	15611	10739	++++
81	III	10.34	-9.17	-	LSC	18758	13360	++++
82	III	8.52	-6.24	-	LSC	20359	12307	++++
83	III	7.54	-6.47	-	LSC	21369	13559	++++
84	III	6.61	-7.88	-	LSC	22457	15994	++++
85	III	6.57	-8.58	-	LSC	22507	16639	++++
86	III	5.17	-9.09	-	LSC	24488	19028	++++
87	III	3.75	-9.53	-	LSC	27143	22019	++++
88	III	5.43	-9.83	-	LSC	24083	19181	++++
89	III	4.98	-0.19	-	LSC	24798	4167	++++
90	III	4.36	-8.53	-	LSC	25897	19988	++++
91	III	6.73	-9.02	-	LSC	22308	16793	++++
92	III	6.39	-9.82	-	LSC	22737	17828	++++
93	III	11.94	-8.77	-	LSC	17569	11855	++++
94	III	6.02	-8.35	-	LSC	23230	17171	++++
95	III	6	-6.6	-	LSC	23257	15581	++++
96	III	16.56	-5.85	-	LSC	14865	6386	++++
97	III	10.45	-7.26	-	LSC	18671	11642	++++

[a]Estimation methods include: AMS, accelerator mass spectrometry; LSC, liquid scintillation counter.

[b]Sources are as follows: + Chen, (2001); ++ Kreuzer et al., (2009); +++ The Institute of Hydrogeology and Environmental Geology (IHEG), (2006), Prospects for sustainable development and utilization of groundwater in North China Plain, unpublished report; ++++ Mao, (2010).

The equation used to calculate the groundwater age by ^{14}C is:

$$Age = \left(5730 / \ln(2)\right) \ln(A_0 / A) \tag{4.3}$$

where 5,730 is the half-life of ^{14}C; A is the ^{14}C concentration in pmc (percent modern carbon) in the groundwater; and A_0 is initial ^{14}C concentration. A_0 is estimated using a ^{13}C correction method of Pearson and Hanshaw (1970). The corrected groundwater age shows an obvious increasing trend with well depth (Figure 4.2).

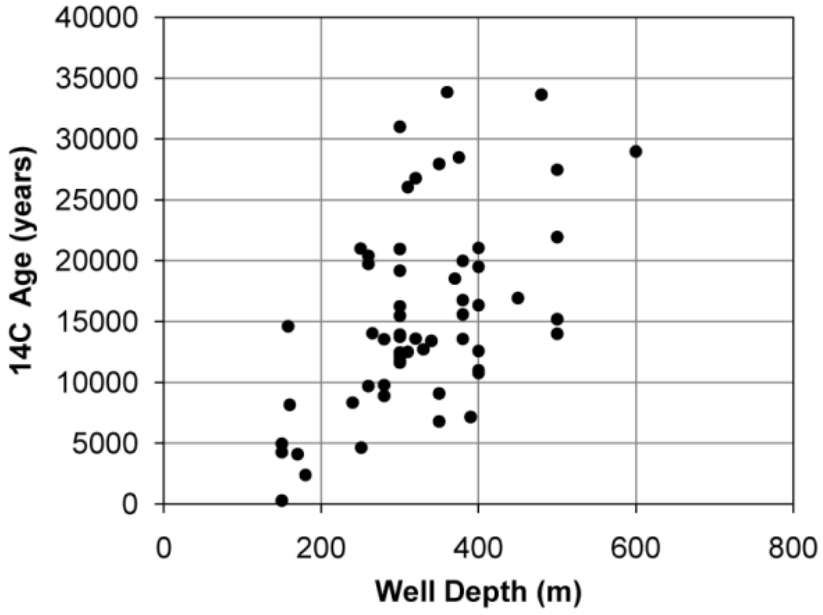

Figure 4.2. Distribution of corrected groundwater ^{14}C age with well depth.

4.2.4. Numerical Simulation of Flow and Transport

Although groundwater age distribution in steady state is of much more interest, a transient flow simulation reproducing the actual flow field from past to present is necessary to illustrate the impact of transient flow (Lemieux et al., 2010; Schwartz et al., 2010). In practical application, however, because no actual recharge data in the past is available, a steady-state flow

filed which is simulated under the current recharge condition is commonly used assuming a steady-state flow in the past. In the NCP, although the paleo-climate change has been interpreted by isotopic data (Chen et al., 2003) for the past 30,000 years, the actual recharge data are not available. Therefore, the flow field in the pre-development period in the NCP simulated by the steady-state flow which has been constructed in Chapter 2 serves as the flow field required by the age model. The effect of paleo-flow conditions of the age distribution is evaluated using a two steady-state stage flow model as used by Sanford et al. (1996). The transient flow model developed in Chapter 2 for the post development period (1970–2008) using MODFLOW 2000 (Harbaugh et al., 2000) with sub-regional water budget calculation code Zonebudget (Harbaugh, 1990) are used to analyze the variation in the recharge rate to the deep groundwater.

Pathlines starting from selected locations were determined by MODPATH (Pollock, 1994) using the three dimensional hydraulic head distributions computed by the flow model. Particles were introduced on the water table at selected model grid cells across the plain and tracked forward to their end points. Advective flowpaths obtained do not account for dispersion, but provide an approximation of the flow pattern. The advective travel time provides an indicator of the time scale of the flowpaths. A value of 25% for effective porosity is used in travel time calculations. The value does not impact flowpaths locations but changes travel times.

The mean age distribution controlled by advection and dispersion was simulated using MT3DMS (Zheng and Wang, 1999; Zheng, 2010) with a steady-state transport simulation option. Because there are no constraints on the dispersivity, sensitivity analysis was conducted by changing the magnitude of longitudinal dispersivity (α_L) and vertical dispersivity (α_V) separately, and the transverse dispersivity (α_T) was taken as one tenth of α_L. The mean and standard deviation of simulated groundwater age at those locations with the ^{14}C age measurement are

listed in Table 4.2. For cases with an effective porosity of 25% and a range of dispersivities, the results did not show a great difference except for the case with a vertical dispersivity of 10 m. The much younger simulated age than the apparent age with a large vertical dispersivity is expected because mixing of deep groundwater with younger groundwater in the shallow aquifer would greatly decrease the age of deep groundwater.

Table 4.2. Sensitivity of simulated mean groundwater age at 97 observation points to dispersivity and effective porosity.

α_L(m)	α_T(m)	α_V(m)	Effective porosity (%)	Average age (kyr)	Standard deviation (kyr)
Without dispersion			25	33.05	31.74
100	10	10	25	3.57	2.45
100	10	1	25	14.13	12.43
100	10	0.1	25	28.64	26.71
1000	100	0.1	25	27.42	25.27
1000	100	0.5	25	18.53	16.45
1000	100	1	25	13.69	11.91
1000	100	1	10	5.48	4.77
1000	100	1	30	16.43	14.30
1000	100	1	S_y	3.55	2.85

Effective porosity is another essential consideration in groundwater age modeling because it is needed to convert the Darcy flux calculated by the flow model to the seepage velocity, and hence travel time. The specific yield of the shallow aquifers ranges from 10 to 30% in the piedmont area, 5 to 20% in the middle alluvial plain, and 5 to 7% in the coastal plain, respectively (Chen, 1999). A uniform effective porosity of 25% used in the sensitivity analysis to dispersivity is considered reasonable. Increasing the effective porosity to 30% did not result in an obvious difference of the simulated ages. The younger ages simulated using an effective porosity

of 10% and the specific yield are expected as smaller effective porosity increases the seepage velocity. A uniform effective porosity of 25% is used in the following simulation.

Automatic model calibration code PEST (Doherty, 2003) was employed to calibrate the recharge distribution based on the water levels and apparent ages converted from carbon-14 data. In this study, a total of 332 observations, including 239 hydraulic heads digitized from the water level contour map and 93 observed groundwater ^{14}C apparent ages were used in the calibration procedure.

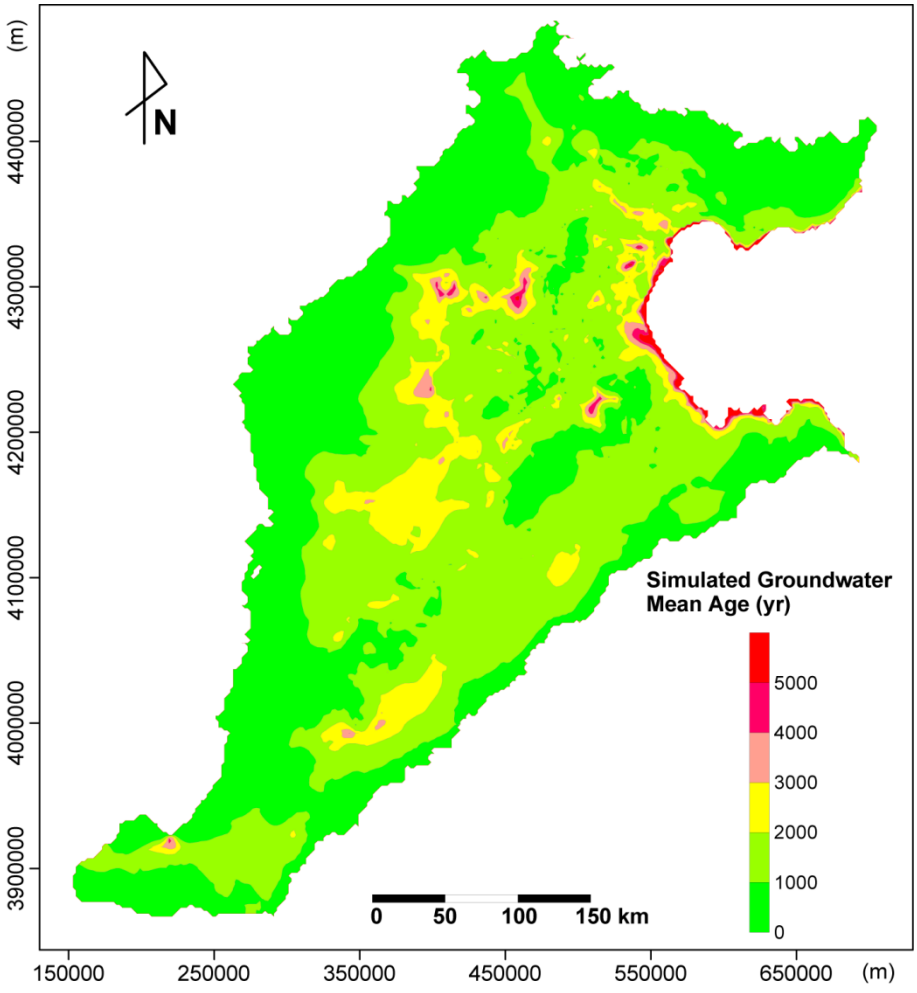

Figure 4.3. Simulated groundwater mean age distribution in the first model layer, which represents the first and second aquifer units in the NCP.

4.3. Results and Discussion

Simulation of hydraulic heads and groundwater mean ages were completed in two stages. The model calibration goal is to obtain the recharge distribution for the flow model that could yield a best fit with the observed water level and C^{14} age data. The results presented here are from the simulation results with the final calibrated recharge rates and hydraulic conductivities.

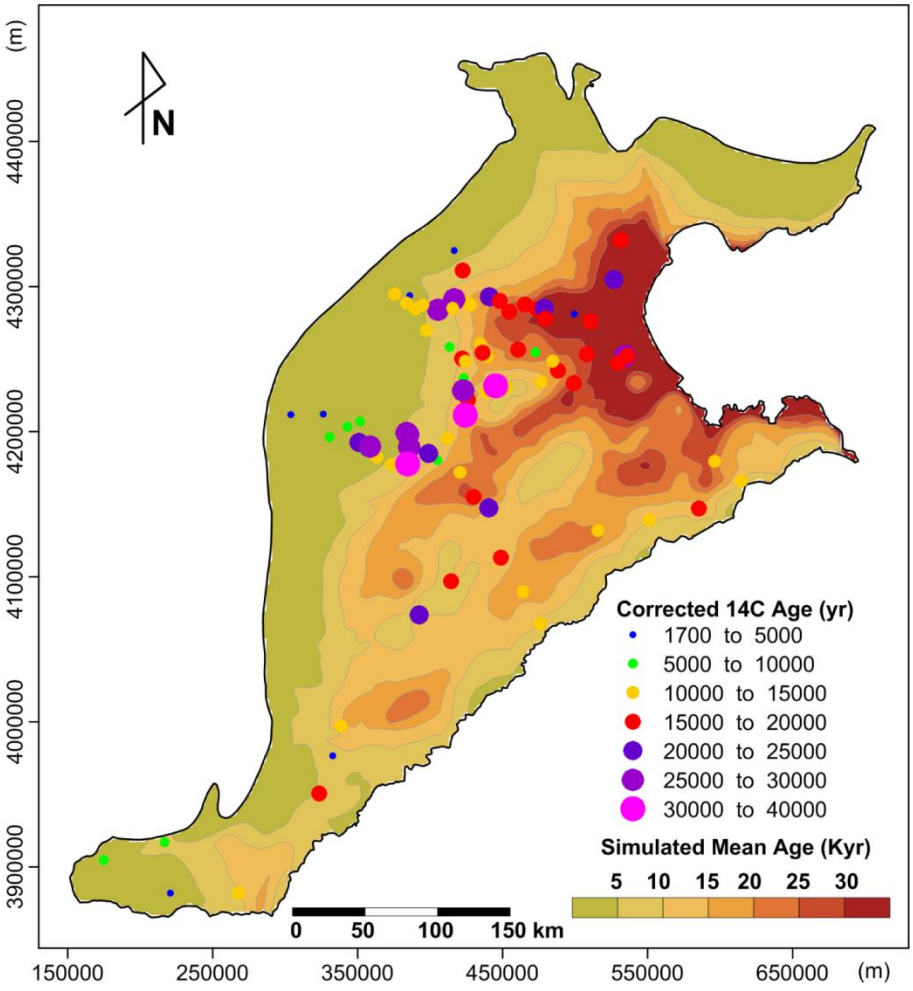

Figure 4.4. Simulated groundwater mean age and the corrected groundwater 14C age in the second model layer, which represents the third aquifer unit.

4.3.1. Mean Steady State Age Distribution with Calibrated Recharge

The simulated mean groundwater age distributions for the shallow and deep aquifer zones are shown in Figure 4.3 and Figure 4.4, respectively. The age pattern has clearly reflected the features of the flow system under natural conditions: age becoming older from the recharge zone to the discharge zone, and younger in the shallow aquifer units and getting older with depth. The mean groundwater age ranges from ~100 years in the piedmont area to > 30,000 years within the fourth aquifer unit in the coastal plain. Younger age of groundwater in the piedmont area and in the shallow aquifer zones suggests that the water has recently entered the aquifer system. The horizontal age distribution along the cross section in the second aquifer unit is shown in Figure 4.5. No significant difference is observed between the simulated advective age and the mean age up to ~120 km from the mountain front, and the advecitve age becomes progressively older than the mean age in the central plain and coastal plain. The advective age reach up to ~200 kyrs in the coastal plain, which is comparable with the ^{36}Cl age (Liu et al., 1993; Dong et al., 2002). The old age of deep groundwater in the central and coastal plains can only indicate the long residence time of groundwater in the aquifer. The enhanced downward leakage of young groundwater by pumping should also be evaluated.

The simulated age and water levels are plotted against the measured age and water levels in Figure 4.6. The mean residual between measured and simulated water levels is -1.6 m, and the RMSE (root mean square error) is 5.3 m. The mean discrepancy between measured ^{14}C ages and the simulated mean ages is 740 years, and the RMSE is 12,200 years. The distribution of simulated mean ages against measured ages shows a more substantial amount of scatter than that of the water levels, even in the log scale. The poorer fit of ^{14}C ages is expected considering that the velocities are a function of the first derivatives of the water potential and then more difficult

to fit, which is confirmed in the study of Sanford et al. (2004). Moreover, hydrodynamic dispersion is also considered in this study and it could improve the fit quality had it not been assumed to be uniform across the plain. However, insufficient data exist to allow the calibration of dispersivity.

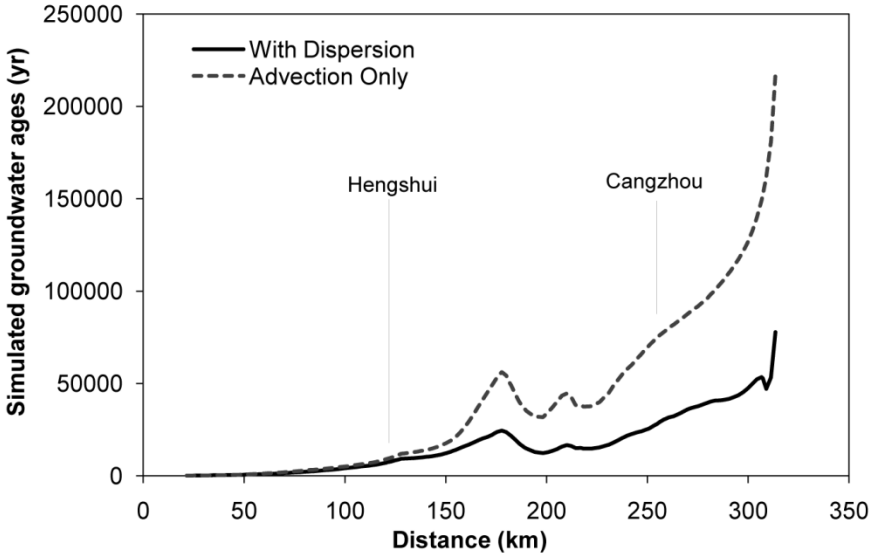

Figure 4.5. Simulated advective age and mean age distribution in the second aquifer along the cross section.

The final calibrated recharge distribution is presented in Figure 4.7. The average recharge is 85 mm/yr. The groundwater recharge is higher in the southeast than in the northwest part of the plain, which shows a similar pattern with the mean annual precipitation in the NCP. The estimated higher recharge rate in the piedmont area along parts of the west boundary is believed to be contributed from the mountain recharge. The net recharge distribution (estimated recharge subtracted by the simulated and specified leakage to river) shows an obvious discharge zone along the boundary between the piedmont plain and the central plain (Figure 4.8). This zone is also spread along the boundary between high hydraulic conductivity zones in the piedmont area

and low hydraulic conductivity zones, the boundary between shallow fresh water and shallow brackish water zones.

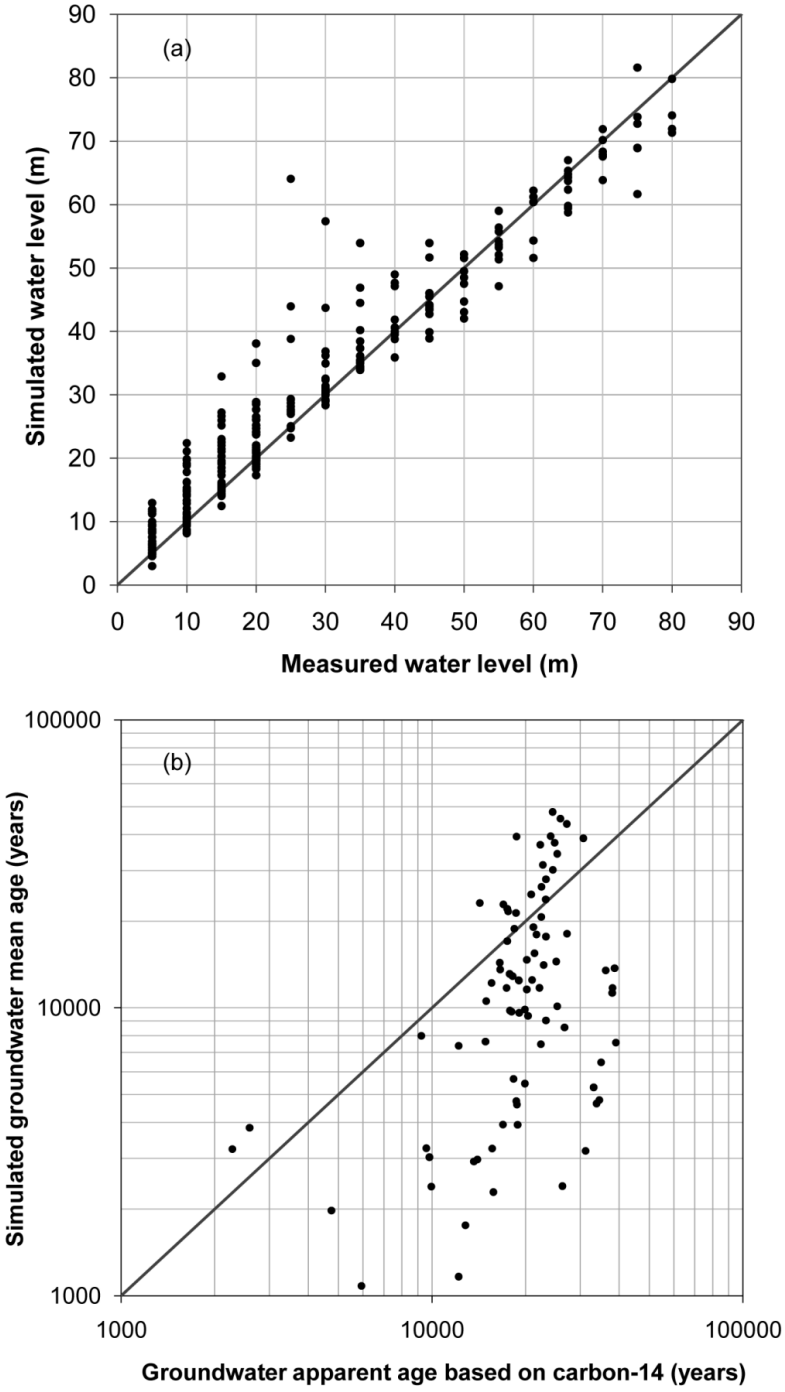

Figure 4.6. Comparison of (a) simulated water level and measured water level and (b) simulated groundwater mean age and measured apparent age based on carbon14.

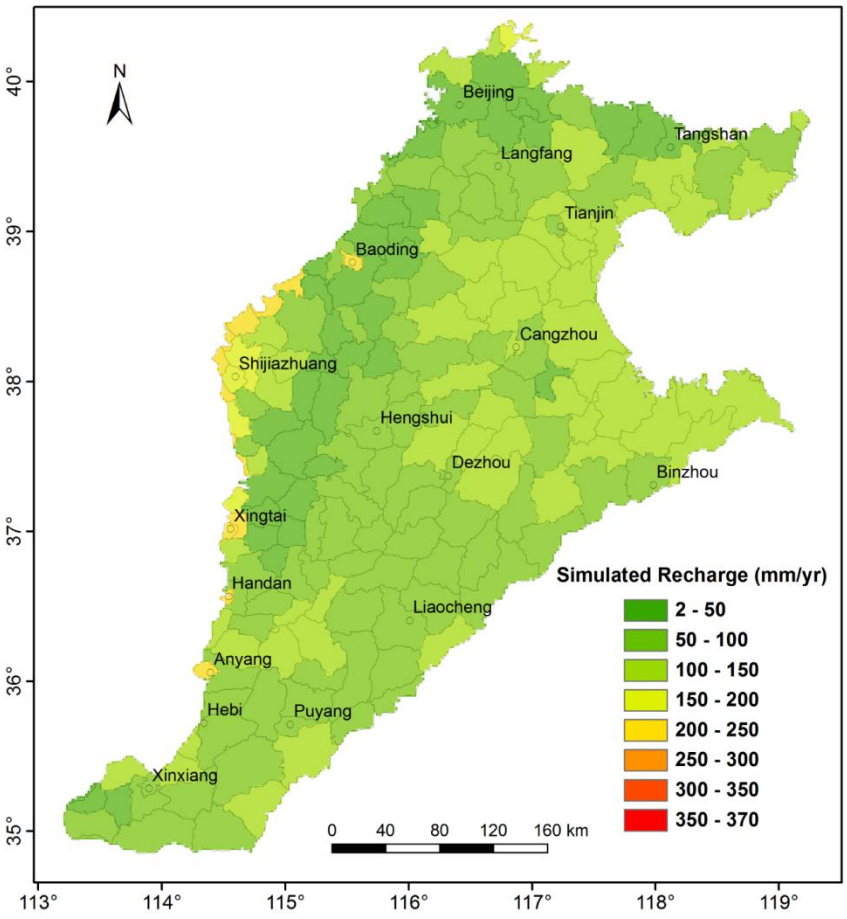

Figure 4.7. Simulated recharge distribution in the NCP.

4.3.2. Impact of Paleo-hydrologic Conditions on Age Simulation

The large discrepancies between simulated and measured ages in the coastal plain are attributed to the assumption of steady-state flow. The conclusion that the period when the groundwater in the third aquifer unit received recharge was the last glacial period has been confirmed by isotopic studies (Chen et al., 2003). It means that the groundwater ages in the third aquifer unit had been affected by the flow conditions in the last glacial period. At the peak of the last glacial period, approximately 18,000 years ago the sea level was 150 m below its present

level in eastern China (Ren, 2006) and the shoreline was 150-180 km east of its present location. These conditions allow higher groundwater velocities than present. To evaluate the effect of the paleo-flow condition on the groundwater age distribution, a simple two steady-state flow modeling method similar to the study of Sanford et al. (1996) is used. Two steady-state flow simulations were first made to represent the flow condition 10,000 years ago and that from 10,000 years ago to present. The simulated age distribution in the third aquifer unit (model layer 2) is plotted together with the residuals between corrected ^{14}C ages and simulated mean ages in Figure 4.9. Although positive residuals, i.e., underestimation, still occur in the piedmont area, the discrepancy between corrected ^{14}C age and simulated mean age are slightly reduced in the coastal plain.

4.3.3. Water Budget of the Deep Groundwater

The main water budget terms for the deep aquifer zone under the brackish water zone is shown in Table 4.3 and Figure 4.10. Both the lateral recharge and leakage from the shallow aquifer zone show an increasing trend with the development of the deep groundwater. The lateral recharge increased from ~0.4 km^3/yr in 1970s to ~0.5 km^3/yr in 2000s, which account for only 13-20% of the pumpage. The low percentage of lateral recharge contributing to the water for pumpage is consistent with the results of the previous water balance evaluation for the Hebei Plain (Chen et al., 1992; Guo et al., 1995; Chen, 1999). The leakage from the shallow aquifer zone increased by ~2.0 km^3 and accounted for 62-85% of the pumpage. The elastic storage release only contributed ~7% of the pumpage.

In this study, the inelastic storage release related to land subsidence was not simulated, which can account for 20–40% of the pumpage (Guo et al., 1995; Wang and Li, 2004). By the end of 2005, the area with cumulative land subsidence greater than 0.5, 1.0, and 2.0 m is 33,400,

8,500 and 940 km^2, respectively (He et al., 2006). The volume of water released from inelastic storage, or compaction of clay layers, can be estimated as the product of the area and the land subsidence. The total volume of water released from inelastic storage was ~43.7 km^3, with a mean annual rate of 1.2 km^3/yr, which accounted for 38% of the mean annul pumpage. The real leakage from the shallow aquifer zone should then be reduced by the water storage change related to land subsidence. In summary, the lateral flow, leakage from the shallow aquifer zone, the elastic and inelastic storage release account for 16%, 39%, 7% and 38% of the pumpage and lateral and vertical outflow, respectively. This indicates that the pumpage of deep groundwater is primarily derived from leakage from the shallow aquifer zone and from aquifer storage.

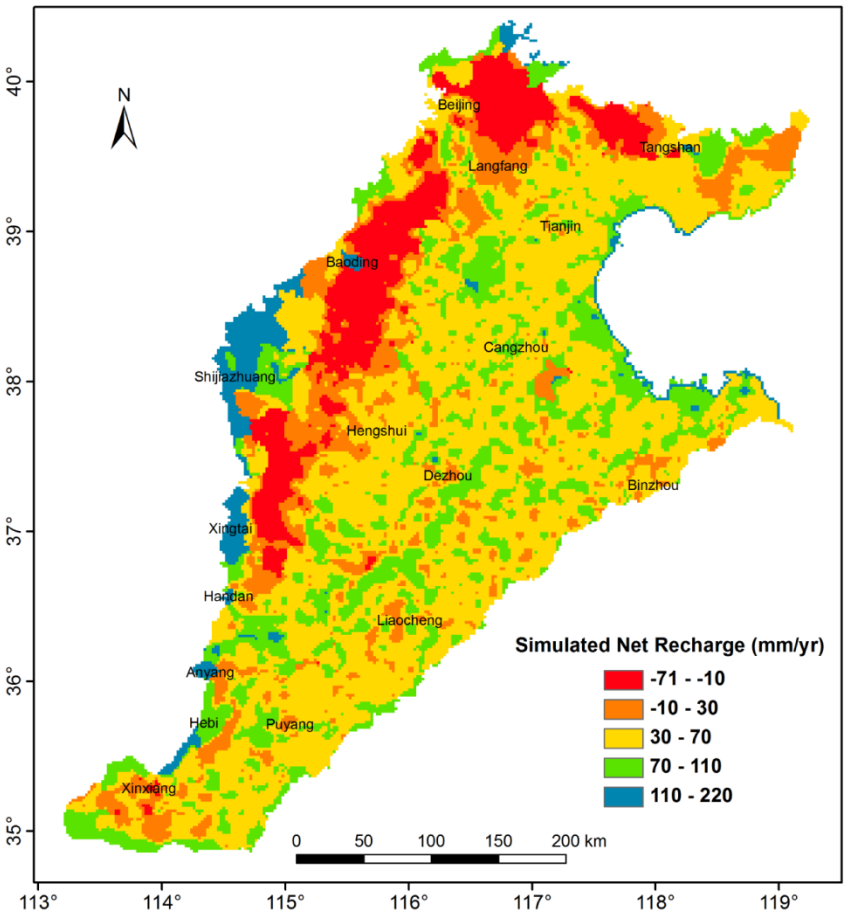

Figure 4.8. Simulated net recharge flux at the water table across the NCP.

The induced significant downward vertical leakage from the shallow aquifer zone has been treated as an important component of the recharge in the water resources evaluation (Chen, 1999; Zhang et al., 2002). However, incipient salinization of deep groundwater has been observed, and the rate of downward migration of the saline/fresh water interface can be up to 0.5–2.0 m/yr in the Heibei and Shandong parts of the NCP in the past 30 years (Ming, 1986; Guo et al., 1995; Song et al., 2007; Fei et al., 2009).

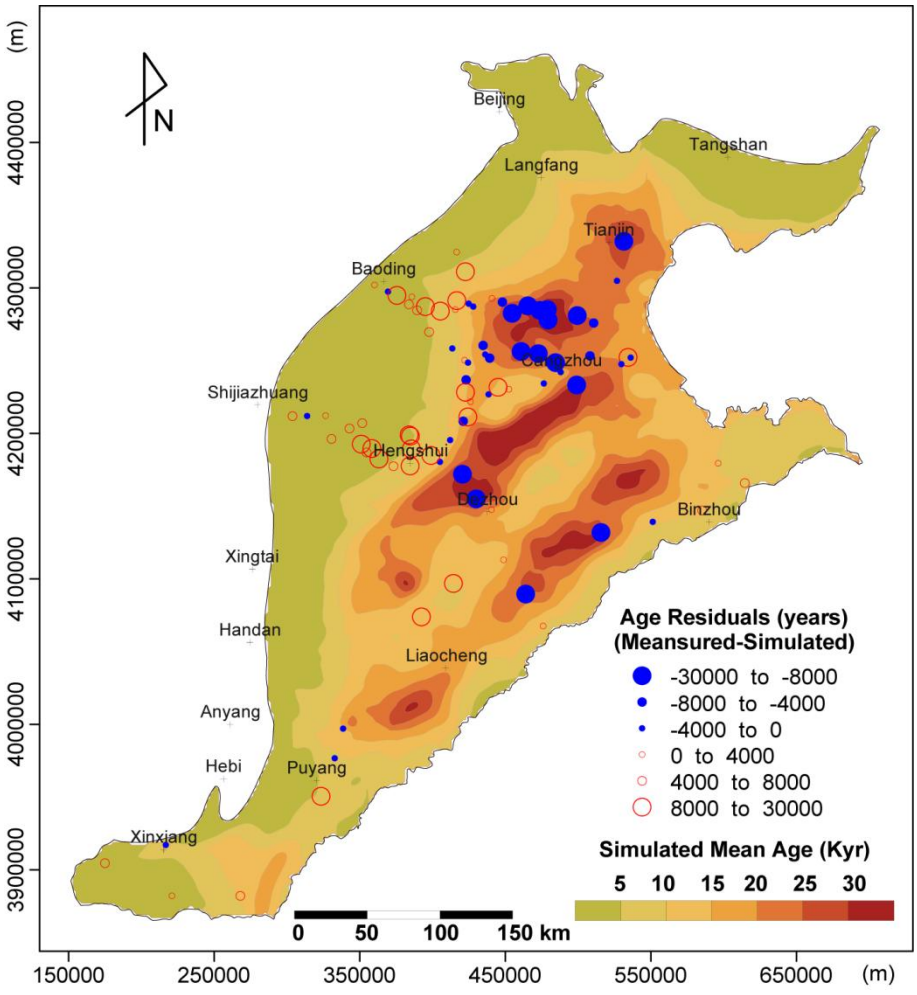

Figure 4.9. Two steady state stage model simulated groundwater mean age and the corrected groundwater ^{14}C age in the second model layer, which represents the third aquifer unit.

4.3.4. Effect of Regional Pumpage on Age Distribution

The numerical test study of Zinn and Konikow (2007) suggested that large scale pumping can have a substantial impact on groundwater age measurements in a heterogeneous layered aquifer system. Most of the ^{14}C activities available in the NCP were sampled during the post-development period, therefore, it is essential to evaluate if the regional pumping had an impact on the age distribution. Moreover, evaluation of the alteration of the age of the deep groundwater can be helpful to evaluate recharge of young groundwater through downward leakage. The transient flow model described in Chapter 2, which simulates the flow dynamics from the predevelopment through 2008, is used to represent the impact of regional pumping on the flow field. The simulated steady-state age distributions are introduced as the initial age distribution of the transient age transport model. Those parameters for the transport model are the same with the final values in the steady-state age model.

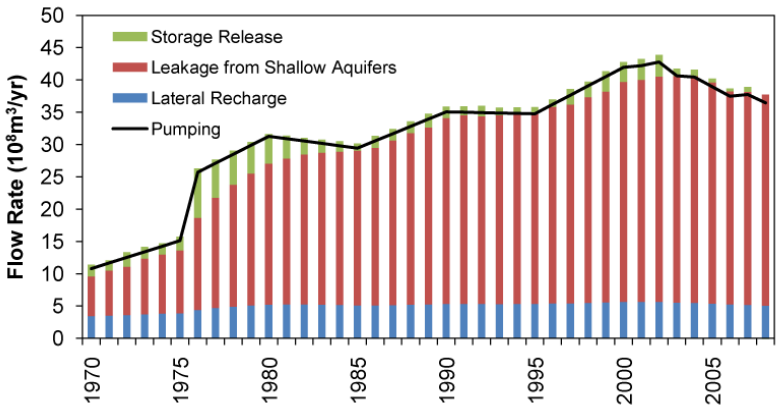

Figure 4.10. Simulated flow rate for inputs (lateral flow recharge, leakage from shallow aquifer zone), pumpage and storage decrease in the deep aquifer zone with TDS>1 g/L for the period of 1970-2008.

Table 4.3. Simulated mean flux rate into the deep aquifer zone under the brackish water zone (unit: $10^8 m^3/yr$)

Period	Lateral Recharge	Leakage From Shallow	Storage Elastic Release	Pumping
1970s	4.10	11.87	3.51	18.89
1980s	5.19	24.26	2.31	31.11
1990s	5.38	30.08	1.71	36.29
2001-2008	5.40	34.04	1.30	39.58

Figures 4.11 and 4.12 show the age distributions in the first and second model layers at the end of 2008, respectively. A comparison of Figures 4.3 and 4.11 demonstrates no obvious alteration of age distribution in the shallow aquifer. An overall decreasing trend of groundwater age can be observed in depression cones with the highest pumping intensity. The primary reason for this changing pattern is the mixing with shallow younger groundwater caused by accelerated downward vertical flow. The highest absolute age change value of ~3,000 years occurs in the coastal plain, which accounts for approximately one tenth of the measured age in this region. All these indicate that the downward vertical flow is the dominant process altering the age distribution in the deep aquifer. This can also be confirmed by the following analysis of the hydraulic gradient between shallow aquifer and deep aquifers.

According to the mass-conservation of the mean age, the mean age of mixed waters is the mass weighted average, or the volume weighted average assuming a constant water density. The pumped volume of water from the deep aquifer is still smaller compared with the aquifer storage, and the transient simulation period is also quite small considering the old groundwater age of deep groundwater. Therefore, the current mean age distribution in the deep groundwater can be treated as a two-component mixture of shallow and deep groundwater age from the

predevelopment condition, assuming that the age mass extracted by pumping and produced in the simulation period can be ignored, as follows:

$$A_{DC} = \lambda A_{SP} + (1-\lambda) A_{DP} \tag{4.4}$$

where A_{DC} is the current age of the deep groundwater, A_{SP} and A_{DP} are the predevelopment groundwater age of the shallow and deep groundwaters, respectively. λ is the volume mixing ratio of shallow groundwater, defined as the ratio of volume of mixed shallow groundwater to the volume of the deep groundwater.

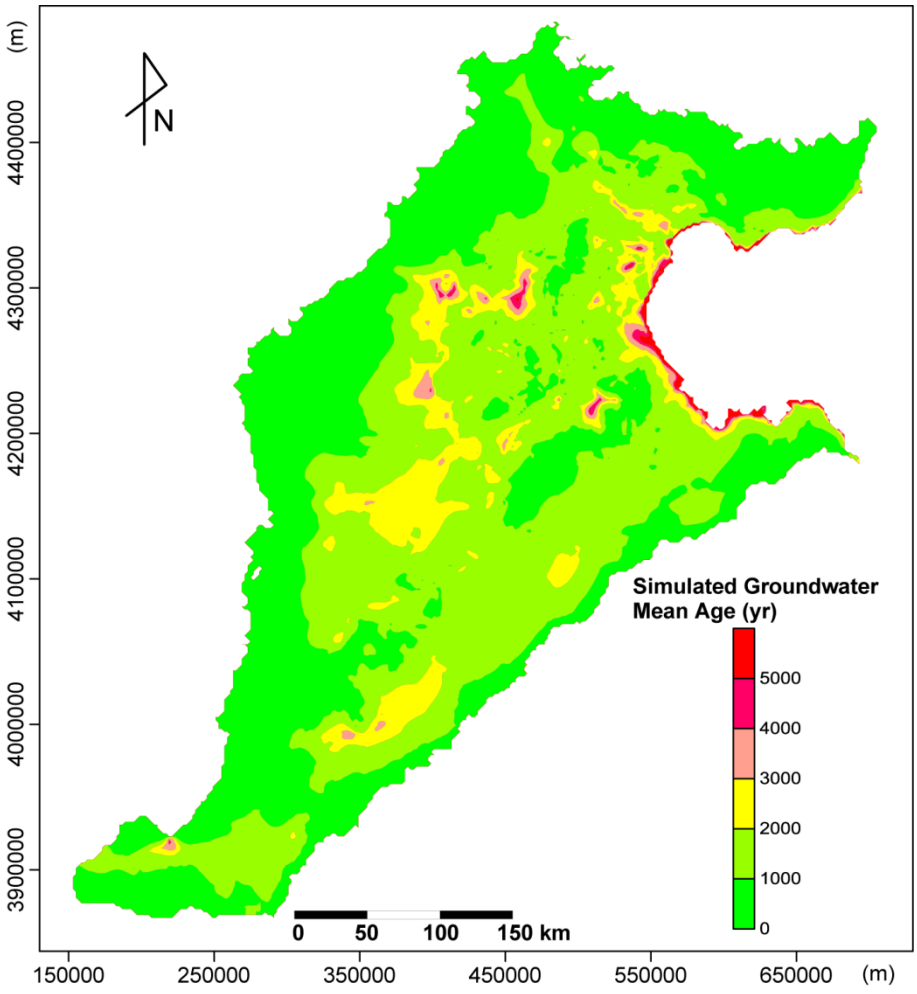

Figure 4.11. Simulated mean age distribution in the end of 2008 in the shallow aquifer zone.

Taking the steady-state age distribution as the predevelopment age into equation (4.4) can yield the distribution of mixing ratio of shallow groundwater to the deep groundwater .The mixing ratio ranges from 20–80% across most areas of the plain, with an average of 47%, which is comparable with the results based on stable isotopes (Sun, 2007) and the water budget calculation in the previous section.

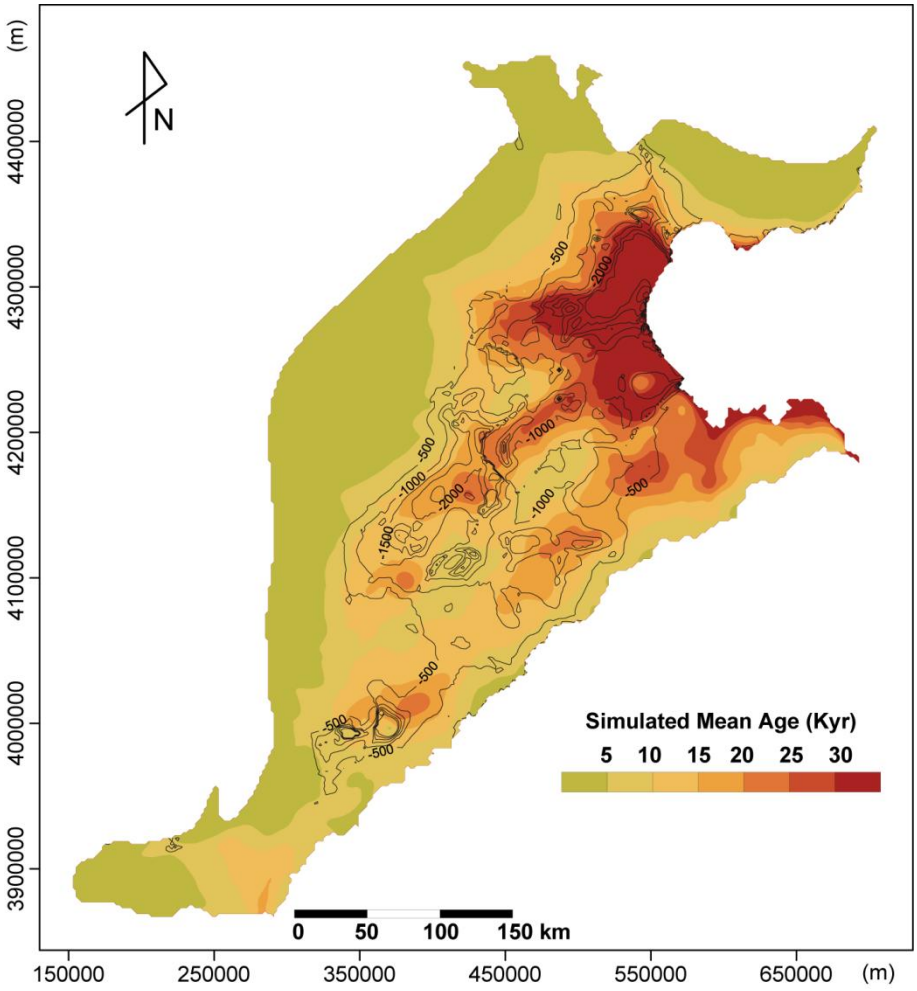

Figure 4.12. Simulated mean age distribution in the end of 2008 with age change compared with the steady stage age in the deep aquifer zone.

4.3.5. Flow Regime Under Natural Conditions and Excessive Exploitation

The water table contours for the shallow aquifer and water level contours map for the deep aquifer under natural conditions suggest a possible regional flow path from the west mountain front toward the east coastal plain. The increasing trend of isotopic ages from the piedmont area toward the coastal plain in the deep aquifer also yields such a plausible flow path (Zhang et al., 1987; Zhang et al., 1997; Chen et al., 2005). Our flow paths simulation does not show the existence of such regional flow paths (Figure 4.13a). The flow paths starting from the west mountain front end in the junction zone between the piedmont plain and the central plain, which is also the zone where both lithology and thickness of the aquifers begin to change. The flowpaths starting from the recharge zone ends in the central and coastal plains only along southwest-northeast direction. This is consistent with the distribution pattern of paleochannels in the central flood plain (Wu et al., 1996). This indicates that the primary lateral recharge source of the deep groundwater in the central and coastal plains is groundwater from the southwest part of the plain. With the current pumping situation, the lateral travel distance of the flow paths has been reduced dramatically, and the flow paths become more vertical (Figure 4.13b).

Vertical gradients in the hydraulic head provide useful information on the vertical flow direction of groundwater. Selected wells along the flow paths from the piedmont area to the coastal plain show a similar pattern of downward gradient (Figure 4.14). Hydraulic gradients plotted in Figure 4.14 were calculated as the difference in water level between shallow and deep screens, or between adjacent shallow and deep well pairs, divided by the vertical distance between the well screen midpoints. Positive gradients indicate the potential for downward water movement in the aquifer. Small gradient is observed in the piedmont area (Figure 4.14a), suggesting an effective connection between the shallow and deep aquifer layers. All other

locations in the central plain and coastal plain shows an increasing trend of positive vertical gradients (Figure 4.14b, c and d). Based on the water level contours in 2001, the horizontal hydraulic gradient in the shallow aquifer in the central and coastal plains is generally 0.1%, which is smaller than the vertical hydraulic gradient between the shallow aquifer and the deep aquifer. The larger vertical hydraulic gradient indicates that vertical flow has become the dominant process controlling the flow pattern in the deep aquifer.

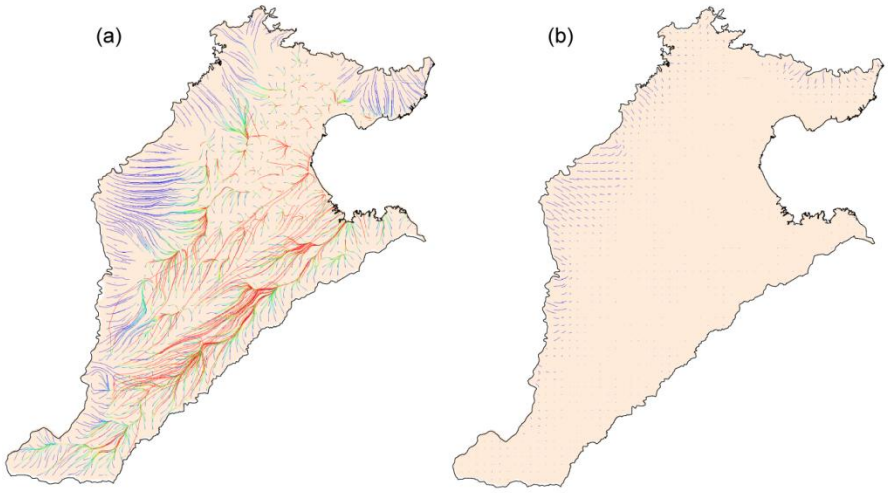

Figure 4.13. Forward tracked advective flow paths starting from selected locations for (a) predevelopment and (b) post-development condition. Colors change with travel time along each flow pathline, beginning with blue at start point and changing to red at advective travel time greater than 10,000 years.

4.3.6. Model Limitation and Future Studies

This study simulated the mean age distribution in the North China Plain, and compared the simulated age and measured ^{14}C age. Furthermore, a two-step steady-state flow model is used to evaluate the effect of paleo-hydrologic conditions on the age simulation. To simulate the age

evolution more realistically, a transient flow model which can represent actual paleo-conditions may be constructed in future study. The groundwater age based on ^{14}C shows a significant increasing trend with depth (Figure 4.2). However, due to limited availability of data, the current model only contains three model layers to represent the aquifer system, which is more complex than a three-layer system. The mixing of younger groundwater from the upper aquifers with older groundwater should be evaluated by a model with a fine vertical grid resolution in future studies.

4.4. Sustainability of Deep Groundwater and Responses

The effects of spatial variations in hydrogeologic parameters on the simulated recharge locations, flow paths and groundwater age indicate the relative importance of the geologic characteristics on flow patterns under natural conditions. Natural predevelopment hydraulic gradients were generated by the relative flat topography across the plain. The human impact on both the shallow and deep flow systems is greater than any geologic control. Both the horizontal and vertical hydraulic gradients have been enhanced by pumping, causing the flowpaths to be more vertical and more locally variable.

Sustainability of the deep groundwater depends primarily on the recharge sources and flow paths. The simulated steady-state age, flow paths and response to regional pumping demonstrate different recharge regimes of the shallow and deep aquifer units. The shallow aquifer receives direct recharge from precipitation and lateral recharge from mountain areas. Spatially distributed recharge and vertical flow are the dominant process shaping the age distribution in the unconfined aquifer.

The recharge regime for the deep aquifer is different in distinct hydrogeological units, and has been altered by extensive pumping. Under natural conditions, the deep water is refreshed through vertical flow in the piedmont area. However, due to the large difference of hydraulic conductivity between the alluvial fans and central plain, the lateral flow from the piedmont area to the central plain is limited. The primary discharge means for the deep groundwater in this region should be the upward flow to the shallow aquifer, and then uptake by evapotranspiration and leakage to rivers. This has been demonstrated by the simulated net recharge flux in natural conditions and the flow paths analysis. The main lateral recharge flux may be from the southwest recharge zone along the SW-NE oriented flow paths. Under developed conditions, due to extensive pumping in the shallow aquifer in the piedmont area, the downward vertical gradient is small, and the amount of shallow groundwater which vertically flows into the deep aquifer is limited. The primary replenishment source of deep groundwater in the middle and coastal plains is the downward vertical flow from the shallow aquifer zone, and maybe the upward vertical flow from much deeper aquifers.

Several water resources management strategies focusing attention on deep groundwater depletion had been proposed or carried out (Duan and Xiao, 2003; Foster et al., 2004; Zhang et al., 2009). Among these strategies, utilization of shallow brackish water for irrigation is thought to be the measure with significant potential for reducing deep groundwater abstraction (Fang et al., 2003; Zhang et al., 2004). Considerable experimental studies on using brackish water for irrigation have been carried out since 1970s (Fang and Chen, 1999). In the Hebei Plain, the current brackish water withdrawal is ~0.3 km^3/yr, which accounts only 25% of the total recharge in the brackish water zone (Zhang et al., 2004). The utilization of brackish water should continue to be encouraged as an alternative to extraction the deep fresh groundwater.

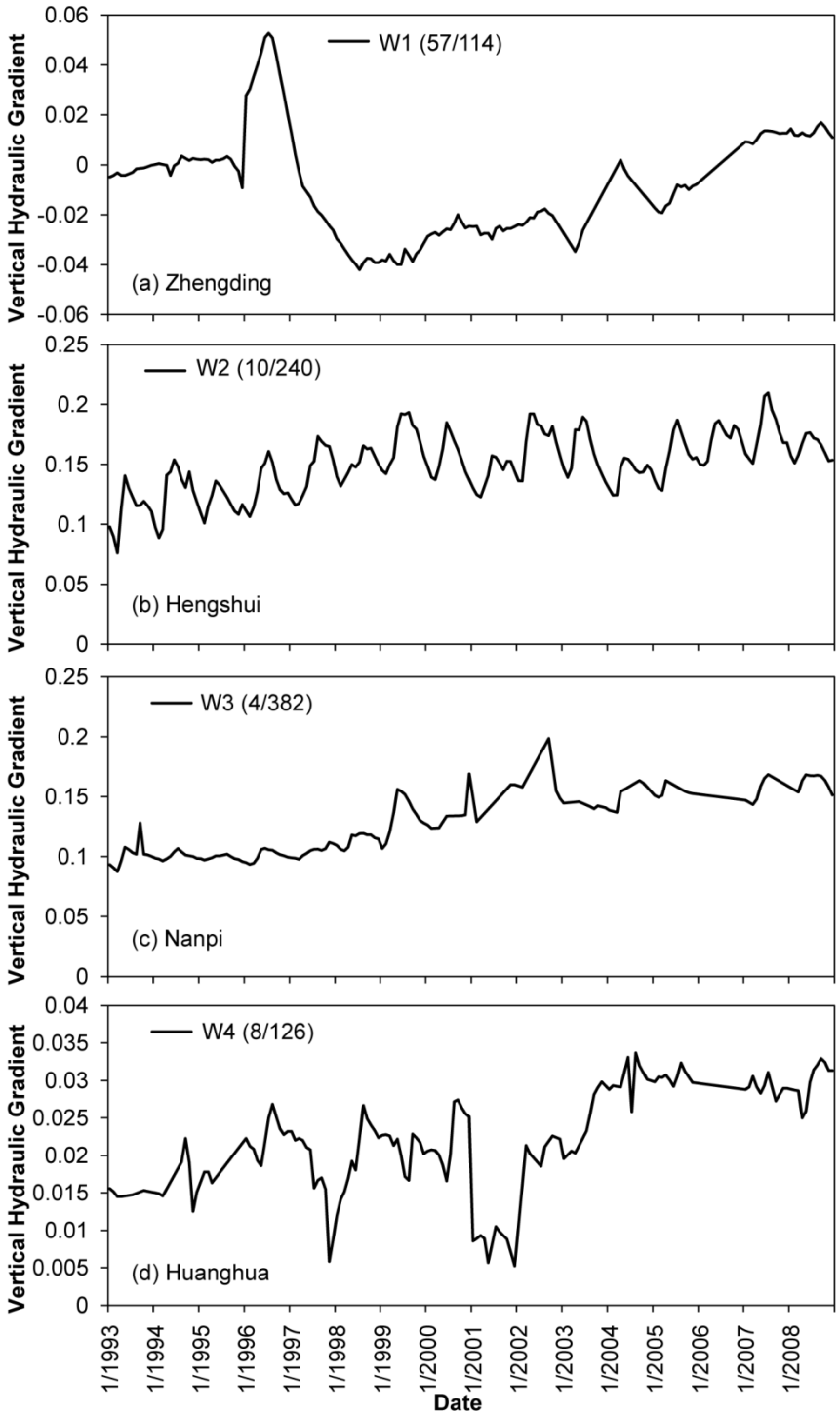

Figure 4.14. Vertical hydraulic gradient at selected sites from (a) Zhengding in the piedmont area, (b) Hengshui and (c) Nanpi in the central alluvial plain to (d) Huanghua in the coastal plain. Water levels measuring depths are given in parenthesis.

4.5. Conclusions

The major findings of this study are summarized as follows:

(1) Groundwater in the shallow aquifer of the NCP receives direct recharge from precipitation and irrigation, and has a higher renewability potential as characterized by younger groundwater age. In the deep aquifer below the central and coastal plains, there exists water recharged during the last glacial period with a limited renewability potential.

(2) The old age of groundwater in the middle and coastal plains does not lend support to the hypothesis of the existence of regional flow paths from the west piedmont area to the central and coastal plains. Lateral flow recharge to the deep aquifer is primarily from the southwest part of the plain, and is enhanced by groundwater pumping.

(3) The extensive groundwater withdrawal had a significant influence on the hydrogeology of the NCP flow system. Widely distributed recharge and vertical flow are the dominant process shaping the flow pattern in both the shallow and deep aquifers in the NCP.

(4) Under overexploitation conditions, groundwater pumped from the productive deep aquifer is primarily replenished by the enhanced downward leakage from the shallow aquifer and also from depletion of elastic and inelastic aquifer storage.

Acknowledgements

This work was supported by the National Basic Research Program of China (grant #2006CB403404) and National Natural Science Foundation of China (grant #40911130505). We appreciate the data support from China Geological Survey and China Institute of Water Resources and Hydropower Research.

References

Amin, I.E., and M.E. Campana. 1996. A general lumped parameter model for the interpretation of tracer data and transit time calculation in hydrologic systems. *Journal of Hydrology* 179, no. 1-4: 1-21.

Bethke, C.M., and T.M. Johnson. 2002a. Ground water age. *Ground Water* 40, no. 4: 337-339.

Bethke, C.M., and T.M. Johnson. 2002b. Paradox of groundwater age. *Geological Society of America* 30, no. 2: 107-110.

Cornaton, F., and P. Perrochet. 2006. Groundwater age, life expectancy and transit time distributions in advective—Dispersive systems: 1. Generalized reservoir theory. *Advances in Water Resources* 29, no. 9: 1267-1291.

Chen, N., X. Zhao, Y. Zang, D. Zhang, and L. Yang. 1992. Development of deep groundwater in the Heilonggang Plain. *Water Resources and Hydropower Engineering* 5: 35-40. (in Chinese)

Chen, W. 1999. Groundwater in Hebei Province. Beijing: Seismological Press (in Chinese).

Chen, Z. 2001. Groundwater resources evolution based on paleo-environmental information from groundwater system in the North China Plain. Dissertation, Jilin University.

Chen, Z.Y., J.X. Qi, J.M. Xu, J.M. Xu, H. Ye, and Y.J. Nan. 2003. Paleoclimatic interpretation of the past 30 ka from isotopic studies of the deep confined aquifer of the North China plain. *Applied Geochemistry* 18, no. 7: 997-1009.

Chen, Z.Y., Z.L. Nie, Z.J. Zhang, J.X. Qi, and Y.J. Nan. 2005. Isotopes and sustainability of ground water resources, North China Plain. *Ground Water* 43, no. 4: 485-493.

Chen, Z., H. Gao, W. Wei, J. Chen, F. Zhang, and Y. Wang. 2009. Groundwater Renewal and Characteristics in the Deep Confined Aquifer in North China Plain. *Resources Science* 31, no. 3: 388-393. (in Chinese with English abstract)

Clark, I.D., and P. Fritz. 1997. *Environmental isotopes in hydrogeology*, CRC Press.

Crosbie, R.S., P. Binning, and J.D. Kalma. 2005. A time series approach to inferring groundwater recharge using the water table fluctuation method. *Water Resources Research* 41, no. 1:1 -9.

Doherty, J. 2003. Version 5 of PEST Manual. Watermark Numerical Computing, Brisbane Australia. Downloadable from: http://www. sspa. com/pest.

Dong, Y., M. He, S. Jiang, S. Wu, and S. Jiang. 2002. Chlorine-36 Age Study for Deep Groundwater of Quaternary Sediments, Hebei Plain. *Earth Science—Journal of China University of Geosciences* 27, no. 1: 105-109. (in Chinese with English abstract)

Duan, Y., and G. Xiao. 2003. Sustainable utilization of groundwater resources in Hebie Plain. *Hydrogeology and Engineering Geology* 30, no. 1: 2-8. (in Chinese with English abstract)

Fang, S., X. Chen, and T.M. Boers. 2003. Sustainable Utilization of Water Resources in The Eastern Part of The North China Plain. *Water Resources Planning and Design* 4: 24-31. (in Chinese with English abstract)

Fei, Y., Z. Zhang, H. Song, Y. Qain, J. Chen, and S. Meng. 2009. Discussion of vertical variations of saline groundwater and mechanism in North China Plain. *Water Resources Protection* 25, no. 6: 21-23. (in Chinese with English abstract)

Ginn, T.R. 1999. On the distribution of multicomponent mixtures over generalized exposure time in subsurface flow and reactive transport: Foundations, and formulations for groundwater age, chemical heterogeneity, and biodegradation. *Water Resources Research* 35, no. 5: 1395-1407.

Ginn, T.R., H. Haeri, A. Massoudieh, and L. Foglia. 2009. Notes on Groundwater Age in Forward and Inverse Modeling. *Transport in Porous Media* 79, no. 1: 117-134.

Goode, D.J. 1996. Direct simulation of groundwater age. *Water Resources Research* 32, no. 2: 289-296.

Gu, Y., S.Z. Nanjing, and Z. Zhong. 1995. The property of deep-lying groundwater resources in Hebei plain and its reasonable evaluation in view of land subsidence. *Journal of China Univeristy of Geosciences* 20, no. 4: 415-420. (in Chinese with English abstract)

Guo, Y., Z. Shen, and Z. Zhong. 1995. Relathionship between saline water downgoing and shallow water desalinization in the Hebei Plain. *Hydrogeology & Engineering Geology* 2: 8-12. (in Chinese with English abstract)

Engesgaard, P., and J. Molson. 1998. Direct simulation of ground water age in the Rabis Creek Aquifer, Denmark. *Ground Water* 36, no. 4: 577-582.

Harbaugh, A.W., E.R. Banta, M.C. Hill, and M.G. McDonald. 2000. MODFLOW-2000, the u. S. Geological survey modular ground-water model-user guide to modularization concepts and the ground-water flow process. U.S. Geological Survey Open-File Report 00-92.

Harbaugh, A.W. 1990. A computer program for calculating subregional water budgets using results from the U.S. geological survey modular three-dimensional finite-difference ground-water flow model. U.S. Geological Survey Open-File Report 90-392.

He, Q., W. Liu, and Z. Li. 2006. Land Subsidence Survey and Monitoring in the North China Plain. *Geological Journal of China Universities* 12, no. 2: 195-209. (in Chinese with English abstract)

Hunt, R.J., D.E. Prudic, J.F. Walker, and M.P. Anderson. 2008. Importance of unsaturated zone flow for simulating recharge in a humid climate. *Ground Water* 46, no. 4: 551-560.

Kazemi, G.A., J.H. Lehr, and P. Perrochet. 2006. *Groundwater age*, Wiley-Interscience.

Kendy, E., P. Gérard-Marchant, M.T. Walter, Y. Zhang, C. Liu, and T.S. Steenhuis. 2003. A soil-water-balance approach to quantify groundwater recharge from irrigated cropland in the North China Plain. *Hydrological Processes* 17, no. 10: 2011-2031.

Lemieux, J.M., and E.A. Sudicky. 2010. Simulation of groundwater age evolution during the Wisconsinian glaciation over the Canadian landscape. *Environmental Fluid Mechanics* 10, no. 1-2: 91-102.

Liu, C., and Z. Wei. 1989. Agricultural Hydrology and Water Resources in the North China Plain. Beijing: Science Press. (in Chinese with English abstract)

Liu, C., P. Wang, L. Zhou, S. Jiang, S. Jiang, H. Guo, and L. Huang. 1993. Cl dating of quaternary groundwater in Hebei Plain. *Hydrogeology and Engineering Geology* 6: 35-38. (in Chinese)

Lu, X., M. Jin, M.T. van Genuchten, and B. Wang. 2011. Groundwater Recharge at Five Representative Sites in the Hebei Plain, China. *Ground Water* 49, no. 2: 286-294.

Ming, M. 1986. Salinization of deep groundwater in Hengshui. *Hydrogeology & Engineering Geology* 5: 42-44 (in Chinese).

Newman, B.D., K. Osenbruck, W. Aeschbach-Hertig, S.D. Kip, P. Cook, K. Rozanski, and R. Kipfer. 2010. Dating of'young'groundwaters using environmental tracers: advantages, applications, and research needs. *Isotopes In Environmental And Health Studies* 46, no. 3: 259.

Pearson, F.J., and B.B. Hanshaw. 1970. Sources of dissolved carbonate species in ground-water and their effects on carbon-14 dating. In: IAEA (Editor), Isotope Hydrology 1970. IAEA, Vienna, pp. 271–285.

Pint, C.D., R.J. Hunt, and M.P. Anderson. 2003. Flowpath Delineation and Ground Water Age, Allequash Basin, Wisconsin. *Ground Water* 41, no. 7: 895-902.

Pollock, D.W. 1994. User's Guide for MODPATH/MODPATH-PLOT, Version 3: A particle tracking post-processing package for MODFLOW, the U.S. Geological Survey finite-difference ground-water flow model. U.S. Geological Survey Open-File Report 94, no. 464: 6.

Ren, M. Sediment Discharge of the Yellow River, China: Past, Present and Future—A Synthesis. *Advances in Earth Science* 21, no. 6: 551-563. (in Chinese)

Richter, J., P. Szymczak, T. Abraham, and H. Jordan. 1993. Use of combinations of lumped-parameter models to interpret groundwater isotopic data. *Journal of Contaminant Hydrology* 14, no. 1: 1-13.

Sturchio, N.C., X. Du, R. Purtschert, et al. 2004. One million year old groundwater in the Sahara revealed by krypton-81 and chlorine-36. *Geophysical Research Letters* 31, L055035.

Smethie, W.M., D.K. Solomon, S.L. Schiff, and G.G. Mathieu. 1992. Tracing groundwater-flow in the borden aquifer using Kr-85. *Journal of Hydrology* 130, no. 1-4: 279-297.

Sophocleous, M. 1992. Groundwater recharge estimation and regionalization: the Great Bend Prairie of central Kansas and its recharge statistics. *Journal of Hydrology* 137, no. 1: 113-140.

Song, H., Z. Zhang, F. Fei, Z. Wang, Y. Qian, and W. Wei. 2007. Down-movement of the fresh-saline groundwater interface in the middle of the Hebei Plain under the condition of exploitation. *Hydrogeology & Engineering Geology* 1: 10-17. (in Chinese with English abstract)

Song, X.F., S.Q. Wang, G.Q. Xiao, Z.M. Wang, X. Liu, and P. Wang. 2009. A study of soil water movement combining soil water potential with stable isotopes at two sites of shallow groundwater areas in the North China Plain. *Hydrological Processes* 23, no. 9: 1376-1388.

Sultan, M., N.C. Sturchio, H. Gheith, Y.A. Hady, and M. El Anbeawy. 2000. Chemical and isotopic constraints on the origin of Wadi El-Tarfa ground water, Eastern Desert, Egypt. *Ground Water* 38, no. 5: 743-751.

Sun, X. 2007. Sustainable utilization study of groundwater resources in Circum-Bohai-Sea region. Dissertaiton, China Univerisy of Geosciences.

Varni, M., and J. Carrera. 1998. Simulation of groundwater age distributions. *Water Resources Research* 34, no. 12: 3271-3281.

von Rohden, C., A. Kreuzer, Z. Chen, R. Kipfer, and W. Aeschbach-Hertig. 2010. Characterizing the recharge regime of the strongly exploited aquifers of the North China Plain by environmental tracers. *Water Resources Research* 46, no. 5: W5511.

Wang, J.B., and P. Li. 2004. Composition of groundwater resources in deep-seated aquifers under the condition of land subsidence in Tianjin Plain. *Hydrogeology and Engineering Geology* 5: 35-37. (in Chinese with English abstract)

Wu, J., A. Zhou, H. Cai, and X. LI. 2007. New understanding of 14C age of groundwater in the Hebei plain. *Hydrogeology & Engineering Geology* 5: 39-44. (in Chinese with English abstract)

Wu, C., Q.H. Xu, Y.H. Ma, and X.Q. Zhang. 1996. Palaeochannels on the North China Plain: Palaeoriver geomorphology. Geomorphology 18, no. 1: 37-45.

Xu, Y., and H.E. Beekman. 2003. Groundwater recharge estimation in Southern Africa. UNESCO IHP Series No. 64.

Zhang, Z., D. Shi, F. Ren, Z. Yin, J. Sun, and C. Zhang. 1997. Evolution of the Quanternary Goundwater in the North China Plain. *Science in China,Ser.D* 2: 168-173. (in Chinese)

Zhang, G., Z. Chen, Y. Fei, and Z. Nie. 2001. Regional Distribution Characteristics of Groundwater Isotopic Ages and Hydrogeological Chemical Types in the Plain of Haihe River

Basin. *Bulletin of Mineralogy Petrology and Geochemistry* 20, no. 4: 412-414. (in Chinese with English abstract)

Zhang, G., and J. Wang. 2002. Mechanism of Confined Groundwater Recharge and Release in the Middle-East Plain of Haihe River Basin. *Hydrology* 22, no. 3: 5-9. (in Chinese with English abstract)

Zhang, G., Y. Fei, J. Shen, and L. Yang. 2007. Influence of unsaturated zone thickness on precipitation infiltration for recharge of groundwater. *Journal of Hydraulic Engineering* 38, no. 5: 611-617. (in Chinese with English abstract)

Zhang, G., Y. Fei, and K. Liu. 2004. Evolution of and countermeasure for the groundwater in the Haihe Plain. Beijing: Science Press. (in Chinese)

Zhang, Z., G. Luo, Z. Wang, C. Liu, Y. LI, and X. Jiang. 2009. Study on Sustainable Utilization of Groundwater in North China Plain. *Resources Science* 31, no. 3: 355-360. (in Chinese with English abstract)

Zheng, C. and P.P. Wang, 1999, MT3DMS: A Modular Three-Dimensional Multispecies Model for Simulation of Advection, Dispersion and Chemical Reactions of Contaminants in Groundwater Systems; Documentation and User's Guide, Contract Report SERDP-99-1, U.S. Army Engineer Research and Development Center, Vicksburg, MS, 1999.

Zheng, C. 2010, MT3DMS v5.3 Supplemental user's guide. Technical Report, Department of geological sciences, University of Alabama, Tuscaloosa, Alabama.

Zhu, C. 2000. Estimate of recharge from radiocarbon dating of groundwater and numerical flow and transport modeling. *Water Resources Research* 36, no. 9: 2607-2620.

Zoellmann, K., W. Kinzelbach, and C. Fulda. 2001. Environmental tracer transport (H-3 and SF6) in the saturated and unsaturated zones and its use in nitrate pollution management. *Journal of Hydrology* 240, no. 3-4: 187-205.

CHAPTER 5

CONCLUDING REMARKS

This study represents a first attempt at a comprehensive assessment of the groundwater recharge and sustainability in the North China Plain (NCP) from a basin-scale, process-based modeling approach. Relying on multiple data sources including meteorological data, land use data, aquifer water level data, soil property data, isotopic groundwater age data, this study yields the spatial and temporal distributions of groundwater recharge between 1993 and 2008 through variably saturated flow modeling, flow budget and flow path analysis, and direct groundwater age simulation. This information provides the basis for quantitative evaluation of the long-term sustainability of groundwater resources in the NCP.

The mathematical models developed in this study include a regional soil-water balance model, a regional variably saturated flow model that couples one-dimensional vertical unsaturated flow with three-dimensional saturated flow, and a regional three-dimensional flow and transport model calibrated with hydraulic heads and isotopic groundwater age data. These models are used to evaluate the groundwater recharge process from different perspectives and to provide comparison and consistency check between the results from different models. The outcome is a comprehensive picture and improved understanding of the groundwater recharge process and overall flow system dynamics in the NCP.

The model-calculated recharge rates are in reasonably good agreement with those from field-based experimental studies at local scales. Although the climatic condition is still the primary factor controlling the recharge distribution for the shallow groundwater, the recharge

and flow regime in the deep aquifer has been alternated significantly by human activities across the entire NCP.

The changes in the groundwater flow system in the NCP aquifer under the long-term stress of extensive groundwater pumping can be illustrated in Figure 5.1. In the shallow aquifer zone, the groundwater is recharged by precipitation in both pre-development and post-development periods. In the deep aquifer zone, there exists groundwater recharged during the last glacial period, and the groundwater is replenished by the precipitation leaked from the shallow aquifer zone.

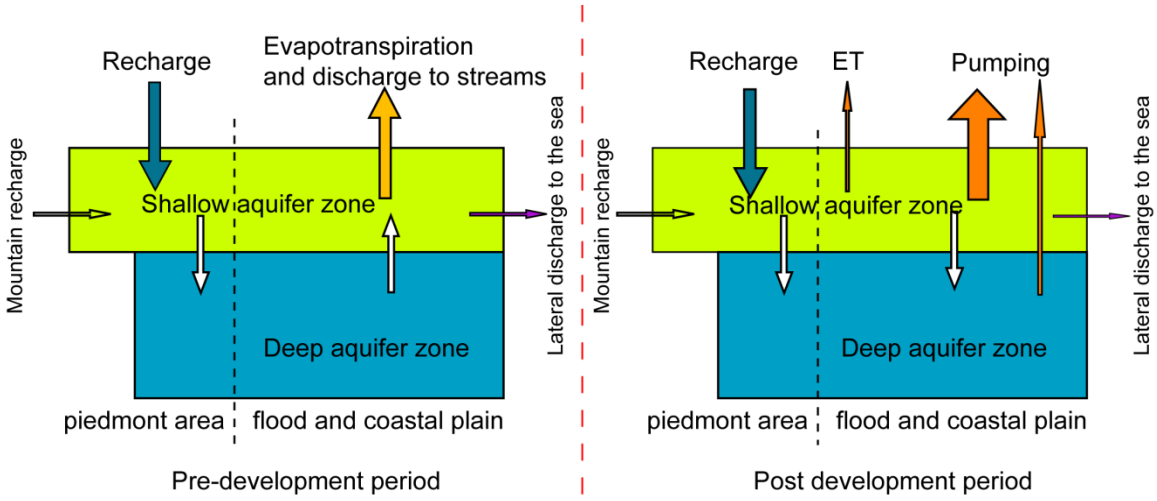

Figure 5.1. Conceptual model illustrating flow pattern changes in the NCP aquifer system

This study focuses primarily on the flow quantity and physical analysis, however, water quality and chemical characteristics of the flow system are another critical aspect with respect to the evaluation of the sustainability of groundwater. Moreover, social, economic and political considerations are also crucial factors. How to quantify the effect of these determinants and integrating with numerical groundwater flow and quality models should be a future research direction.

Although reducing irrigated acreage and changing the land use and crop system to dryland farming has the most significant potential in reducing groundwater overuse, whether it is applicable is still in doubt because of the current food security policies in China. The main applicable strategies towards sustainable groundwater development in the NCP include: groundwater recharge enhancement with excess surface runoff, improvement of the efficiency of irrigation system and water use efficiency, utilization of brackish groundwater water for irrigation, desalination of seawater for industrial and domestic water use in coastal cities, and conjunctive use of groundwater and surface water from water transfer projects.